Modulation of Chondroitin Sulfation by Lithium-Inhibited Bisphosphate Nucleotidase 2

By

Brynna Suzanne Eisele

Dissertation

Submitted to the Faculty of the

Graduate School of Vanderbilt University

in partial fulfillment of the requirements

for the degree of

DOCTOR OF PHILOSOPHY

in

Pharmacology

December 18, 2021

Nashville, Tennessee

Approved:

Christine Konradi, Ph.D.

John D. York, Ph.D.

Lisa Monteggia, Ph.D.

Jeffrey Neul, MD. Ph.D.

Fiona Harrison, Ph.D.

Sun Peck, Ph.D.

ACKNOWLEDGEMENTS

This research was supported by the National Institutes of Health (T32GM007347) and Vanderbilt University.

I would like to thank my advisor, John York, for all of the discoveries he made prior to this work, which allowed me to step into an exciting project that aligned so closely with my own interests. I am grateful for the level of independence that he afforded me to develop and to test my own ideas. He instilled in me the importance of practicing science from a place of curiosity, instead of getting wrapped up in how the science should serve a specific purpose. I believe that this approach breeds the most open and honest scientific inquiry, and I am grateful to have seen it in practice. Thank you, John, for also teaching me that it is important to pursue the career path that is meaningful, not just what may be expected.

I am grateful for the people who led me to pursue scientific training, including Iva Zovkic and Andrew Kennedy. The path was not easy, but I do feel I have benefitted immensely. Thank you for encouraging me in this direction.

I am grateful for the people I conversed with and consulted with frequently, including Lucia Plant, Andrew Hale, Bradley Clarke, Jane Wright, Joseph Weiss, Ryan Irving, and Celeste Greer. I learned from each of you, and I am glad you were willing to help when I needed it.

Thank you to Zigmund Luka, who established the HPLC protocols almost from scratch, and who spent his last week before retirement tirelessly preparing and running my samples. Thank you for being so thorough. Thank you for being so kind. Thank you for being in the lab to greet me every morning.

I want to specifically thank my undergraduate Alice Wu, for willingly taking on so many of the crucial tasks, and for being so reliable. Thank you for also being a lab companion, and for teaching me an important lesson: the data might not always be significant, but the people are.

Thank you to Garrett Kaas, for being a mentor to me even when you didn't have to be. I'm not sure how anyone makes it through graduate school without someone like you. Thank you not only for your knowledge and expertise, but also for your encouragement when times got tough. Thank you for reminding me that there are bigger and brighter things ahead for both of us.

I am forever grateful for my parents, David and Deborah Paulukaitis, for encouraging me in whatever I do. I am also grateful to my in-laws, Fred and Linda Eisele, who have been exceptionally helpful throughout my time in Nashville.

Finally, I want to express how much I love and appreciate my husband, Scott Eisele, for bearing with me throughout the ups and the many downs over the course of the last 5 years. Thank you for finishing your PhD, for showing me that it could be done. Thank you for listening. Thank you for understanding. I look forward to the things we will learn together.

TABLE OF CONTENTS

LIST OF TABLES

LIST OF FIGURES

LIST OF ABBREVIATIONS

AAV	adeno-associated virus
AMP	5’-adenosine monophosphate
ATP	adenosine triphosphate
BPNT	bisphosphate nucleotidase
C0S	unsulfated chondroitin
C4S	chondroitin-4-sulfate
C4ST	chondroitin-4-sulfotransferase (encoded by *Chst11*)
C6S	chondroitin-6-sulfate
C6ST	chondroitin-6-sulfotransferase (encoded by *Chst3*)
ChABC	chondroitinase ABC
CHST	carbohydrate sulfotransferase
CNS	central nervous system
CSPG	chondroitin sulfate proteoglycan
CST	cerebroside sulfotransferase
DSPG	dermatan sulfate proteoglycan
DMMB	1,9-dimethylmethylene blue
ECM	extracellular matrix
FBP	fructose bisphosphatase
GAG	glycosaminoglycan
GFP	green fluorescent protein
GPAPP	Golgi-resident 3’-phosphoadenosine-5’-phosphate phosphatase (also known as BPNT2)
GSK	glycogen synthase kinase
HPLC	high-performance liquid chromatography
HPRT	hypoxanthine phosphoribosyltransferase
HSPG	heparan sulfate proteoglycan

IMPA	inositol monophosphatase
IMPAD1	inositol monophosphatase domain-containing 1 (also known as BPNT2)
INPP	inositol polyphosphatase
JAWS	“joints abnormal with splitting” (also known as BPNT2)
KO	knockout
KSPG	keratan sulfate proteoglycan
LiCl	lithium chloride
MEF	mouse embryonic fibroblast
MMP	matrix metalloproteinase
N2A	neuroblastoma-2a cells
PAP	3’-phosphoadenosine 5’-phosphate
PAPS	3’-phosphoadenosine 5’-phosphosulfate
PAPSS	phosphoadenosine phosphosulfate synthase
PAPST	phosphoadenosine phosphosulfate transporter (encoded by *SLC35b2* and *SLC35b3*)
PNGaseF	peptide N-glycosidase F
PNN	perineuronal net
SULT	sulfotransferase
SV40	simian virus 40
WFA	*Wisteria floribunda* agglutinin
WT	wild-type

CHAPTER I

INTRODUCTION

Introduction to bisphosphate nucleotidase 2 (BPNT2)

Lithium-sensitive phosphatases.

Lithium has been used in the treatment of neuropsychiatric disease since the 1950s[1,2]. Classically, lithium is used to treat bipolar disorder—a disorder characterized by extreme mood fluctuations[3]. Patients with bipolar disorder experience intense periods of excitement (mania, or hypomania) interspersed with periods of depression which both inhibit normal daily function and increase risk of suicide[4,5]. Despite lithium's broad side effect profile[6–8] and the advent of novel therapeutics for the treatment of bipolar disorder[9], lithium remains the first-line treatment for acute mania[10] and the only available therapy that decreases suicide risk[11]. However, the mechanism of action of lithium remains unclear. Several potential targets have been identified, including glycogen synthase kinase 3β (GSK-3β) and inositol phosphatases, but resultant hypotheses about how targeting these enzymes treats mood fluctuation have not been definitively validated[12].

Inositol phosphatases have been shown to be directly regulated by lithium and other metal cations[13–15]. Investigations into a potential metal-binding site among these enzymes led to the identification of a common sequence motif [D-P-(I/L)-D-(G/S/A)-(T/S)], which directly coordinates lithium (Li^+) binding and is involved in enzyme catalysis[16,17]. Overlaying the structures of lithium-inhibited inositol phosphatases around this sequence led to the further identification of an apparent three-dimensional structural motif [D-X_n-EE-X_n-DP(I/L)D(G/S/A)(T/S)-X_n-WD-X_{11}-GG][16]. This motif was used to identify additional enzymes—all of which demonstrated phosphomonoesterase activity and were potently inhibited by lithium ions, and activated by magnesium ions. The identification of this novel family of enzymes (displayed in the dendrogram shown in **Figure 1**) led to the discovery of additional candidate targets of lithium.

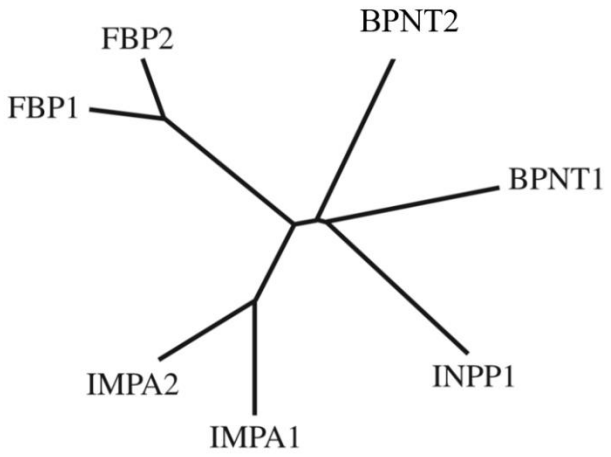

Figure 1. Phylogenetic tree of lithium-inhibited phosphatases defined by a common metal-binding structural motif. Enzymes and relationships depicted as identified from *Mus musculus*. Family members include fructose bisphosphatases 1 and 2, inositol monophosphatases 1 and 2, inositol polyphosphatase, and bisphosphate nucleotidases 1 and 2. Figure adapted from Frederick et al. 2008[18].

Among this family were the previously known inositol monophosphatases (IMPA1 and IMPA2), as well as inositol polyphosphate 1-phosphatase (INPP1), along with the fructose 1,6-bisphosphatases (FBP1 and FBP2). Two novel family members were also identified: the bisphosphate nucleotidases (BPNT1 and BPNT2)[19,20]. At the time of their discovery, only the function of BPNT1 was known[21]. BPNT1 exhibits lithium-inhibitable phosphatase activity against the nucleotide phosphoadenosine phosphate (PAP), a by-product of intracellular sulfation[19,22], and homologs of this enzyme exist in both yeast[23] and bacteria[24], suggesting an important evolutionary role for PAP phosphatase.

The function of the second enzyme (now known as BPNT2), which shares approximately 26% sequence homology with BPNT1, was not elucidated until several years later. While investigating BPNT2, it was discovered that residues 7-29 encoded a transmembrane domain, and it contains an N-link glycosylation consensus sequence (at N257); these features suggest localization to an endoplasmic reticulum or Golgi membrane[18]. Subsequent work demonstrated that BPNT2 is indeed localized to the Golgi (with its catalytic core contained within the Golgi lumen), and that deletion of the transmembrane domain prevents Golgi localization[18]. In these studies, insect cells were used to express BPNT2, given the presence of glycosylation mechanisms in insect cells which assist in proper glycoprotein folding[25]. Insect-cell-

produced BPNT2 demonstrated lithium-inhibitable catalytic activity against PAP, similar to BPNT1[18]. It was thus concluded that BPNT2 metabolizes PAP specifically in the Golgi. Because Golgi membranes are not present in prokaryotes, BPNT2 is less highly conserved compared to BPNT1. Yeast homologs of BPNT2 have not been reported, but BPNT2 is conserved across mammals[18].

Sulfur assimilation pathways.

As previously stated, PAP is a by-product of sulfation reactions. Understanding the function of the bisphosphate nucleotidases requires an understanding of the sulfur assimilation pathway.

Sulfur is an essential dietary micronutrient. It is primarily consumed as the amino acids methionine and cysteine. Methionine can be demethylated to form homocysteine, which is then converted to cystathionine. Cystathionine can then be converted to cysteine (which is why methionine, and not cysteine, is considered an essential amino acid). Cysteine can either be converted to cysteine sulfinate or desulfurated to ultimately yield inorganic sulfate[26]. These pathways are illustrated in **Figure 2**.

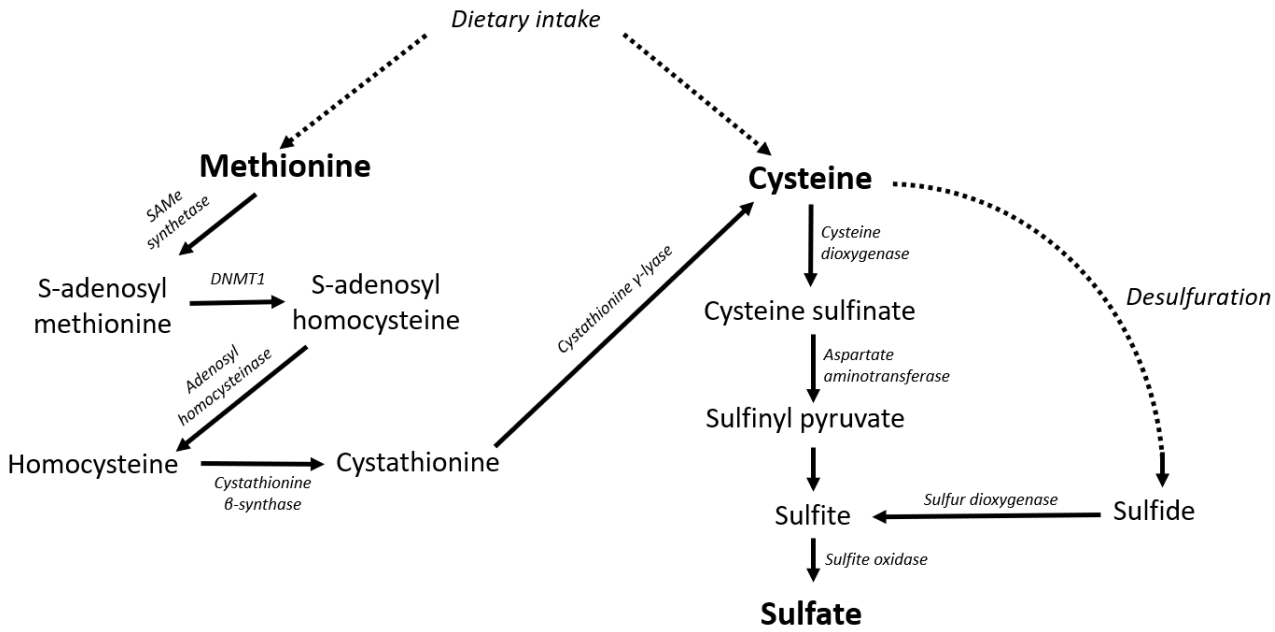

Figure 2. Summary of sulfur amino acid metabolism. A diagram of predominant pathways for the conversion of sulfur-containing amino acids into inorganic sulfate, and relevant enzymatic steps. Both methionine and cysteine can be obtained through diet, or cysteine can be synthesized from methionine. Cysteine can then undergo conversion to cysteine sulfinate to ultimately yield sulfinate, or undergo desulfuration to yield sulfide, which is then oxidized to sulfite. Sulfite oxidase converts sulfite to inorganic sulfate, which can be excreted or utilized for sulfation reactions.

Sulfate is utilized by metazoans to produce a variety of organic compounds. To do so, inorganic sulfate (SO_4^{2-}) is transported across the plasma membrane by the sulfate transporter (SLC26A2)[27]. Once inside the cell, the sulfate must be converted into a usable form. The usable form is phosphoadenosine phosphosulfate (PAPS), also known as the universal sulfate donor. PAPS is synthesized from sulfate and adenosine triphosphate (ATP) by the bifunctional enzyme PAPS-synthase (PAPSS)[28]. PAPSS contains a sulfurylase domain which attaches the sulfate to the ATP, yielding adenosine phosphosulfate (APS). APS is then phosphorylated by the kinase domain of PAPSS to yield PAPS. PAPS serves as the substrate for sulfotransferases, which transfer the sulfate to a target molecule, yielding PAP as a by-product. PAP is then hydrolyzed to adenosine monophosphate (AMP) by the bisphosphate nucleotidases: BPNT1 in the cytosol, and BPNT2 in the Golgi. These pathways are illustrated in **Figure 3**. Of note, PAPS is synthesized specifically in the cytosol, then imported into the Golgi by solute carrier enzymes known as PAPS transporters (PAPST1 and PAPST2, also known as SLC35B2 and SLC35B3 respectively)[29].

Sulfotransferases can be classified based on their subcellular localization to either the cytosol or the Golgi membrane.

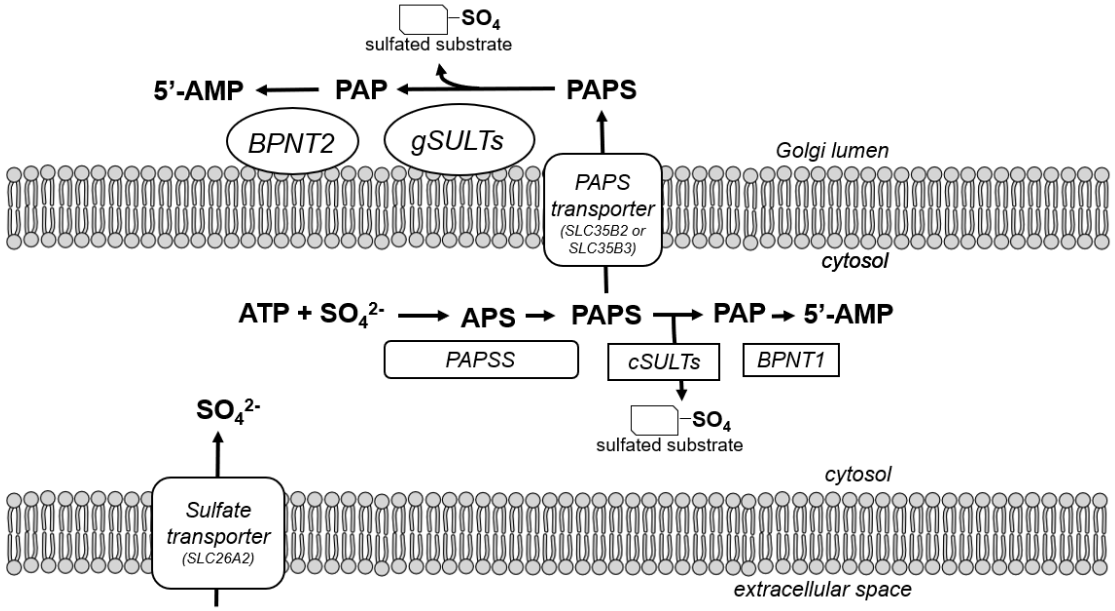

Figure 3. Sulfation pathways in the cytosol and Golgi. Inorganic sulfate crosses the plasma membrane through a sulfate transporter, where it joins with ATP to generate PAPS. PAPS can be utilized for sulfation in the cytosol, or it can be transported into the Golgi by PAPST. Resultant PAP from sulfation reactions is metabolized to AMP by BPNT1 in the cytosol and BPNT2 in the Golgi.

The subcellular localization of the BPNT enzymes is significant because of the unique types of sulfation reactions that occur in the cytosol versus in the Golgi. Cytosolic sulfotransferases (the classical SULT family of enzymes, including SULT1A1, SULT2E1, etc.) are known for their roles in drug metabolism, as the sulfation of xenobiotics is an important step in drug processing and excretion[30,31]. Cytosolic SULTs can also sulfate hormones and other endogenous small molecules[30]. Genetic variations in SULTs are often associated with alterations in drug metabolism and pharmacokinetic parameters[31–33]. Genetic alterations in Golgi-resident sulfotransferases, however, are often associated with overt disease states[34–38].

The Golgi-resident sulfotransferases are carbohydrate sulfotransferases (the CHST family of enzymes). These enzymes catalyze the sulfation of larger endogenous substances, especially glycosaminoglycans[39].

Glycosaminoglycan (GAG) sulfation.

Glycosaminoglycans (GAGs, also known as mucopolysaccharides) are large, secreted substances which are principally comprised of chains of repeating disaccharide units. These polysaccharide chains can be conjugated to core proteins to form proteoglycans[40]. Proteoglycans are an important component of the extracellular matrix, wherein they facilitate movement of substances between cells (especially ions and water) and can interact with other secreted proteins to form cartilage (which facilitates movement at the organismal level). The functionality of many GAGs can be traced in part to their high degree of sulfation, which makes them highly polar. GAGs are frequently sulfated at specific loci on each disaccharide unit. The major components of GAGs and proteoglycans are illustrated in **Figure 4**.

GAGs are classified by their specific disaccharide composition as well as the locus of sulfation on the disaccharide. One particularly abundant GAG is chondroitin (a major component of cartilage), which is comprised of repeating units of N-acetylgalactosamine and glucuronic acid. Chondroitin can be sulfated at the fourth carbon position on N-acetylgalactosamine, yielding the species known as chondroitin-4-sulfate. Additional species of chondroitin include chondroitin-6-sulfate (sixth carbon position on N-acetylgalactosamine), chondroitin-2,6-sulfate (sixth carbon of N-acetylgalactosmine and second carbon of glucuronic acid), as well as unsulfated chondroitin.

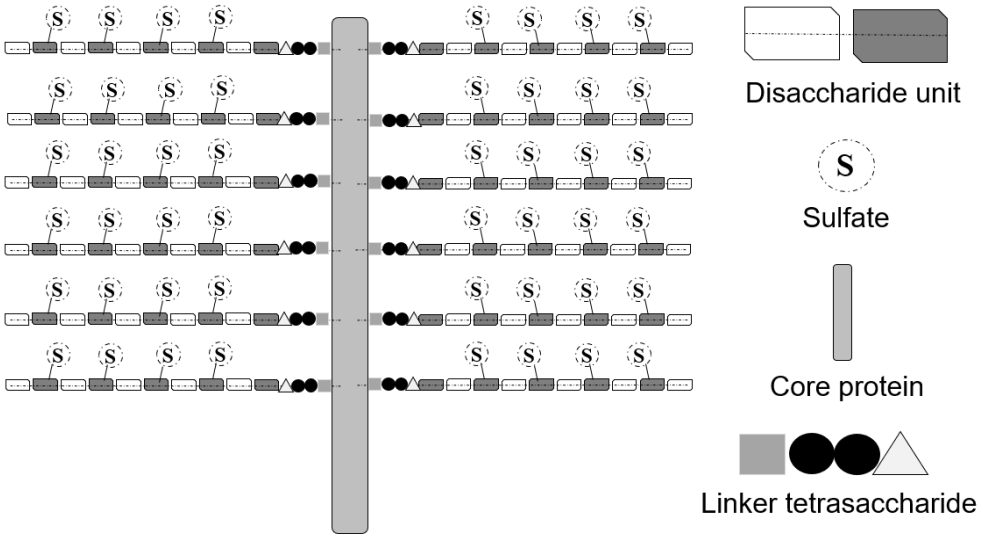

Figure 4. Structural features of glycosaminoglycans and proteoglycans. Chains of disaccharides, which often contain sulfated loci, are linked together to form GAGs. GAGs can organize around core proteins to form tree-like proteoglycans. GAGs are joined to core proteins by tetrasaccharide linkages.

Chondroitin-4-sulfate is particularly abundant in cartilage, which is essential for skeletal development and joint function. Other major species of GAG include heparan-sulfate, keratan-sulfate, deramatan-sulfate, and hyaluronan. These are all components of the extracellular matrix in various tissues, including cartilage, blood vessels, skin, and cornea, among others. These GAGs are comprised of distinct disaccharide units, and can also be sulfated at distinct loci[40], with the exception of hyaluronan, which is not sulfated.

GAGs are synthesized and sulfated primarily in the Golgi. The synthesis of the sugar chains has been described in detail by others[41,42]. The process of sulfation in the Golgi mirrors that of sulfation in the cytosol. To reiterate, the sulfate donor PAPS is synthesized from inorganic sulfate and ATP in the cytosol. It is transported into the Golgi by PAPS transporters (PAPST). Once inside, Golgi-resident sulfotransferases catalyze the transfer of the sulfate from PAPS to a substrate molecule (most frequently the carbohydrate moieties of GAGs), yielding a sulfated product and PAP. PAP is further metabolized to AMP by BPNT2.

BPNT2.

As part of the intial characterization of BPNT2, our laboratory generated BPNT2 knockout mice by insertion of a gene-trap vector downstream of the first exon of *Bpnt2*[18,43]. Homozygous BPNT2-null mice were conceived in Mendelian ratios to heterozygous breeding pairs, but they exhibited severely shortened long bones (**Figure 5**) and died shortly after birth (presumably due to underdeveloped rib cages causing pulmonary insufficiency)[18]. This work was corroborated by other groups, who also noted abnormalities in BPNT2-null pups such as ectopic digital joints and cleft palate[43,44]. It was discovered that this phenotype was markedly similar to the phenotype of mice lacking the chondroitin-4-sulfotransferase enzyme (C4ST1)[45], which is also characterized by aberrant long bone development and perinatal lethality.

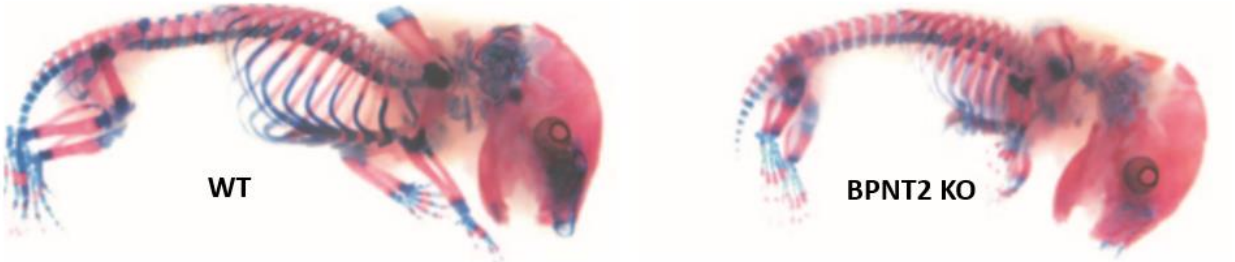

Figure 5. Phenotype of BPNT2 knockout mice. Skeletons of WT and BPNT2-KO littermates, shown at approximately E18.5. Images are of whole-mount preps originally stained with Alizarin red (bone) and Alcian blue (cartilage). Long bones of BPNT2-KO mouse are shortened, including ribs and limbs. Images adapted from Frederick et al. 2008[18].

This led our laboratory to investigate levels of chondroitin sulfation in BPNT2-knockout mice. Chondroitin species were extracted from both full mouse embryos as well as cartilaginous tissues of E18.5 pups. Extracts were digested with chondroitinase ABC and the resultant disaccharide units were resolved by high-performance liquid chromatography (HPLC). As is seen in C4ST1-knockout mice, BPNT2-knockouts displayed diminished chondroitin-4-sulfate (C4S) levels that corresponded with increases in unsulfated chondroitin (C0S) (**Figure 6**)[18]. It was concluded that the phenotype of mice lacking functional BPNT2 was likely a result of this sharp decrease in chondroitin-4-sulfate. As described above, chondroitin-4-sulfate is a major component of cartilage. Long bones are formed by endochondral ossification, which describes the process of a cartilage matrix being laid down first, then filled in with bone tissue. This is in contrast to intramembranous ossification (which is how the skull and axial skeleton form), which does not require a preliminary cartilage matrix. The loss of chondroitin-4-sulfate would impair the formation of this cartilage matrix, inhibiting elongation of long bones, which explains the apparent dwarfism phenotype. Meanwhile, there are no impairments in intramembranous ossification, which explains why both C4ST1- and BPNT2-knockout mice do not exhibit gross abnormalities in skull development[18,45].

BPNT2 mutation in humans.

Following the publication of the BPNT2-knockout mouse phenotype, a novel human chondrodysplastic disorder, characterized by autosomal recessive *BPNT2* mutations, was described[46,47]. This disorder recapitulates the mouse phenotype in that patients display shortened long bones with apparently normal axial skeleton, as well as abnormalities of digital (among other) joints. This disorder bears resemblance to other chondrodysplastic disorders, but genomic testing did not identify mutations in any known disease-associated loci. However, homozygous mutations were later identified in *BPNT2*. Given the apparent similarity to the published mouse phenotype, researchers concluded that these mutations likely underlied the disorder. At the time, the disorder was termed "Chondrodysplasia-Golgi PAP Phosphatase (GPAPP) Type."[46]

While exceptionally rare (just six published cases, all in offspring of apparently healthy consanguineous parents), Chondrodysplasia-GPAPP Type represents a monogenic Mendelian disorder with recessive inheritance. Each patient had one of four different mutations in *BPNT2*: Arg187X, Ser108ArgfsX48, Asp177Asn, and Thr183Pro. According to follow-up studies published by Nizon et al., disease severity does not appear to be related to the specific mutation that is present[47], but this analysis is obviously limited by the very small sample size. It is interesting to note that some patients had full siblings who had similar phenotypes but died in infancy or were stillborn, despite presumably having the same *BPNT2* mutations. A summary of all confirmed cases (as well as suspected cases in siblings) and their disease phenotypes is shown in **Table 1**. Data used to generate **Table 1** were published in the following papers: [46–48].

	Patient 1	Patient 2	Patient 3	Patient 4	Patient 5	Patient 6	Patient 7	Patient 8
Mutation	D177N	T183P	T183P	R187X	R187X	S108RfsX48	Presumed S108RfsX48	Presumed S108RfsX48
Last reported age	23 years	11 years	2 years	Deceased at 5 days (aspiration pneumonia due to cleft palate)	5 years	3 months	Deceased at 13 days	Full term stillbirth
Country of origin	Germany	Turkey	Turkey	India	Turkey	Turkey	Turkey	Turkey
Birth length	≤2 SD	≤2 SD	≤2 SD	-4 SD	NR	-4 SD	"short extremities"	"short extremities"
Joint hyperlaxity	-	+	NR	+	+	+	NR	NR
Hand and foot anomalies	+	+	+	+	+	+	NR	NR
Cleft palate and micrognathia	+	+	+	+	+	+	+	NR
Growth retardation	-8 SD	-7.5 SD	≤4 SD	NR	-6 SD	NR	NR	NR
Spinal anomalies	-	+	+	+	+	+	+	+
Intellectual disability	-	+	-	NR	-	NR	NR	NR
Siblings	NR	Full siblings (also had one unaffected full sibling)		NR	NR	Full siblings (mother had one additional spontaneous abortion at an unreported gestational age)		

Table 1. Summary of patients with chondrodysplasia-associated BPNT2 mutations. NR: not reported. SD: standard deviation.

It is understandable how the nonsense (Arg187X) and frameshift (Ser108ArgfsX48) could truncate the BPNT2 protein sufficiently as to render it dysfunctional, but it is interesting that two missense mutations (Asp177Asn and Thr183Pro) could disrupt the protein enough to cause an equally severe phenotype. It is also interesting to note that these two mutations occur in close proximity, both to each other and to the core sequence of the metal-binding structural motif [DP(I/L)D(G/S/A)(T/S), specifically $DPLDAT_{174\text{-}179}$ in human BPNT2] which was used to identify BPNT2 in the first place. This motif is illustrated in **Figure 7**. Indeed, Asp177 is one of the conserved residues directly in the middle of this sequence. While Thr183 is not one of the motif-defining residues, it is only a few amino acids away and remains highly conserved across species[46], and proline mutations are known to alter protein secondary structures[49,50]. It is thus conceivable that the Asp177Asn mutation alters the catalytic activity of the enzyme, and that the Thr183Pro mutation alters protein folding sufficiently as to disrupt normal BPNT2 functioning. However, the precise mechanisms for how these mutations result in human disease remains unknown.

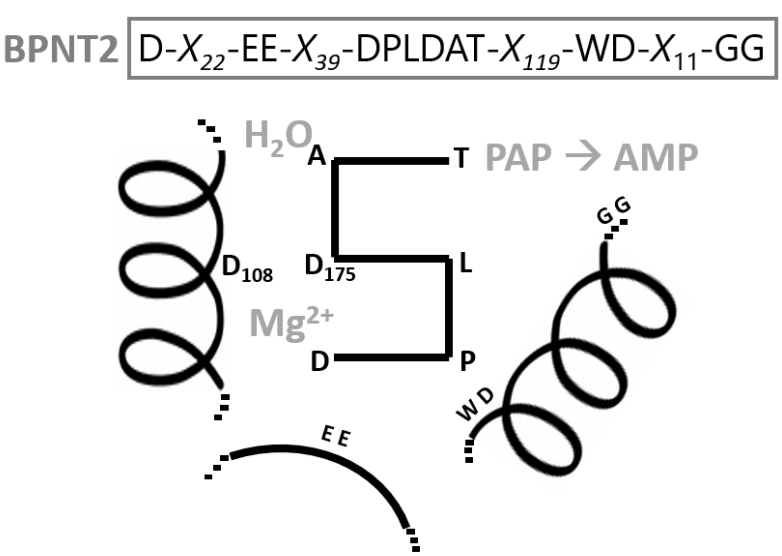

Figure 7. Illustration of metal-binding/catalytic structural motif of BPNT2. Murine BPNT2 metal-binding motif sequence is depicted at the top of the figure. Relevant residues are depicted in the figure. The 3 aspartic acid residues (D108, D172, and D175) make up the metal-binding pocket. For phosphate hydrolysis to occur, magnesium must be present in this pocket. Lithium displaces the magnesium cofactor to inhibit catalytic activity.

To summarize so far, BPNT2 was initially identified based on a defining structural motif that characterizes lithium-inhibited phosphatases. BPNT2 is a PAP phosphatase, which metabolizes PAP (the major by-product of sulfation reactions) to AMP specifically in the Golgi, where glycosaminoglycan sulfation occurs. Loss of BPNT2 in mice results in a dysplastic skeletal phenotype which stems from a

decrease in chondroitin-4-sulfation, which impairs cartilage development and therefore disrupts endochondral ossification. Homozygous mutations in BPNT2 in humans cause a similar chondrodysplastic disorder, characterized by impairments in endochondral ossification and joint abnormalities. It is unclear how the loss of BPNT2 impairs the process of chondroitin sulfation and causes the observed phenotypes.

BPNT2 in the central nervous system (CNS)

BPNT2 as a target of lithium.

As previously discussed, the bisphosphate nucleotidases (BPNT1 and BPNT2) were identified based on a three-dimensional structural motif[16,19,20] which directly coordinates the binding of metal ions. The likely catalytic pocket contained within this motif is bordered by three aspartic acids (as shown in **Figure** 7), which are negatively charged. The activity of this family of enzymes depends on the binding of a positively charged magnesium ion (Mg^{2+}) at this site, which generates an electrochemically favorable environment for water to be ionized, thus permitting the hydrolysis of a phosphate off of the substrate molecule[51]. The binding of lithium (Li^{+}, a monovalent cation) to this site in place of magnesium inhibits enzyme activity. The inhibition pattern is uncompetitive[18,19,22] (meaning it occurs only when substrate is already bound to the enzyme). For BPNT1 and BPNT2, inhibition occurs at sub-millimolar concentrations (K_i = ~150 μM for BPNT1[19] and K_i = ~175 μM for BPNT2[18]).

Lithium remains one of the most efficacious treatments for bipolar disorder, despite it's unclear biochemical effects in the central nervous system (CNS). The identification of the bisphosphate nucleotidases as targets of lithium has led us to seek to understand their function in the brain. The therapeutic window for lithium as a mood stabilizer is approximately 0.6-1.2 mM[8,52], meaning both BPNT1 and BPNT2 are potently inhibited at subtherapeutic concentrations, and are in fact the most potently inhibited targets of lithium that are currently known. Given the array of other potential targets of lithium, it would be reasonable to assume that lithium's mechanism of action is broader than its effect on one single

enzyme, but it is clear that the bisphosphate nucleotidases are indeed inhibited when lithium is present at therapeutic doses, and therfore could be contributing to either lithium's efficacy or its side effect profile.

The consequences of BPNT1 knockout in the CNS have not been fully elucidated, though the neurobehavioral characterization of BPNT1 knockout mice is likely to be complicated by their metabolic phenotype[53]. Nonetheless, this remains an important area of future research.

The consequences of BPNT2 knockout in the CNS (prior to this work) were also undetermined, as the BPNT2-knockout mouse died in the perinatal period, prohibiting any neurobehavioral analysis. However, BPNT2 expression patterns were previously examined in E18.5 pups, and are shown in **Figure 8**[18]. From this figure, it is evident that BPNT2 is highly expressed in the brain and spinal cord, at least during this stage of development. While this is a nonspecific finding, it could point to an important role for BPNT2 in the CNS.

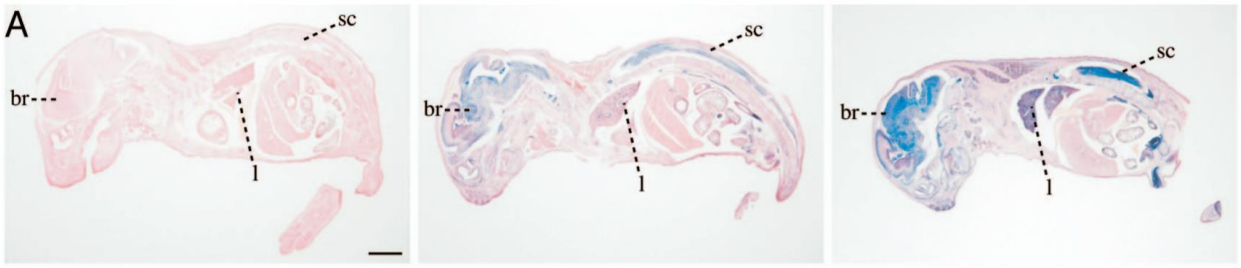

Figure 8. BPNT2 expression pattern in E18.5 mouse pups. Gene trapped alleles (Bpnt2 knockout alleles) included a LacZ cassette as part of the gene-disruption paradigm. Blue stain is beta-galactosidase, which indicates localization of gene-trapped *Bpnt2* allele. Staining indicates abundance of Bpnt2 in the brain (br) and spinal cord (sc), as well as the liver (l). This figure is also Fig. S3 from Frederick et al. 2008. Scale bar – 2mm. Left-to-right: $Bpnt2^{+/+}$, $Bpnt2^{+/gt}$, $Bpnt2^{gt/gt}$.

In contrast to BPNT2-knockout mice, many of the patients identified to have homozygous BPNT2 mutations (Chondrodysplasia-GPAPP Type) have survived infancy. The exceedingly small sample size (as well as the fact that many of the identified patients were still young children) prevents us from making conclusive statements regarding their neurologic or psychiatric condition. However, it should be noted that neurodevelopmental delay has been reported in at least one of these patients[47]. This finding, in conjunction

with high expression of BPNT2 in the developing mouse brain and the inhibition of BPNT2 at therapeutic concentrations of lithium, has led us to question what role BPNT2 may play in the CNS.

Chondroitin-sulfate in the CNS: perineuronal nets (PNNs).

As discussed, the phenotypes of BPNT2-knockout mice and patients with Chondrodysplasia-GPAPP Type seem to stem from impaired chondroitin-4-sulfation. While chondroitin-4-sulfate (C4S) is the most prevalent GAG in the body generally, it is especially enriched in the skeletal system and in the central nervous system[42].

There is extensive evidence suggesting a crucial role for chondroitin-4-sulfate in neuronal function. Multiple populations of neurons are surrounded by a specialized extracellular matrix known as the perineuronal network, which has become an emerging interest in the field of neurobiology[54–59]. Perineuronal nets (PNNs) consist primarily of condensed chondroitin sulfate, with C4S being the major species in the adult brain and chondroitin-6-sulfate (C6S) comprising the minority[60]. This condensation of GAGs around neuronal cell bodies is perceived to act as a type of insulation, and the term "net" implies they provide some dimension of stability. This has led PNNs to generally be viewed as barriers to neuroplasticity[61]. Prior work has found that PNNs indeed play important roles in the stabilization of neural circuitry (such as that underlying stable long-term memories[62,63] and addiction[54]). Throughout postnatal development, neuroplasticity tends to decrease, correlating with increased PNN density over time[64–66]. Given their presumptively restrictive role, PNNs are also thought to negatively regulate neurite outgrowth and axon extension.

While they are not strictly expressed around only one specific group of neurons[67], PNNs predominantly surround parvalbumin-expressing, GABAergic interneurons[68] and are thought to regulate the balance between excitatory and inhibitory signaling in the brain; this balance is disrupted in psychiatric disease states (such as acute mania and psychosis)[61,69] as well as in neurodevelopmental disorders (such as Fragile X and Angelman syndromes). There is some evidence to suggest that GABAergic interneurons are dysregulated in mood disorders[70], and that lithium (along with other mood stabilizers) has a positive effect

on GABAergic signaling[12,71] and could shift hyper-excited brain states (which are suspected to underlie mania) toward inhibitory states[72].

PNNs and neuropsychiatric disease.

Given the capacity for BPNT2 to modulate chondroitin sulfation, and the role of chondroitin sulfate in the composition of perineuronal nets in the brain, we conceived that it may be possible that the inhibition of BPNT2 by lithium could contribute to its therapeutic mechanism. The putative hypothesis in this scenario would be that chondroitin-sulfation (perhaps especially chondroitin-4-sulfation) is abnormally high (or PNNs are abnormally dense) in psychiatric disorders which respond to lithium. Inhibition of BPNT2 by lithium could correct this abnormality by limiting the production of chondroitin-4-sulfate.

Alterations in PNNs have indeed been reported in psychiatric diseases[55,61,73], including schizophrenia[66] and bipolar disorder[74,75]. Specifically, *decreases* in PNNs have been reported in the amygdala, entorhinal cortex, and prefrontal cortex of patients with schizophrenia, according to post-mortem tissue analyses[66,73]. *Decreases* in PNN density have also been reported in the prefrontal cortex[76] and thalamic reticular nucleus[75] of subjects with bipolar disorder, and more generally in patients with a history of psychotic episodes[76]. However, further analyses revealed decreases specifically in neuronal chondroitin-6-sulfate in the amygdala[74]. Chondroitin-6-sulfate (C6S) is the minor chondroitin species in the brain, and there is evidence to suggest it functionally opposes chondroitin-4-sulfate, in that C6S permits cellular plasticity[60,77,78] while C4S limits it[79]. There were also correspondent *increases* in PNN densities in amygdalar glial cells, as well as *increases* in the number of glial *cells* which stained positive for PNNs[73]. In patients with bipolar disorder, there are also notable increases in PNN staining *within glial cells* in the amygdalar nuclei, though they are less widespread[73]. The effect of chronic lithium treatment in the population of subjects with bipolar disorder was considered, and authors noted that while not statistically significant, there may be a mild corrective effect of lithium on these observed glial cell abnormalities[73].

There have also been noted alterations in mRNA expression of lectican proteins that serve as the backbones for chondroitin sulfate proteoglycans (CSPGs). In amygdalar tissue taken from patients with

schizophrenia, there has been reported overexpression of versican[73] and aggrecan[74], which are two of the four major lecticans comprising CSPGs in the CNS[80,81]. Similar overexpression patterns were not reported in bipolar disorder, but it should be noted that genome-wide association studies have identified a variant in neurocan (another major CSPG lectican) as a risk factor for bipolar disease[82].

Unlike schizophrenia and bipolar disorder, histological changes in PNN expression have not been identified in major depressive disorder[76], which is a common psychiatric diagnosis. However, decreases in PNN density have recently been correlated with depressive behaviors in rats[83], and subjecting mice to chronic restraint stress (a protocol used to induce depressive behaviors in rodents[84]) increases PNN expression in the medial prefrontal cortex[85]. There is also research which shows that chronic treatment with commonly prescribed antidepressants (including venlafaxine and fluoxetine) decreases PNN expression in the medial frontal cortex[86] and in the hippocampus[87,88] of mice. The authors of these studies proposed that these changes may contribute to the efficacy of these drugs, and suggested that upregulation of a matrix metalloproteinase (MMP9) may in part underlie the therapeutic effects of venlafaxine[87]. While these drugs (monoamine reuptake inhibitors) are not commonly prescribed for bipolar disorder, it is noteworthy that the degradation of PNNs may contribute to the alleviation of depressive symptoms.

Because the synthesis and expression of PNNs is itself a developmental process, many have investigated PNNs in the context of neurodevelopmental disease. PNN abnormalities have been reported in developmental disorders, both in human patients[89] and in mouse models[90,91]. Post-mortem tissue obtained from patients with Rett Syndrome (a disorder characterized by developmental regression and mutations in *MeCP2*) shows deficits in PNN staining in the motor cortex[89]. In a mouse model of Angelman syndrome (a disorder which causes severe developmental delay and which is characterized by loss of the maternal copy of the gene *UBE3A*), there is a striking overabundance of PNNs in the dentate gyrus of the hippocampus, which correlates with an increased susceptibilty to seizures[90]. In the mouse model of Fragile X Syndrome (a disorder which causes intellectual disability and distinctive facial features, and which is characterized by silencing of the *FMR1* gene), there were decreases in the number of PNN+ cells in the

auditory cortex during early postnatal development[91]. These changes coincided with enhanced expression of a matrix metalloproteinase[91].

Table 2 summarizes the alterations in PNNs that have been identified in various neuropsychiatric conditions. While not described in this summary, it is worth mentioning that alterations in PNNs have also been identified in neurological disorders including Alzheimer's disease[92] and epilepsy[93].

Disease state	Species	Change in PNN staining
Schizophrenia	Human Human Human	↓ Lateral amygdalar nucleus[73] ↓ Lateral entorhinal cortex[73] ↓ Prefrontal cortex[66]
Bipolar disorder	Human Human Human	↑ Amygdalar glial cells[73] ↓ Prefrontal cortex[76] ↓ Thalamic reticular nucleus[75]
Depression	Mouse Rat	↑ Medial prefrontal cortex[85] ↓ Prelimbic cortex[83]
Rett syndrome	Human	↓ Motor cortex[89]
Angelman syndrome	Mouse	↑ Dentate gyrus[90]
Fragile X syndrome	Mouse	↓ Auditory cortex[91]
Alzheimer's disease	Human	↓ Cortex[92,94]
Epilepsy	Rat	↓ Hippocampus[93]
Addiction	Rat	↓ Ventral tegmental area[95]

Table 2. Summary of neuropsychiatric disorders with reported abnormalities in PNNs.

PNNs and neurobehavior.

Previous work has shown that disrupting chondroitin synthesis during brain development alters PNN morphology and rodent behavioral characteristics. Mice lacking a critical chondroitin synthesis enzyme (CSGalNAcT1, which facilitates elongation of the chondroitin disaccharide chain) exhibit altered performance on tasks of motor coordination, increased basal activity, increased social interaction, and a heightened startle response relative to wild-type littermates[96]. These traits coincided with decreases in PNNs throughout the cerebral cortex, as identified by immunohistochemistry[96]. Similarly, disruption of aggrecan

expression in the developing mouse brain using a Cre-lox system is associated with diminished PNNs and enhancement of spatial memory as measured by an object recognition task[97].

Other changes in PNNs have been identified in mice lacking various other proteoglycan core proteins (including brevican and neurocan), and while overt behavioral alterations were not observed, these changes appeared to alter several electrophysiological characteristics of neurons[80,98–100].

Much of the work that has investigated PNNs in the context of neurobehavioral traits has involved post-developmental disruption of existing PNNs in mature adult mice. For example, degradation of PNNs following intracerebral administration or overexpression of an enzyme which degrades chondroitin (chondroitinase ABC, ChABC) has been associated with renewed neuronal plasticity[62,63] and memory enhancement[101,102]. However, the behavioral consequences of chondroitin degradation (particularly in the context of behavioral tasks used to investigate memory) appear to be influenced by the brain region subjected to chondroitinase treatment and the timing of the treatment relative to the behavioral task. Prior work suggests that degradation of PNNs with chondroitinase may improve memory acquisition (i.e. learning), but PNN degradation in regions where memories are stored may adversely affect the ability to recall such memories. For instance, chondroitin digestion in a rodent cerebellum prior to a cerebellar-dependent learning protocol appears to enhance learning, but may impair memory retrieval[102]. Impairments in memory retrieval have also been reported when chondroitinase is administered to a rat's hippocampus three hours prior to a contextual fear-learning protocol (a paradigm for hippocampal-dependent learning)—though the rats learn to associate a novel context with an aversive stimulus, they do not appear to recall this memory when tested 48 hours later[99]. Likewise, administration of chondroitinase to the mouse amygdala prior to an amygdalar-dependent learning protocol does not alter memory acquisition (i.e. learning), but it does render the memory more susceptible to erasure via extinction training[63]. A general unifying notion is that the lack of PNNs during memory formation is associated with a plastic state that facilitates learning[103]. Once a memory is formed, however, PNNs may be necessary for stabilizing and maintaining it; loss of PNNs at this stage of memory consolidation would render the memory vulnerable to loss or disruption[62,63].

Potential for lithium modulation of PNNs.

As previously discussed, there is evidence that some psychiatric medications (such as venlafaxine[87] and fluoxetine[86], which treat major depression) can down-regulate PNNs. We are especially interested in whether lithium may be able to modulate PNNs, perhaps by altering chondroitin sulfate synthesis by inhibition of BPNT2.

Prior studies have shown that lithium regulates chondroitin-sulfate proteoglycans (CSPGs) in the CNS. These studies focused on lithium's modulation of chondroitin to promote axon regeneration at neuronal growth cones within the spinal cord[104–106]. Lithium is therefore being investigated for its pharmacologic potential to treat spinal cord injury by facilitating axon guidance and neurite outgrowth[107,108], processes which are normally attenuated by PNNs[109,110]. These findings are of particular relevance not only because they connect the pharmacodynamics of lithium to chondroitin sulfate, but also because the expansion of neuronal growth cones is a common mechanism of action for multiple drugs used to treat bipolar disorder[111,112]. This suggests that chondroitin-sulfate proteoglycan dysregulation may be a fundamental mechanism contributing to the pathophysiology of bipolar disorder. Beyond its traditional application in bipolar disorder, lithium has also been shown to treat cognitive and behavioral symptoms in patients with neurodevelopmental disorders, including those with known alterations in PNNs[113–115], though the mechanistic basis for these observations is unknown.

Summary and Motivation

BPNT2 was discovered because of a structural motif that defines lithium-inhibited enzymes. Despite knowing it is inhibited by lithium, the function of the enzyme was not known until a knockout mouse was generated. The *Bpnt2*-knockout mouse exhibits chondrodysplasia, due to impaired chondroitin-4-sulfation.

My interest in this work stems from the observation that BPNT2 is inhibited by lithium, and lithium is an old, enigmatic, and uniquely efficacious psychotropic drug. Could lithium alter chondroitin sulfation via BPNT2 inhibition, and could such an alteration contribute to lithium's therapeutic effects? This question

looms large, and answering it thoroughly is unfortunately beyond the scope of this work. However, this project sought to begin this undertaking by answering two sets of questions.

The first question: does the impairment in chondroitin sulfation seen with loss of BPNT2 stem from a loss of the catalytic function of the protein, or from a non-catalytic function? A protein may have a known enzymatic role, but that does not mean it is its only role. For example, if BPNT2 supports chondroitin sulfation by acting in some structural role, then inhibiting it with lithium will not affect that structural purpose, so we could not anticipate an effect of lithium on chondroitin sulfation, at least not one that is mediated by BPNT2. However, if it is BPNT2's catalytic function that somehow sustains proper chondroitin sulfation, then it is conceivable that lithium could affect sulfation by inhibiting BPNT2. Chapter II of this dissertation describes my efforts to answer this question. In it, I generate an *in vitro* model of impaired glycosaminoglycan sulfation resulting from knockout of BPNT2, and I generate a cell line which expresses only catalytically inactive BPNT2. I show that the loss of the catalytic activity alone is sufficient to impair both overall sulfation and, specifically, chondroitin-4-sulfation. I further show that lithium treatment also diminishes sulfation in wild-type cells, but treating BPNT2-knockout cells with lithium does not exacerbate the effects on sulfation. This suggests that lithium's effect on sulfation is mediated through BPNT2.

The follow-up question, then, is whether BPNT2 plays an important functional role in the nervous system. We know that the loss of BPNT2 in an animal model impairs skeletal development, but the lethality of the somatic BPNT2-knockout mouse prevented investigation of the function of BPNT2 in the brain, which is (of course) where lithium acts to alleviate mania and depression. What happens when BPNT2 is lost in the nervous system? Is chondroitin sulfation decreased? Because chondroitin sulfate is crucial for perineuronal nets, are perineuronal nets affected? Because alterations in perineuronal nets are associated with neuropsychiatric disease and altered neurobehavioral traits, would loss of BPNT2 exclusively in the nervous system produce observable behavioral change? These questions motivated the work described in Chapter III. In this chapter, I describe the generation of a nervous-system specific BPNT2-knockout mouse. I demonstrate that this mouse (which is viable into adulthood and does not display gross physical

abnormalities) indeed displays impaired chondroitin-4-sulfation in brain tissues. I also describe an analysis of perineuronal nets in brain tissue from these mice, as well as a neurobehavioral analysis. While we did not observe alterations in either perineuronal nets or behavioral traits, this does not overshadow the discovery of measurable biochemical alterations in chondroitin sulfate profiles of these experimental animals.

Chapter IV of this dissertation concludes this research by addressing the implications of these findings, and describing important follow-up questions which will guide future experiments. On the whole, this work achieves two goals: 1. Establishes that BPNT2 exerts an effect on chondroitin sulfation by way of its catalytic function, which can be targeted with lithium, and 2. Demonstrates that BPNT2 activity regulates chondroitin sulfation specifically in the brain, where lithium elicits its therapeutic effects. Chapter IV then discusses important limitations, including that this work, while answering critical questions, does not establish BPNT2 as the mediator of lithium's efficacy. Future work will determine whether lithium-mediated inhibition of BPNT2 contributes at all to the alleviation of the symptoms of bipolar disorder. Independent of lithium, this work establishes BPNT2 as a critical regulator of chondroitin sulfation in the brain, which is an important contribution to the fields of both neurochemistry and glycobiology.

CHAPTER II

MECHANISM OF IMPAIRED GLYCOSAMINOGLYCAN SULFATION VIA MUTATIONS IN BPNT2

Introduction

The work contained in this chapter was published in 2021 in the *Journal of Biological Chemistry*[116].

Sulfation is a ubiquitous biological process in eukaryotes wherein a sulfate group from phosphoadenosine-phosphosulfate (PAPS, the universal sulfate donor) is transferred to a target substrate by sulfotransferase enzymes. This reaction yields the by-product 3'-phosphoadenosine-5'-phosphate (PAP), which is further catabolized to 5'-adenosine monophosphate (AMP) by the bisphosphate nucleotidases (BPNT1 and BPNT2)[18,19,53,117,118]. BPNT1 is localized to the cytoplasm, where sulfation of small molecules (such as hormones and xenobiotics) occurs[19]. BPNT2 (previously known as LPM, IMPAD1, gPAPP) is localized to the Golgi, which is the site of glycosaminoglycan (GAG) sulfation[18]. Sulfated GAGs are important components of the extracellular matrix that serve important structural roles and facilitate cell-to-cell signaling[119].

A role for BPNT2 in regulating GAG sulfation was discovered through the generation of *Bpnt2*-knockout mice. These mice die in the perinatal period, but pups have shortened limbs indicative of chondrodysplasia[18,44]. Further analysis of tissue from *Bpnt2*-knockout pups on embryonic day 18.5 (E18.5) identified a significant decrease in GAG sulfation, particularly of chondroitin-4-sulfate[18], which is necessary for the production of the cartilage matrix that precedes endochondral ossification of long bones. Subsequent studies by other groups identified an autosomal recessive human disorder caused by mutations in *BPNT2* and characterized by chondrodysplasia[46–48], reminiscent of the knockout mouse phenotype, as well as other disorders of GAG sulfation[120]. However, the mechanism by which loss or mutation of *Bpnt2* impairs GAG sulfation is not currently known.

The BPNT enzymes are members of a family of magnesium-dependent, lithium-inhibited phosphatases[16,18,117]. The precise mechanism and location of lithium-mediated inhibition of these enzymes was recently reported, establishing this family of enzymes as direct targets of lithium[17]. Lithium has been used for more than a half-century as a treatment for psychiatric disorders[1,2], but its therapeutic mechanism remains unclear[12]. Prior work suggests that lithium may modulate chondroitin sulfate[74,104], but the mechanisms by which this could occur remain unknown. BPNT2 is a known modulator of chondroitin sulfation and a direct target of lithium[18]. Thus, BPNT2 inhibition is a candidate mechanism for lithium's purported effects on chondroitin sulfate, and this inhibition may contribute to the therapeutic consequences or side effects of lithium treatment. However, previous studies have not established whether the consequences of *Bpnt2*-knockout originate from a loss of BPNT2's catalytic activity (namely, the conversion of PAP to 5'-AMP) or from another non-catalytic function. As more becomes known about non-enzymatic roles of proteins and the genes encoding them, including structural functions (e.g. formation of protein complexes and substrate channeling[121]) and signaling functions (e.g. genes containing non-coding microRNAs that regulate pertinent pathways[122]), we cannot assume that a phenotypic consequence of knocking out a gene is necessarily due to loss of a catalytic function.

The objective of this study was to investigate whether the loss of BPNT2's catalytic function underlies the chondrodysplastic phenotype observed in mice and humans. We established a model system to study BPNT2's effects on GAG sulfation *in vitro* using embryonic fibroblasts cultured from *Bpnt2*-knockout mice. We then utilized genetic complementation to examine the impact of mutations in *Bpnt2* on GAG sulfation. We studied 3 *Bpnt2* mutations, which happen to be in close proximity to the active site/metal-binding domain (1 which ablates catalytic activity, 2 which are known to cause chondrodysplasia in humans[46]). We demonstrate herein that these mutations impair GAG sulfation. We further show that treatment of MEF cultures with lithium chloride decreases GAG sulfation; these effects are dependent on the presence of BPNT2, consistent with BPNT2 being an *in vivo* target of the drug.

Methods.

MEF harvesting and culture methods. Cells were obtained from the *Bpnt2*-knockout mouse line previously generated by our laboratory and available through Jackson Laboratory mouse repository (Jackson #012922). Details regarding the development of this mosue line can be found in Frederick et al. 2008[18]. Mouse embryonic fibroblasts were obtained from E12.5 pups from heterozygous (*Bpnt2*+/-) breeding pairs. Cells from each pup were genotyped (according to Frederick et al. 2008) and cultured in DMEM +4.5 mg/dl glucose and L-glutamine (Gibco), with 10% FBS and 1% penicillin/streptomycin (basal medium). Cells were incubated at 37C with 5% CO2 for the duration of culture. Cells were immortalized by lentiviral expression of SV40 large and small T antigens—briefly, SV40 T antigen lentiviral plasmid (Addgene #22298) was packaged in HEK 293T cells using helper plasmids pMD2.G (Addgene #12259) and psPAX2 (Addgene #12260). 48 hours after transfection of all three plasmids, 3 mL of cell media was collected, filtered through a 0.45 um sterile filter, and added directly to MEF culture medium containing 8 ug/mL polybrene.

Promotion of chondrogenesis in MEFs. To enhance production of GAGs while in three-dimensional culture, basal medium was changed to chondrogenic medium: DMEM +4.5 mg/dl glucose and L-glutamine (Gibco), with 10% FBS, 1% penicillin/streptomycin, 1% ITS+ supplement (Corning), 0.1 uM dexamethasone, 200 uM ascorbic acid, and 10 ng/mL TGF-β1 (Peprotech). For chondrogenic three-dimensional pellet culture, approximately 1 million cells were seeded in sterile screw-cap 1.7-mL conical tubes and centrifuged at 500g for 5 minutes to form pellets. Cells were cultured as pellets in these tubes with the caps loosened. Pellet media (700 uL per tube) was changed 2 times weekly until cells were harvested for downstream analysis, 14 days after seeding. For lithium experiments, medium contained 10 mM LiCl or NaCl for the duration of pellet culture.

Generation of mutant Bpnt2 MEF lines. Mouse *Bpnt2* cDNA was cloned into the pBABE-puro (Addgene #1764) retroviral vector using BamHI and SalI restriction sites. The plasmid was subsequently mutagenised using traditional site-directed mutagenesis methods to generate D108A, T181P, and D175N

mutants, and mutagenesis was verified by Sanger sequencing. Retroviral vectors were each co-transfected with VSV.G (Addgene #14888) and gag/pol (Addgene #14887) vectors into HEK 293T cells using GenJet DNA transfection reagent (SignaGen). 2 mL of viral supernatant was harvested 48 hours post transfection, filtered to remove cells, and added directly to separate *Bpnt2*-KO MEF cultures containing 8 ug/mL polybrene (Invitrogen). Approximately 24 hours post viral transduction, 3 ug/mL puromycin was added to kill non-transduced cells. Cells were incubated in puromycin media for 3 days before being passaged into media without puromycin. Efficacy of transduction was confirmed by measuring *Bpnt2* mRNA and protein expression.

Quantitative PCR. RNA was collected from culture samples using Qiagen RNeasy Mini Kit, including treatment with Qiagen DNase I. cDNA was synthesized from 1 ug of RNA using iScript cDNA Synthesis Kit from Bio-Rad. PCR reaction was carried out using SsoAdvanced Universal SYBR Green Supermix (Bio-Rad) according to manufacturer instructions. Bpnt2 mRNA expression was normalized to HPRT mRNA expression to determine relative transcript enrichment. Primer sequences can be found in **Appendix A**.

Immunoblotting. Protein was collected from cells lysed in RIPA buffer with protease inhibitor (Roche). Protein extracts were passed through a 25g needle to break up DNA and quantified using BCA assay. 10 ug of total protein was loaded per lane onto a 12% SDS-PAGE gel (Bio-Rad), which was run at 100 V for 2 hours. Proteins were transferred to a 0.2 um PVDF membrane (Bio-Rad) using TransblotTurbo (Bio-Rad) at 1.3A for 7 minutes. Blots were incubated in primary antibodies (sheep anti-BPNT2, 1:1000, Invitrogen #PA5-47893; mouse anti-Actin, 1:1000, Invitrogen #MA1-744) overnight at 4C, washed 3 times in 0.1% TBS-Tween then in secondary antibodies (AlexaFluor680 anti-sheep 1:20,000; AlexaFluor800 anti-mouse 1:20,000) for 2 hours at room temperature and washed 3 times in 0.1% TBS-T. Blots were imaged on LiCor Odyssey.

PNGaseF digestion. 10 ug of protein extract were digested with PNGaseF (NEB) according to manufacturer instructions. Full digest products were subsequently run on gel as described above.

Measurement of PAP in MEFs. Briefly, approximately 1 million cell MEF pellets which had been cultured as pellet for 14 days were boiled for 3 min in 150 μL of PAP isolation buffer (50 mM glycine, pH 9.2) and disrupted mechanically with a tissue pestle. Homogenates were clarified by centrifugation at 16100 × g, 4 °C for 20 min. Then 0.2 volumes of chloroform ($CHCl_3$) was added, and samples were vortexed to mix. Samples were again centrifuged at 16100 × g, 4 °C for 20 min. The upper aqueous phase was then collected and used for the assay. To quantify PAP levels, we used a colorimetric microplate absorbance assay in which recombinant mouse SULT1A1-GST is used to transfer a sulfate group from p-nitrophenyl sulfate to 2-naphthol, using PAP as a catalytic cofactor[123]. Briefly, 20 μL of the tissue lysate was incubated with 180 μL of PAP reaction mixture [100 mM bis·Tris propane (pH 7.0), 2.5 mM β-mercaptoethanol, 2.5 mM p-nitrophenyl sulfate, 1 mM β-naphthol, and 1 μg of PAP-free recombinant mouse SULT1A1-GST]. Reactions velocities were determined by monitoring the production of 4-nitrophenol at 405 nm. Concentrations of PAP in lysates were determined by comparing reaction rates acquired from kinetic analysis to those of a series of PAP standards run concurrently on the same plate.

Dimethylmethylene blue (DMMB) assay. Media was collected from cell pellets upon harvest and kept at -20C until used for downstream analyses. After removing media, cell pellets were rinsed in 1X PBS. Pellets were then incubated in 300 ul 10mM Tris-HCl (pH 7.5) solution containing 100ug/mL proteinase K (Roche) at 60C overnight followed by 30 min at 90C to denature Proteinase K. 40 ul of each sample was loaded onto a clear-bottom 96-well plate in duplicate, and 200 ul of pH 1.5 DMMB reagent (prepared according to Zheng and Levenston 2015[124]) was added using a multichannel pipette. Absorption was immediately measured at 525 and 595 nm, and 595 measurement was subtracted from 525 to yield final reading. Quantity of sulfated GAG was determined by comparison to a standard curve of bovine chondroitin-4-sulfate (Sigma) prepared in 10mM Tris-HCl. Amount of sulfated GAG was normalized to cell count across samples. For analysis of secreted sulfated GAG in media, 60ul media was added directly to clear-bottom 96-well plate in duplicate, and readings were compared against bovine chondroitin-4-sulfate standards prepared in culture medium.

High performance liquid chromatography analysis of chondroitin-sulfate disaccharides. 1-million-cell pellets were homogenized in 400 ul GAG preparation buffer (50 mM Tris, pH 8.0, 10 mM NaCl, 3 mM $MgCl_2$), containing 4 ul of 2mg/mL Proteinase K, using tissue pestle. Sample was incubated overnight at 56C. After digest, the samples were heated at 90C for 30 minutes to denature Proteinase K. Precipitated material was separated by centrifugation. Sample buffer was changed to 0.1 M ammonium acetate, pH 7.0 by using 3 kDa Millipore concentrator by concentration/dilution until initial concentration of homogenization buffer decreased 500-times. The volume of concentrated samples was adjusted to 70 ul and 3 ul of Chondroitinase ABC (1.4 U/ml Stock solution, containing BSA, SEIKAGAKU) was added to each sample. Reaction mixture was incubated at 37C for 4 hours. After chondroitinase ABC cleavage, 130 ul of water was added. Released disaccharides were filtered through a 10 kDa concentrator. This procedure was repeated once more to improve yield. GAG samples were lyophilized using a SpeedVac at 25 °C overnight. Lyophilized samples were stored at -80C until fluorescent labeling. Labeling of disaccharides was performed with 2-aminobenzamide (2-AB) by published procedure[125]. An aliquot of 5-7 ul of labeling mixture (0.35 M 2-AB, 1 M $NaCNBH_3$ solution in 30% acetic acid in dimethyl sulfoxide) was added to lyophilized samples or disaccharide standards and the mixture was incubated for 3 hours at 65C. Labeling reaction mixtures were spotted on a strip of Whatman 3MChr paper and washed with 1 ml of acetonitrile six times. Cleaned disaccharides were eluted with three aliquots of 50, 75 and 75 ul of water by using 0.2 um centrifugal device. The analysis of labeled disaccharides was performed by HPLC. The HPLC system included Waters 515 Pumps, Waters 517plus Autosampler, Waters Pump Control Module II and Shimadzu RF-10Axl spectrofluorometer detector under Waters Empower software. Sample analysis was performed on Supelco-LC-NH_2 25 cm x 4.6 mm (Sigma). Column was equilibrated with 16 mM NaH_2PO_4 with flow rate of 1 ml/min. The samples of 50-100 ul were injected and eluted with 60 min linear gradient 16 mM – 800 mM NaH_2PO_4 with flow rate of 1 ml/min as in Yoshida et al. 1989[126]. Disaccharide elution was monitored by fluorescence at 420 nm with excitation at 330 nm. Peaks were identified by comparison to 4S, 6S, and 0S chondroitin standards (Sigma). Calculations were determined by integrating each peak on

the resultant chromatogram and calculating ratios of chondroitin species. Chromatograms were analyzed by Empower software.

Generation of an *in vitro* model system to analyze GAG sulfation.

BPNT2 is a Golgi-resident protein which has a demonstrated role in Golgi-localized sulfation reactions. The major components of this sulfation pathway are illustrated in **Figure 9A**. Loss of BPNT2 is known to impair the upstream sulfation of GAGs, but previous studies have not established whether this effect stems from the loss of BPNT2 catalytic activity or another non-catalytic function. To investigate this mechanism, we first sought to generate an immortalized cell system to study the function of BPNT2 with respect to alterations in GAG sulfation. We elected to use embryonic fibroblasts because: 1. These cells were easily attainable from the *Bpnt2*-knockout mouse line developed by our laboratory (Jackson #012922); 2. MEFs derive from mesenchyme, which give rise to connective tissues which are primarily responsible for GAG synthesis *in vivo*, and 3. MEFs can be readily immortalized to facilitate genetic manipulations and prolonged study. MEFs were harvested on embryonic day 12.5 of pregnancies resulting from *Bpnt2*-heterozygous crosses. *Bpnt2* wild-type (WT) and knockout (KO) MEFs obtained from littermates were then immortalized by lentiviral expression of SV40 T antigens. Absence of BPNT2 in these lines was further confirmed by analyzing mRNA expression using quantitative PCR (**Figure 9B**), and by immunoblotting for BPNT2 protein (**Figure 9C**). For our analyses, the most relevant property of the cells was their ability to synthesize and secrete sulfated GAG, the most abundant of which is chondroitin sulfate. The cells primarily responsible for chondroitin sulfate production *in vivo* are chondrocytes, but chondrocytes are not well suited to long-term culture involving repeated passaging. However, chondrocytic properties can be induced in cells of mesenchymal origin by maximizing cell-cell contact in cultures and supplementing media with certain growth factors[127]. This method of culturing immortalized MEFs allowed us to investigate the effects of BPNT2 on GAG sulfation *in vitro*, without having to repeatedly harvest primary cells, and allowed us to manipulate gene expression to generate stable cell lines expressing mutant versions of

BPNT2. *Bpnt2*-KO MEFs display decreased total GAG sulfation as measured by dimethylmethylene blue (DMMB) assay assay (**Figure 9D**), normalized to cell number. KO MEFs also secrete fewer sulfated GAGs into the culture medium (**Figure 9E**). We were also interested in whether these cells displayed measurable alterations in PAP level, which might be expected in the absence of BPNT2, but we did not detect any difference in PAP between WT and KO cells (**Figure 9F**). Nonetheless, the alterations in sulfation in immortalized MEFs recapitulate impairments in sulfation seen in *Bpnt2*-KO mice. We therefore deemed this an appropriate model for our investigations.

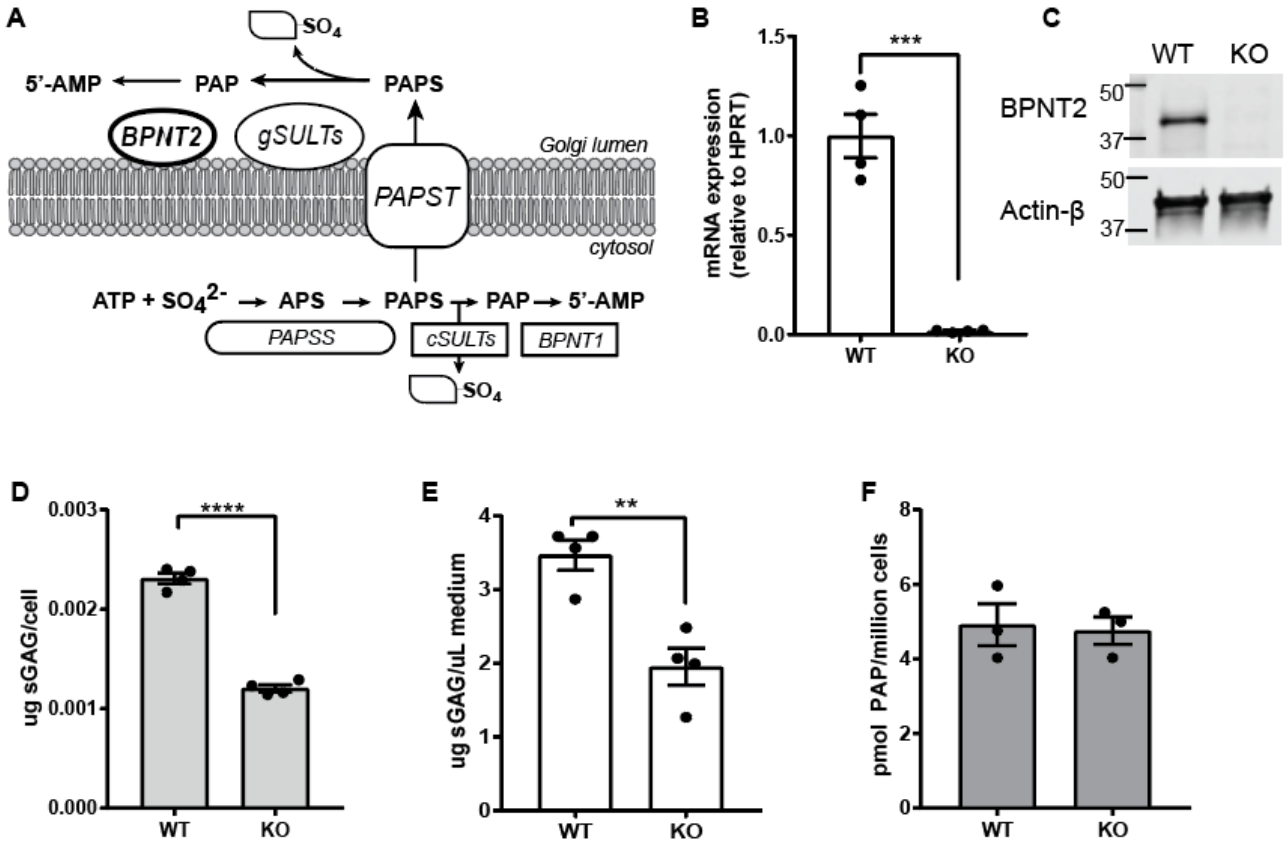

Figure 9. Loss of Bpnt2 impairs glycosaminoglycan sulfation, but does not alter PAP level. A. Illustration of intracellular sulfation pathways, wherein BPNT2 hydrolyzes PAP, a by-product of sulfation, to AMP. B. Absent expression of Bpnt2 mRNA (***p=0.0001) in Bpnt2-KO MEFs as determined by quantitative PCR and C. absent BPNT2 protein in Bpnt2-KO MEFs, as determined by western blot. D. Bpnt2-KO MEFs exhibit decreased levels of both intracellular (left, ****p<0.0001) and E. secreted (right, **p=0.0034) sulfated glycosaminoglycans, as determined by DMMB assay. F. Bpnt2-KO MEFs do not show changes in PAP level relative to WT cells. Bars show mean +/-SEM. Significance analyses are results of unpaired student's t test (2-sided). ATP: adenosine triphosphate, APS: adenosine phosphosulfate, PAPSS: PAPS synthase, PAPS: 3',5'-phosphoadenosine phosphosulfate, PAP: 3',5'-phosphoadenosine phosphate, AMP: 5'-adenosine monophosphate, cSULTs: cytosolic sulfotransferases, PAPST: PAPS transporter, gSULTs: Golgi-resident sulfotransferases.

***Bpnt2* mutations that cause chondrodysplasia are located near the metal-binding/catalytic domain.**

Murine BPNT2's three-dimensional core structural motif (which defines the family of lithium-inhibited phosphatases) has been simplified and represented graphically in **Figure 10A**. This region of BPNT2 is highly conserved across species[46]. Three aspartic acid (D) residues provide a negatively-charged environment conducive to the binding of positively-charged metal cations: divalent magnesium is a necessary cofactor for phosphate hydrolysis, whereas monovalent lithium inhibits this hydrolysis[17]. Mutation of the first aspartic acid which composes this pocket ($D110^{human}/D108^{mouse}$) to alanine renders family members catalytically inactive[17,128]. Interestingly, two missense mutations in *Bpnt2* localized near this locus are known to cause chondrodysplasia in humans[46,47]. A summary of these mutations is shown in **Figure 10B**. These mutant versions of *Bpnt2* have previously been predicted to have effects on the enzymatic activity, due to localization near the presumed active site, based on structural comparisons to BPNT1 (PDB: 2WEF)[46], as no structure has yet been determined for BPNT2. Indeed, one of these mutations, $D177N^{human}/D175N^{mouse}$, is in another of the three aspartic acid residues that compose the negatively-charged pocket, while $T183P^{human}/T181P^{mouse}$ is located just 6 amino acids further downstream.

A

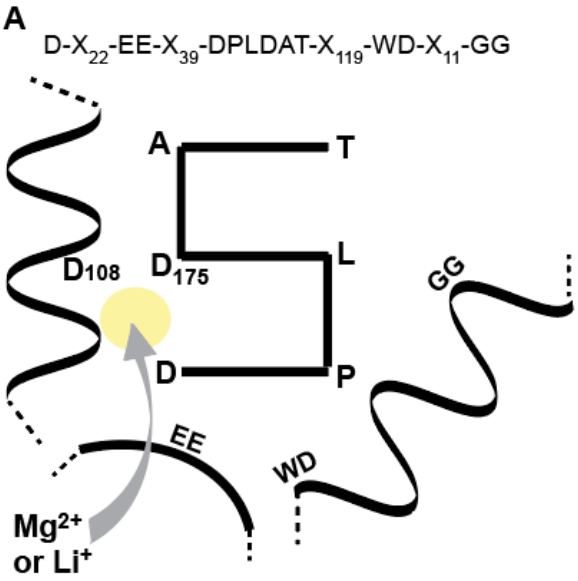

B

Mutation	Putative consequence	Citation
D110A^{human}/ D108A^{mouse}	Catalytic inactivity	Dollins et al. 2020, Hale et al. 2020
T183P^{human}/ T181P^{mouse}	Chondrodysplasia in humans	Vissers et al. 2011, Nizon et al. 2012
D177N^{human}/ D175N^{mouse}	Chondrodysplasia in humans	Vissers et al. 2011, Nizon et al. 2012

Figure 10. Summary of *Bpnt2* mutations in relation to the metal-binding/catalytic domain. A. Graphical simplification of metal-binding/catalytic domain defining magnesium-dependent/lithium-inhibited phosphatases; numbered amino acids are those in murine *Bpnt2*; yellow circle represent metal-binding pocket, where magnesium binds under active conditions and lithium binds under inhibitory conditions. B. Table showing mutations investigated herein, which are in close proximity to the metal-binding structural motif.

Expression of *Bpnt2* mutants revealed a novel N-glycosylation locus on chondrodysplasia-associated mutant *Bpnt2*^{D175N}.

We next utilized site-directed mutagenesis and a retroviral expression system to generate MEF lines which exclusively express mutant forms of murine *Bpnt2*: *Bpnt2*^{D108A}, *Bpnt2*^{T181P}, and *Bpnt2*^{D175N}. We also generated a wild-type *Bpnt2*-complemented cell line (KO+WT) as a control, as well as WT and KO lines transduced with empty vector (EV) control retrovirus. Success of viral transduction was determined by western blotting for BPNT2 (**Figure 11A**). Surprisingly, BPNT2^{D175N} mutant protein appeared to be partially shifted upward, displaying a second band of higher molecular weight relative to other BPNT2 isoforms. Native BPNT2 is localized to the Golgi, and like other membrane-associated proteins, it contains an N-glycosylation consensus sequence (N-X-S/T^{129}) at N259^{human}/N257^{mouse}**.** The novel asparagine in BPNT2^{D175N} made us inquire as to whether an additional N-glycosylation locus was generated by this mutation, as a secondary glycosylation event could explain the increased molecular weight of the detected protein. **Figure 11B** shows a section of cDNA for both human and mouse *Bpnt2*. In both human and mouse, the mutation of this aspartic acid to asparagine results in the generation of an N-glycosylation consensus sequence: N-A-T. To test whether the heavier band was indeed due to an additional N-glycosyl modification, protein extracts from cell lines were treated with PNGaseF. Native BPNT2's one glycosylation site at N259^{human}/N257^{mouse} is cleaved with PNGaseF treatment, resulting in a downward shift of the protein. Treatment of BPNT2^{D175N} with PNGaseF cleaves both N-glycosyl groups, eliminating the double band and producing a protein of the same size as those seen in all other PNGaseF-treated cell lines (**Figure 11C**). The generation of this additional N-glycosylation site has not been previously described in association with this mutation.

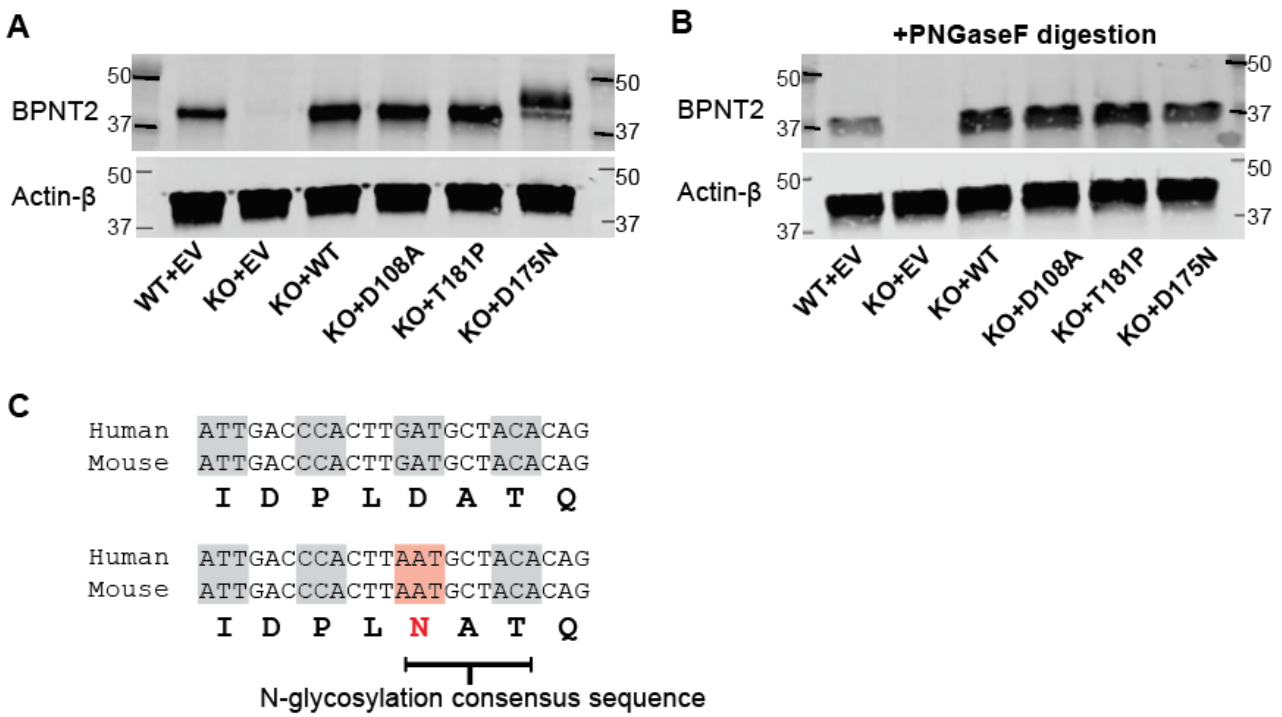

Figure 11. Generation of mutant *Bpnt2* MEF lines. A. Blot for BPNT2 and actin on protein extracted from *Bpnt2* MEF lines; arrows in D175N lane denote 2 bands, representing singly and doubly glycosylated protein. B. A selection of *Bpnt2* sequence from mouse and human *Bpnt2*. In both, the D175N/D177N mutation results in generation of an N-glycosyl consensus sequence. C. Blot of proteins extracted from MEF lines, treated with PNGaseF to remove N-glycosyl groups; PNGaseF removes both glycosyl groups, resulting in a single band for BPNT2-D175N. Note that all bands shift downward with PNGaseF, as native murine BPNT2 has one N-glycosylation site at N257.

Wild-type *Bpnt2* rescues impairments in overall sulfated GAGs, while mutant *Bpnt2* constructs do not.

We next sought to examine the consequences of these mutations on GAG sulfation. To facilitate the synthesis of GAGs and extracellular matrix components, we cultured three-dimensional cell pellets for each MEF line over a period of 7-14 days. Media was collected from pellets immediately prior to harvest. Total sulfated GAG from cell pellets was quantified using a colorimetric dimethylmethylene blue (DMMB) assay, then normalized to cell count. These results are depicted in **Figure 12A**. We observed a significant decrease in sulfated GAG in the knockout line, which was rescued by expressing wild-type *Bpnt2*. In contrast, expression of *Bpnt2*^{D108A} did not rescue this decrease, nor did *Bpnt2*^{T181P} or *Bpnt2*^{D175N}. Level of secreted sulfated GAG in media (collected at pellet harvest) was also measured, and are shown in **Figure 12B**. Again, we observed a significant decrease in secreted/extracellular sulfated GAG in the knockout line, which was not rescued with expression of *Bpnt2*^{D108A}, but did appear to be rescued with expression of other *Bpnt2* mutants.

Mutant *Bpnt2* constructs do not rescue specific alterations in chondroitin sulfation.

We next used high-performance liquid chromatography (HPLC) to evaluate specific alterations in chondroitin sulfation. Isolated glycosaminoglycans can be digested by chondroitinase enzymes to yield individual sulfated chondroitin disaccharides. These disaccharides can then be fluorescently labeled and resolved by HPLC to identify specific sulfation moieties. Previous work has demonstrated that *Bpnt2*-KO mouse embryos exhibit impairments in overall levels of 4-sulfated disaccharide (Δdi-4S, or 4S) that correspond with increased levels of unsulfated chondroitin (Δdi-0S, or 0S)[18]. We observed a decrease in the ratio of 4S to total chondroitin disaccharides (4S+6S+0S) in KO+EV MEFs relative to WT+EV MEFs, which was in large part rescued by complementing WT *Bpnt2* back into the line (KO+WT). However, this decrease was not rescued by expression of catalytic-dead *Bpnt2* or either chondrodysplasia-associated

mutant *Bpnt2* (**Figure 12C**). Interestingly, we observed a correspondent increase in the ratio of chondroitin-6-sulfate (Δdi-6S, or 6S) in KO cells, which was partially restored with WT complementation, and which remained elevated in mutant *Bpnt2* lines (**Figure 12D**). The increase in 6S has not been previously reported in association with *Bpnt2*-KO. However, overall ratios of unsulfated chondroitin are increased in KO cells, restored to near-WT levels with back-complementation, and significantly elevated in mutant *Bpnt2* lines (**Figure 12E**). These changes are summarized in **Figure 12F**.

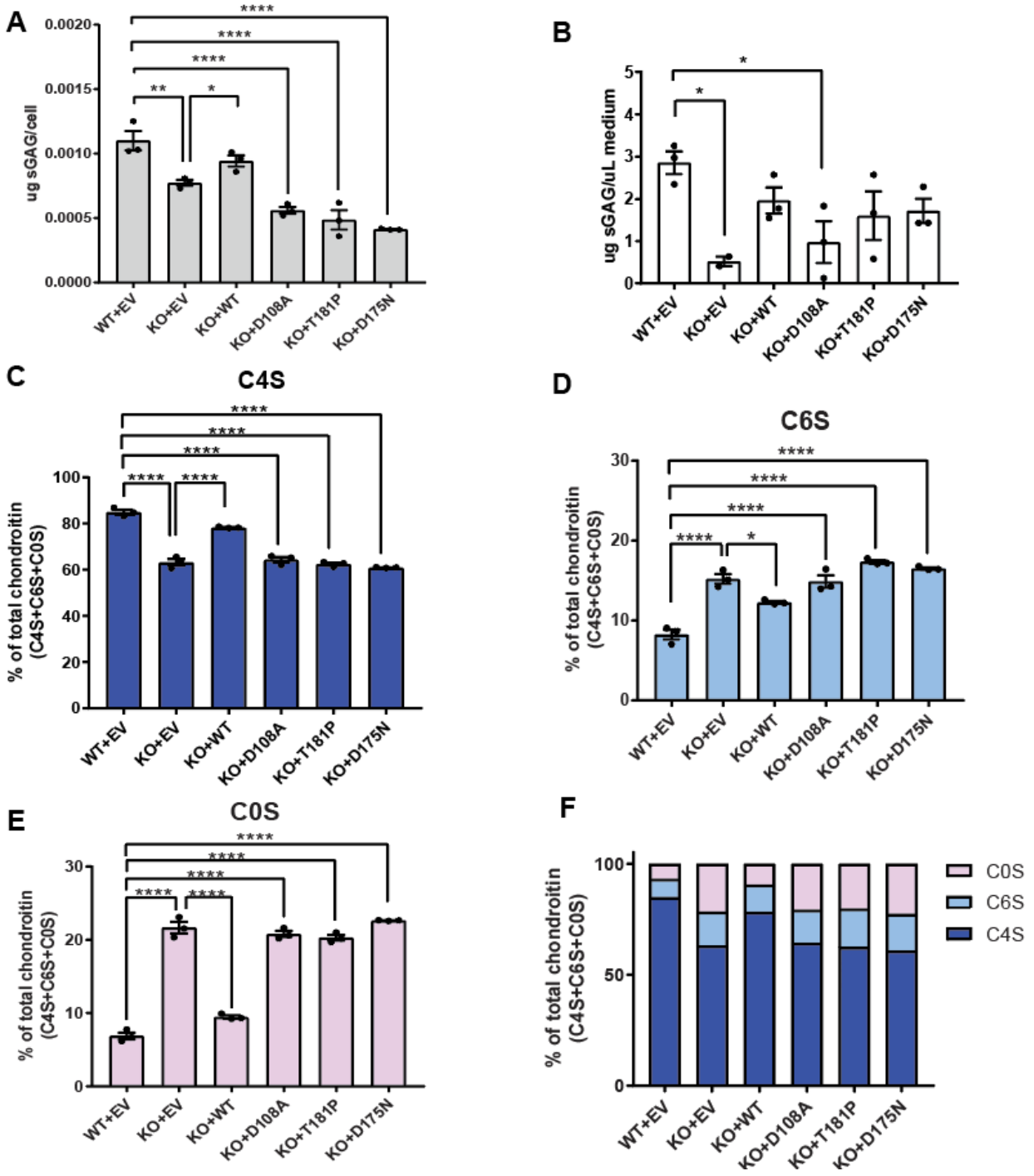

Figure 12. MEFs expressing mutated Bpnt2 exhibit decreased sulfated glycosaminoglycans, including decreased chondroitin-4-sulfate. A. Sulfated GAG levels in Bpnt2-mutant cells, as measured by DMMB assay. B. Sulfated GAG levels in medium of Bpnt2-mutant cell cultures, as measured by DMMB assay. Alterations in C. chondroitin-4-sulfate, D. chondroitin-6-sulfate, and E. unsulfated chondroitin levels in Bpnt2-mutant cell cultures, as measured by chondroitin disaccharide HPLC. F. Summary of alterations in chondroitin-sulfation profile across Bpnt2-mutant lines. Error bars show mean +/- SEM. Denoted significance indicates results of Tukey's post-hoc tests after significant one-way ANOVA. *p<0.05, **p<0.01, ***p<0.001, ****p<0.0001.

Lithium decreases intracellular and extracellular sulfated GAG, including chondroitin-4-sulfate.

The discovery that the loss of BPNT2 catalytic function underlies impairments in overall GAG sulfation is particularly relevant because BPNT2 is potently inhibited by the psychopharmacologic agent lithium[18]. To test whether lithium impairs total GAG sulfation, we treated both WT and *Bpnt2*-KO MEFs with 10 mM lithium chloride (LiCl), using an equal concentration of sodium chloride (NaCl) as a control. We observed a decrease in intracellular GAG sulfation in lithium-treated WT MEFs, as compared to sodium-treated WT MEFs (**Figure 13A**). Loss of *Bpnt2* in cells treated with sodium resulted in a marked reduction in GAG sulfation similar to WT MEFs treated with lithium (**Figure 13A**). Importantly, treatment of *Bpnt2*-KO MEFs with lithium did not further reduce sulfation of GAGs (**Figure 13A**). Likewise, we observed a significant reduction in sulfation of GAGs secreted into the culture medium in lithium-treated as compared to control sodium-treated samples (**Figure 13B**). Again, *Bpnt2*-KO MEFs treated with LiCl did not exhibit any additional decrease in secreted sulfated GAG.

We next used HPLC to resolve chondroitin disaccharides in WT and *Bpnt2*-KO cells treated with lithium, and we observed a significant decrease in 4S (**Figure 13C**) in LiCl-treated WT cells alongside significant increases in 6S (**Figure 13D**), and 0S (**Figure 13E**). *Bpnt2*-KO cells did not exhibit these alterations when treated with LiCl, demonstrating that lithium does not have any additional effects on chondroitin sulfation patterns in cells that lack *Bpnt2*. Collectively, the similarity between sulfation patterns in LiCl-treated cells and *Bpnt2*-KO cells can be appreciated in **Figure 13F** and are consistent with a role for *Bpnt2* in mediating lithium's effect on GAG sulfation. As a follow-up to these experiments, we evaluated whether lithium treatment altered PAP level in WT or *Bpnt2*-KO MEFs, and we did not observe significant alterations (**Appendix B**), nor did we observe alterations in expression of key members of the chondroitin sulfation pathway (**Appendix C**).

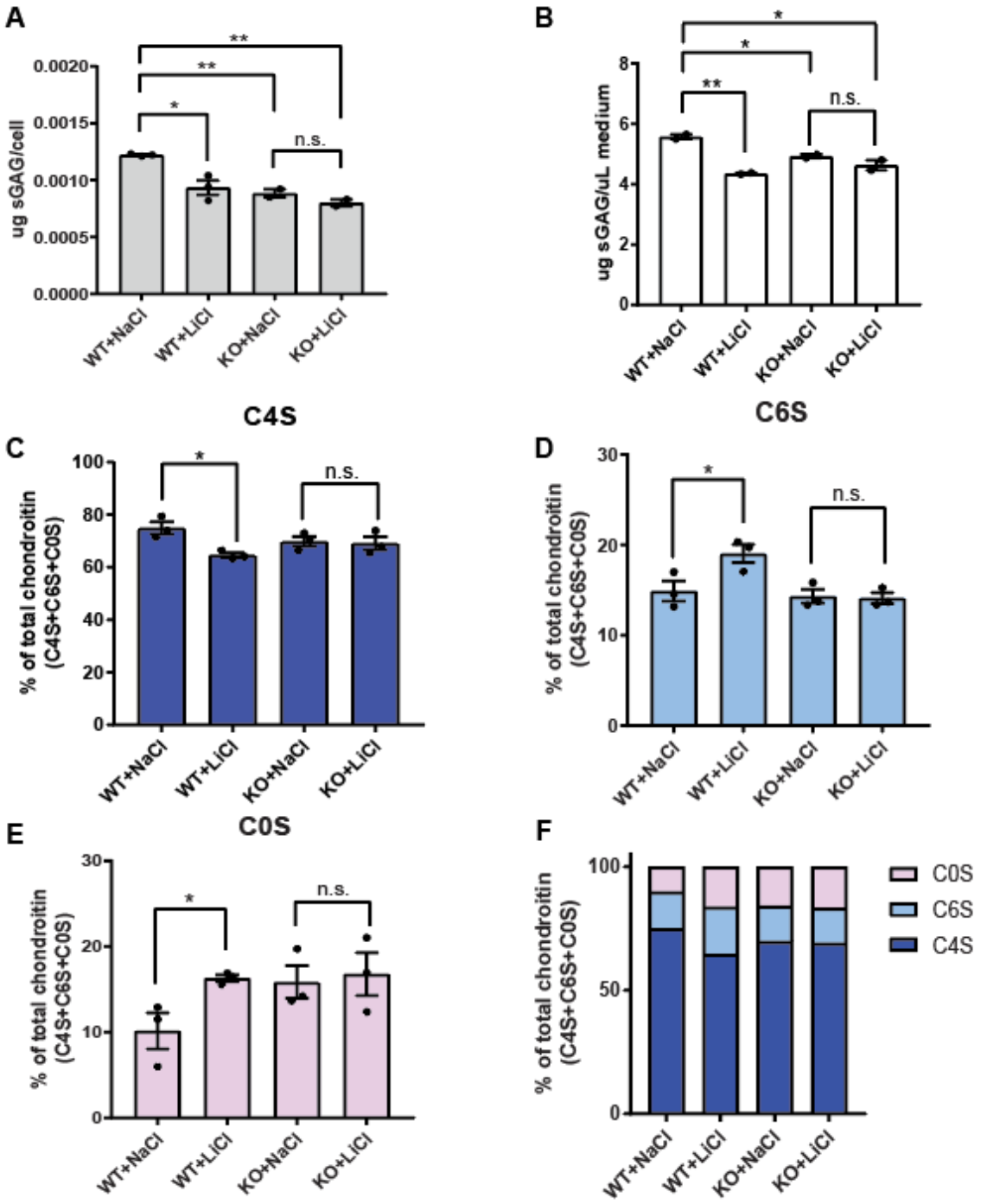

Figure 13. Lithium treatment decreases overall GAG sulfation, including chondroitin-4-sulfation, in wild-type cells, but not Bpnt2-knockout cells. A. Sulfated GAG analyses performed on cells treated with 10 mM NaCl or LiCl. B. Sulfated GAG analysis performed on culture medium of cells treated with 10mM NaCl or LiCl. Alterations in C. chondroitin-4-sulfate, D. chondroitin-6-sulfate, and E. unsulfated chondroitin levels in treatment groups, as measured by chondroitin disaccharide HPLC. F. Summary of alterations in chondroitin-sulfation profile across treatment groups. Error bars show mean +/- SEM. Denoted significance indicates results of two-sided student's t-test. *$p<0.05$, **$p<0.01$, n.s. = not significant.

Discussion.

In this work, we utilize an *in vitro* fibroblast model to demonstrate that knockout of a lithium-inhibited enzyme, BPNT2, impairs overall GAG sulfation (especially chondroitin-4-sulfation), and that this impairment stems specifically from a loss of the catalytic activity of BPNT2, as a catalytic-dead construct does not rescue these impairments. We also evaluated two missense mutations in BPNT2 which are associated with chondrodysplasia in humans and are adjacent to the core catalytic motif. We therefore suspect that these mutations interfere with BPNT2 catalysis. Vissers et al., who initially described these mutations, posited that the mutation of threonine 183 to proline in human *BPNT2* would produce a helix-breaker effect, which would alter secondary BPNT2 structure[46]. They also suggested that the loss of the charged aspartic acid side chain in the D177N mutation would affect the binding of metal cations at the active site[46]. In this work, we recapitulated impairments in chondrogenesis caused by these two missense mutations, and we further report that the D(177/175)N mutation generates an N-glycosylation consensus sequence in both human and mouse *Bpnt2*. N-glycosylation is a protein modification that occurs co-translationally[130], which may affect protein folding. Additional kinetic and protein biochemical assays will be important in understanding precisely how these mutations influence BPNT2 catalysis.

As previously reported, we identified decreases in chondroitin-4-sulfate (4S) and increases in unsulfated chondroitin (0S) as a result of the loss of BPNT2, which we also attribute to disrupted BPNT2 catalytic activity. Of note, we also identified *increases* in chondroitin-6-sulfate (6S), which were not previously identified in tissues (whole embryo preparations) from *Bpnt2*-KO mice. Contrasting roles for 4S and 6S have been described, wherein 4S is more abundant in developing cartilage, while 6S is more abundant in mature and articular cartilage[131]. In the nervous system, 6S is more abundant in the developing brain, where it promotes synaptic plasticity, whereas 4S is more abundant in the adult brain, where it limits plasticity and promotes synaptic stability[78,79]. Importantly, decreases in 6S have been identified in the brains of human patients with bipolar disorder[74] and lithium treatment is associated with increases in 6S[74], thought to be corrective. We now present evidence that inhibiting the catalytic activity of a molecular target of lithium can increase 6S levels in a mammalian cell model. The increase in 6S could be a result of shunting

or flux given the reductions in 4S and significant elevation of 0S. It is notable that GAG sulfation overall was still decreased in response to the loss of BPNT2 activity, as measured by DMMB assay, which is not specific for any species of sulfated GAG.

While our results clearly indicate that BPNT2 activity is required for altering sulfated GAG/chondroitin sulfation, we are not able to distinguish exactly how this is accomplished. Is it through altering the production of 5-AMP or through defects in the consumption of PAP? In our previous studies of BPNT2's cytosolic counterpart BPNT1, we found clear evidence of PAP accumulation in mutant animals and cells, which resulted in metabolic toxicity[53,118,128]. An accumulation of PAP with BPNT2-knockout could feedback-inhibit sulfotransferases[132], impairing GAG sulfation. However, we did not observe an increase of PAP in *Bpnt2*-KO cells. It may be that PAP only needs to locally accumulate within the Golgi, where BPNT2 is located, in order to effectively inhibit Golgi-resident sulfotransferases. Meanwhile, BPNT1 is still metabolizing PAP in the cytosol. The relative proportion of PAP accumulation in the Golgi to the total amount of PAP in the cell may be too small for such a difference to be detectable by our assays. Isolating only the PAP that is located within the Golgi-lumen has thus far proven to be a technically complex undertaking, as traditional subcellular fractionation studies by our group have not yielded measurable PAP levels in Golgi-associated fractions. If, on the other hand, the phenotypes observed in BPNT2 mutants are due to failure to produce 5'-AMP, then it is possible that PAPS transport into the Golgi is impaired. Studies of the PAPS transporter, which moves the sulfate donor PAPS from the cytosol into the Golgi, indicate it is a member of the antiporter family of proteins that may exchange PAPS for 5'-AMP[133,134]. The diminished production of 5'-AMP in the Golgi resulting from loss of BPNT2 activity could prevent PAPS from entering the Golgi and being utilized for sulfation. Notably, we did not observe alterations in expression of the PAPS transporters or chondroitin sulfotransferases in WT or KO cells treated with lithium (**Appendix C**), but there are other mechanisms by which the functions of these proteins could be altered. Further work will be required to determine which, if any, of these mechanisms underlies the observed sulfation impairments.

In this work, we also show that treatment of MEFs with 10mM lithium chloride alters sulfation, and that this alteration is dependent on the presence of BPNT2. Prior work suggests that lithium negatively

regulates chondroitin sulfate proteoglycans which would otherwise prevent axon regeneration after spinal cord injury[104]. It has also been shown that lithium promotes neurite outgrowth[112,135], a process which is normally restricted by chondroitin sulfate[110]. Consistent with these prior findings, we identified decreases in sulfated GAG when MEFs were treated with lithium. *Bpnt2*-KO MEFs displayed impaired GAG sulfation in a manner that mimicked WT MEFs treated with lithium, and did not exhibit additive decreases in sulfation with lithium treatment. When specifically analyzing chondroitin disaccharides, we identified alterations in WT MEFs treated with lithium consistent with the effects previously identified in *Bpnt2*-KO MEFs, but we did not identify additional alterations when *Bpnt2*-KO MEFs were treated with lithium. These data suggest that lithium's effects on chondroitin sulfation are mediated by BPNT2.

The field of psychopharmacology has yet to reach a consensus on how lithium remains so effective in treating bipolar disorder, despite a vast array of other recent psychopharmacologic advances. While this work does not decisively establish lithium's mechanism of action, it does present evidence that loss of the catalytic activity of known target of lithium, BPNT2, mediates decreases in sulfated GAG, and observable lithium-mediated decreases in sulfation may be due to the loss of BPNT2. On the whole, this work provides a basis for an interesting new hypothesis into how lithium could elicit its psychiatric effects.

Additional data pertaining to this chapter can be found in the Appendix. **Appendix D** demonstrates effective immortalization of MEFs using SV40 T antigen, as described in the methods. **Appendix E** shows that C4ST1 does no co-immunoprecipitate with BPNT2. **Appendix F** shows that treatment of wild-type BPNT2 with PNGaseF cleaves a native N-glycosylation locus, confirming that BPNT2 is N-glycosylated at N257. **Appendix G** shows that all mutant lines localize appropriately to the Golgi apparatus. **Appendix H** shows that chondrogenic culture methods of MEFs enhance production of sulfated GAGs.

CHAPTER III

CONSEQUENCES OF THE LOSS OF BPNT2 IN THE CENTRAL NERVOUS SYSTEM

Introduction.

Bisphosphate nucleotidase enzymes metabolize the by-products of intracellular sulfation reactions[117]. These enzymes are also inhibitory targets of lithium, the first-line pharmacologic agent for bipolar disorder[136]. Despite an unclear mechanism of action and a vast side effect profile, lithium is an important therapeutic agent that is continually being investigated as a treatment for an array of psychiatric and neurologic disorders [108,137–139]. Understanding the biochemical consequences of lithium treatment on the bisphosphate nucleotidases therefore could shed light on the pharmacologic mechanisms or toxic effects of lithium.

Bisphosphate nucleotidase 2 (BPNT2, previously known as IMPAD1[47], JAWS[44], GPAPP[18]) is a Golgi-resident nucleotidase[18]. BPNT2 acts downstream of Golgi-localized sulfotransferases, which utilize the sulfate group from phosphoadenosine phosphosulfate (PAPS) to yield sulfated products and the by-product phosphoadenosine phosphate (PAP). BPNT2 then catalyzes the breakdown of PAP to adenosine monophosphate (AMP)[18]. Golgi-sulfotransferases are primarily carbohydrate sulfotransferases which sulfate glycosaminoglycans[39]. Loss of BPNT2 disrupts sulfation of glycosaminoglycans (GAGs), especially chondroitin-4-sulfate[18], which is a major component of cartilage. *Bpnt2*-knockout mice exhibit a chondrodysplastic phenotype, characterized by shortened long bones and joint abnormalities[18,43,44] due to impaired bone and cartilage development. These mice die in the perinatal period, likely due to pulmonary insufficiency secondary to an underdeveloped ribcage. Notably, an autosomal recessive human chondrodysplasia caused by mutations in *BPNT2* has also been identified[46,47], implicating BPNT2 as an important regulator of chondrogenesis in humans.

We recently reported that the defects in sulfation seen with *Bpnt2*-knockout stem from a loss of the catalytic activity of the enzyme, and that human disease-associated mutations are located in close proximity to the catalytic motif[116]. We also demonstrated that lithium impairs sulfation *in vitro* in a BPNT2-dependent

fashion[116]. Given lithium's relevance in the treatment of neuropsychiatric disease, we wanted to investigate whether the loss of BPNT2 in the nervous system could elicit alterations in brain chemistry or behavior.

There is substantial evidence suggesting chondroitin-sulfate is involved in neuronal function[79,141]. Multiple populations of neurons are surrounded by a specialized extracellular matrix known as the perineuronal network: an emerging interest for many neuroscientists[54–58]. Perineuronal nets (PNNs) consist primarily of condensed chondroitin sulfate, with chondroitin-4-sulfate being the major species in the adult brain and chondroitin-6-sulfate comprising the minority[60]. PNNs are generally seen as barriers to neuroplasticity[61], and may be involved in stabilization of neural circuitry (such as that underlying long-term memories[62,63] and addiction[54]). Throughout postnatal development, plasticity tends to decrease; this correlates with an increase in PNN density over time[64–66,79]. Given the "restrictive" nature of PNNs, they are also believed to negatively regulate neurite outgrowth and axon extension. Classically, PNNs surround inhibitory interneurons[68], and they are thus thought to regulate the balance between excitatory and inhibitory signaling in the brain—a balance which is disrupted in acute mania and psychosis[61,69]. Interestingly, alterations in perineuronal nets have been reported in psychiatric diseases[55,61,73], including schizophrenia[66] and bipolar disorder[74].

Previous work has shown that disrupting the formation of chondroitin alters PNN morphology and rodent behavioral characteristics, including performance on tasks of motor coordination, activity, startle response, and object recognition memory[96,97,142]. These traits coincided with decreases in PNNs throughout the brain, as identified by immunohistochemistry[96,97,142].

Given BPNT2's role in chondroitin sulfation, we hypothesized that BPNT2 is important for the sulfation of GAGs (especially chondroitin-4-sulfate) in the brain, and for the development of PNNs and PNN-associated behaviors. Because of the perinatal lethality of the conventional *Bpnt2*-knockout mouse, we have previously been unable to study BPNT2 in the adult mouse brain. In this work, we generated a nervous system-specific *Bpnt2*-knockout mouse (*Bpnt2*$^{fl/fl}$ Nestin-Cre), which is viable and does not display gross physical abnormalities. We then analyzed GAG sulfation patterns, including the chondroitin sulfation profile. We utilized the common histological PNN marker, *Wisteria floribunda* agglutinin

(WFA) to analyze PNN histology, and subjected experimental animals to a selection of neurobehavioral assays which are associated with PNNs.

Methods.

Animals. All animal experiments were carried out in compliance with the Vanderbilt University Institutional Animal Care and Use Committee (IACUC). Mice were housed on a 12hr light/dark cycle. All assessments were conducted during the light phase. The mouse strain used for this research project, C57BL/6N-Bpnt2tm1a(KOMP)Wtsi/Mmucd, RRID:MMRRC_048210-UCD, was obtained from the Mutant Mouse Resource and Research Center (MMRRC) at University of California at Davis, an NIH-funded strain repository, and was donated to the MMRRC by The KOMP Repository, University of California, Davis; Originating from Ramiro Ramirez-Solis, CSD. Tm1a (targeted allele) animals were bred with mice expressing FLP recombinase (Jackson Labs, #011065) to generate *Bpnt2*-floxed (tm1c, conditional allele) mice. Floxed mice were bred with mice expressing Nestin-driven (Jackson Labs, #003771) Cre recombinase to knock out *Bpnt2* (producing the tm1d, null allele) in the nervous system (neurons and astrocytes). Mice were identified by ear-tagging and tail DNA was used for genotyping. Genotyping primers to detect *Bpnt2* alleles were: Bpnt2.Fwd: TTAGAAAGGTCCCAGGTTGGCTTCC and Bpnt2.Rev: AAGCTCTGGTACATGCCTACCATCC. For wild-type allele, the primers yielded a 684 bp product, and for conditional allele, primers yielded a 786 bp product. Nestin-Cre genotyping was performed with primer sequences available from Jackson Labs. Nestin-Cre was kept heterozygous in all mice used for breeding and experiments. All mice used for experiments were of mixed C57BL/6N and C57BL/6J background. Both male and female mice were used; sex differences were not detected in molecular or behavioral results. All analyses were run on adult mice between 12 and 18 weeks of age.

Quantitative PCR. Mice were sacrificed by decapitation. Brains were extracted and one hemisphere was dissected and tissues were flash frozen on dry ice. RNA was extracted using Qiagen RNeasy Mini Kit using Qiagen DNase I. cDNA was synthesized from 1 ug of RNA using iScript cDNA synthesis kit (Bio-Rad). PCR reaction was carried out using SsoAdvanced Universal SYBR Green Supermix (Bio-Rad)

according to manufacturer instructions. *Bpnt2* mRNA expression (F: 5'-CGCCGATGATAAGATGACCAG-3' and R: 5'-GCATCCACATGTTCCTCAGTA-3') was normalized to *Hprt* mRNA expression (F: 5'- GCAGTACAGCCCCAAAATGG-3' and R: 5'-ATCCAACAAAGTCTGGCCTGT-3') to determine relative transcript enrichment.

Immunoblotting. Protein was collected from cells lysed in RIPA buffer with protease inhibitor (Roche). Protein extracts were quantified using BCA assay and passed through a 25g needle to break up DNA. 10 ug of total protein was loaded per lane onto a 12% SDS-PAGE gel (Bio-Rad), which was run at 100 V for 90 minutes. Proteins were transferred to a 0.2 um PVDF membrane (Bio-Rad) using TransblotTurbo (Bio-Rad) at 1.3A for 7 minutes. Blots were incubated in primary antibodies (sheep anti-BPNT2, 1:1000, Invitrogen #PA5-47893; mouse anti-Actin, 1:1000, Invitrogen #MA1-744) overnight at 4C, washed 3 times in 0.1% TBS-Tween then in secondary antibodies (AlexaFluor680 anti-sheep 1:20,000; AlexaFluor800 anti-mouse 1:20,000) for 2 hours at room temperature and washed 3 times in 0.1% TBS-T. Blots were imaged on LiCor Odyssey and analyzed using ImageJ.

Glycosaminoglycan analysis. Flash-frozen brain regions (10-15 mg of tissue) were homogenized in 400 ul GAG preparation buffer (50 mM Tris, pH 8.0, 10 mM NaCl, 3 mM $MgCl_2$) using tissue pestle. 50 ul of homogenate was taken and centrifuged at 12000rpm, and supernatant was used to determine soluble protein content using Pierce BCA assay. 4 ul of Proteinase K (2 mg/ml) was added to the remaining homogenate, and sample was incubated overnight at 56C. After digest, the samples were heated at 90C for 30 minutes to denature Proteinase K. Precipitated material was separated by centrifugation. **Dimethylmethylene blue (DMMB) assay.** An aliquot of supernatant was used for DMMB analysis of total sulfated GAGs. 20 ul of each sample was added to a 96-well clear-bottomed microplate in duplicate. 200 ul of pH 1.5 DMMB reagent (prepared according to Zheng and Levenston[124]) was added to each well using a multichannel pipette. Absorption was immediately measured at 525 and 595 nm, and 595 measurement was subtracted from 525 measurement to yield final reading. Quantity of sulfated GAG was determined by comparison to a standard curve of bovine chondroitin-4-sulfate (Sigma) prepared in GAG preparation buffer. Amounts of sulfated GAG were normalized to protein concentration. **High-performance liquid**

chromatography (HPLC). Sample buffer was changed to 0.1 M ammonium acetate, pH 7.0 by using 3 kDa Millipore concentrator by concentration/dilution until initial concentration of homogenization buffer decreased 500-times. The volume of concentrated samples was adjusted to 70 ul and 3 ul of Chondroitinase ABC (1.4 U/ml Stock solution, containing BSA, SEIKAGAKU) was added to each sample. Reaction mixture was incubated at 37C for 4 hours. After chondroitinase ABC cleavage, 130 ul of water was added. Released disaccharides were filtered through a 10 kDa concentrator. This procedure was repeated once more to improve yield. GAG samples were lyophilized using a SpeedVac at 25 °C overnight. Lyophilized samples were stored at -80C until fluorescent labeling. *2-AB derivatization*. Labeling of disaccharides was performed with 2-aminobenzamide (2-AB) by published procedure (4). An aliquot of 5-7 ul of labeling mixture (0.35 M 2-AB, 1 M $NaCNBH_3$ solution in 30% acetic acid in dimethyl sulfoxide) was added to lyophilized samples or disaccharide standards and the mixture was incubated for 3 hours at 65C. Labeling reaction mixtures were spotted on a strip of Whatman 3MChr paper and washed with 1 ml of acetonitrile six times. Cleaned disaccharides were eluted with three aliquots of 50, 75 and 75 ul of water by using 0.2 um centrifugal device. *HPLC.* The analysis of labeled disaccharides was performed by HPLC. The HPLC system included Waters 515 Pumps, Waters 517plus Autosampler, Waters Pump Control Module II and Shimadzu RF-10Axl spectrofluorometer detector under Waters Empower software. Samples analysis performed on Supelco-LC-NH_2 25 cm x 4.6 mm (Sigma). Column was equilibrated with 16 mM NaH_2PO_4 with flow rate of 1 ml/min. The samples of 50-100 ul were injected and eluted with 60 min linear gradient 16 mM – 800 mM NaH_2PO_4 with flow rate of 1 ml/min as in (5). Disaccharide elution was monitored by fluorescence at 420 nm with excitation at 330 nm. Peak identities were determined by running Δdi-0S, Δdi-6S, and Δdi-4S standards (Sigma) prior to running samples. Chromatograms were analyzed by Empower software.

Immunofluorescence. Mice were sacrificed by decapitation. Brains were extracted and one hemisphere was flash frozen in OCT compound then sectioned into 30-um-thick slices on a Leica cryostat at -20C. Tissue slices were fixed in 4% paraformaldehyde for 15 minutes then rinsed twice in 1X PBS containing 0.3% Triton X-100 (PBS-T), 10 minutes per wash. Slides were blocked in blocking buffer (PBS-

T containing 10% goat serum) for 30 minutes at room temperature, then covered in primary antibody (WFA-biotin conjugate, 1:500, Sigma #L1516) in blocking buffer diluted 1:3 in PBS-T and incubated for 1.5 hours at room temperature. Slides were then washed in diluted blocking buffer 3 x 5 minutes, then covered in secondary antibody (Streptavidin-AlexaFluor488, 1:500) in diluted blocking buffer for 1 hour at room temperature in a humidified container, protected from light. Slides were washed in diluted blocking buffer 3 x 5 minutes. Coverslips were affixed to slides using ProLong™ Gold Antifade Mountant with DAPI (Life Technologies) and allowed to dry overnight before imaging the following day. Images were taken at 4X and 20X magnification on a Nikon Eclipse Ti inverted fluorescent microscope. 20X images were taken in z-stacks of 25 images, 0.4 um apart. Summed-stack images were used for PNN analysis using commercially available PipsqueakAI software (Rewire Neuro). PNNs from approximately 8 fields of view from each of 2 slices of tissue (per region analyzed) were measured from each animal (3-7 animals per genotype). PNN fluorescence measurements from each animal were averaged, and individual animal averages were used for statistical calculations between genotypes[143].

In vivo behavior (in order of testing). **Elevated zero maze.** Mice were placed individually on the open arm of an elevated zero maze (Med Associates) and behavior was tracked using AnyMaze software for 5 minutes. **Open field activity analysis.** Open-field behavior was examined for 45 min using the infrared photobeam Med Associates system for mice. **Novel object recognition.** Mice were habituated to a Y-maze for 2 days (5 minutes per day). On training day, 2 identical objects were placed in each of the 2 non-starting arms of the maze, and the mouse was allowed to explore objects for 5 minutes. On testing day, one of the two objects was replaced with a novel object, and the mouse was allowed to explore objects for 5 minutes. The 5 minute training and testing phases were recorded using AnyMaze software, and time spent interacting with objects was measured by 2 independent scorers, blinded to mouse genotype. Scores were averaged, and averages were used to determine discrimination ratios. **Accelerating rotarod.** Mice were placed on a cylinder (~3 cm in diameter) which initially rotates at 4 rpm and accelerates to 40 rpm. The latency to falling off the rotarod was measured as an index of motor coordination (maximum trial length of 300 seconds). Trials were repeated 3 times daily, over a course of 3 days. **Tail suspension.** Mouse tails

were taped to a vertical aluminum bar connected to a strain gauge inside a commercial tail suspension test chamber (Med Associates). Motion was recorded over 6 minutes. **Startle/Prepulse inhibition.** The startle response to 40-ms 120-dB white noise and its inhibition by a prepulse was examined using the Acoustic Startle Reflex Package for mice from Med Associates. Mice were placed in a clear plastic cylinder (~5 cm diam) within a ventilated sound-attenuating enclosure, and given 5 minutes to acclimate. Startle stimulus was presented in the presence or absence of a 20-ms prepulse presented at 70, 76, 82, or 88 dB, 100-ms before the stimulus. The maximal startle amplitude recorded during a 65-msec sampling window after stimulus presentation was used as the dependent variable. Stimuli were presented in a total of 54 trials, and startle response or prepulse inhibition were averaged across trials.

Generation of a nervous system-specific *Bpnt2*-knockout mouse.

An illustration of the knockout strategy is shown in **Figure 14A**. The second exon of the *Bpnt2* gene was flanked by loxp sites, generating a "floxed" (fl) allele. When bred with a Nestin-Cre mouse, the second exon was excised, preventing functional protein expression in nervous system tissues. A section of cerebral cortex was used to confirm near-absence of *Bpnt2* mRNA expression (**Figure 14B**) and BPNT2 protein expression (**Figures 14C, 14D**) in $Bpnt2^{fl/fl}$ Nestin-Cre mice relative to $Bpnt2^{fl/fl}$ and heterozygous $Bpnt2^{fl/+}$ Nestin-Cre controls. $Bpnt2^{fl/fl}$ Nestin-Cre animals were viable and did not display gross physical abnormalities.

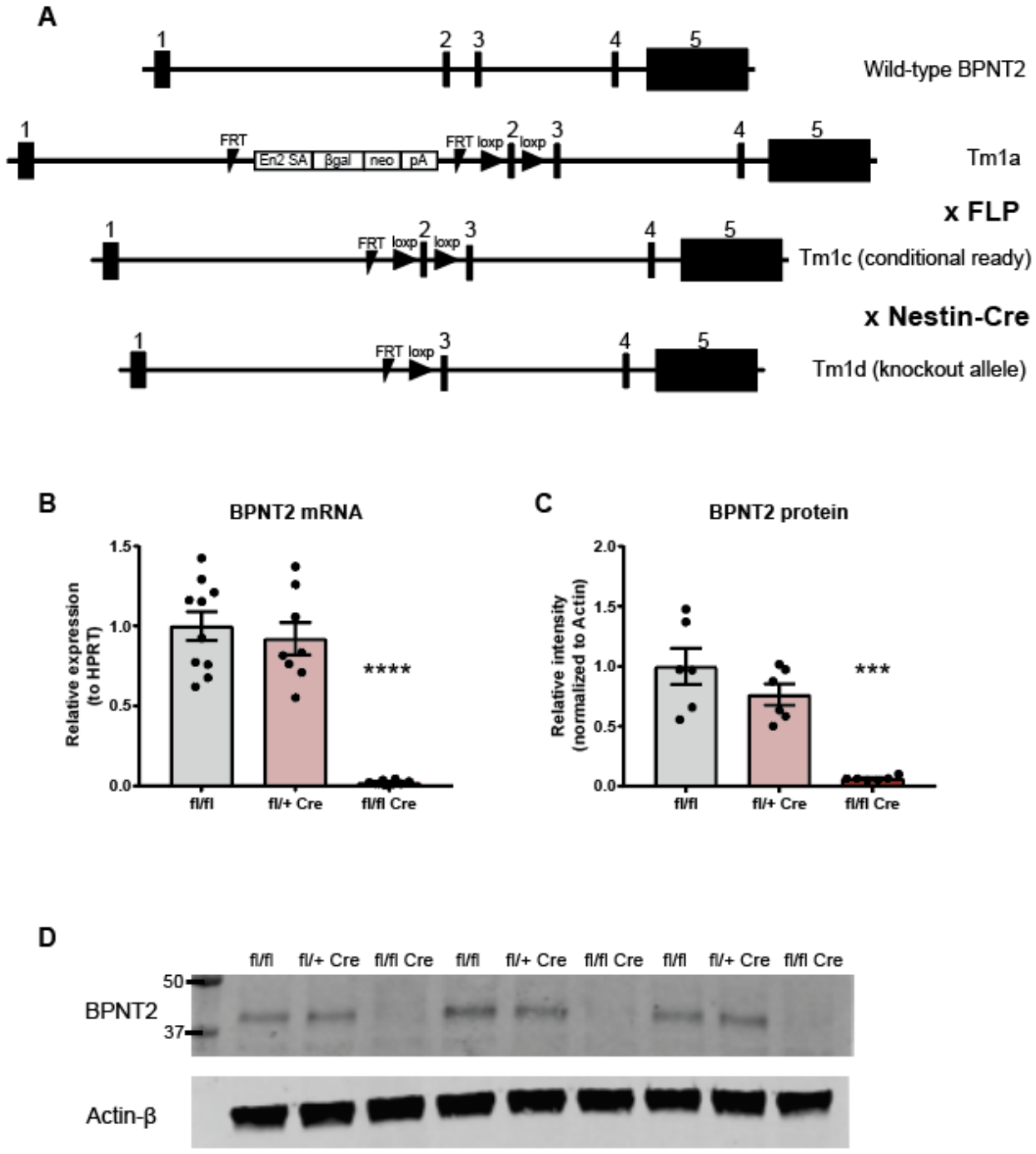

Figure 14. Generation of conditional and nervous system-specific *Bpnt2*-knockout mouse. A. Schematic of knockout strategy. Tm1a mice obtained from UC-Davis KOMP and bred with FLPo-10 mice (Jackson #011065) to generate Tm1c (floxed) mice, which were then crossed with Nestin-Cre mice (Jackson #003771) to yield knockout (Tm1d allele) in nervous system tissues (neurons and astrocytes). B. mRNA expression of *Bpnt2* in cortical brain tissue. C. Quantification of protein expression from western blot and D. Western blot showing BPNT2 protein expression in cortical brain tissue. P-values are results of one-way ANOVA: ***p<0.001, ****p<0.0001.

Glycosaminoglycan sulfation in brain tissue from *Bpnt2*$^{fl/fl}$ Nestin-Cre mice is impaired.

We next investigated whether overall GAG sulfation was altered in the brains of *Bpnt2*$^{fl/fl}$ Nestin-Cre mice. We analyzed total GAG sulfation in two brain regions associated with perineuronal nets: visual cortex[144] and hippocampus[73]. Total sulfated GAG was measured in tissue homogenates using dimethylmethylene blue assay, and sulfated GAG content was normalized to total protein concentration. As predicted, *Bpnt2*$^{fl/fl}$ Nestin-Cre mice exhibited decreased sulfated GAG (per protein content) in both visual cortex and hippocampus relative to Nestin-Cre-only, *Bpnt2*$^{fl/fl}$, and *Bpnt2*$^{fl/+}$ Nestin-Cre controls (**Figures 15A, 15B**).

Chondroitin sulfation patterns are altered in brain tissue from *Bpnt2*$^{fl/fl}$ Nestin-Cre mice.

To more specifically analyze sulfated moieties, we next sought to analyze alterations in chondroitin sulfation patterns in the visual cortex and the hippocampus. Because we did not identify alterations in overall sulfation among the three control groups (Nestin-Cre-only, *Bpnt2*$^{fl/fl}$, and *Bpnt2*$^{fl/+}$ +Nestin-Cre), we elected to analyze only *Bpnt2*$^{fl/fl}$ and *Bpnt2*$^{fl/fl}$ Nestin-Cre brain tissues. Following digestion of samples with chondroitinase ABC, chondroitin disaccharides were fluorescently labeled and resolved by high-performance liquid chromatography (HPLC). We analyzed ratios of each of the major species of chondroitin (0S, 4S, and 6S) to the total peak area of all three species. Using this approach, we identified clear and signficant decreases in 4S disaccharide (Δdi-4S), which corresponded with a significant increase in unsulfated disaccharide (Δdi-0S). These findings recapitulate those seen in the cartilage extracts from germline *Bpnt2*-knockout mice[18]. Interestingly, we also observed an *increase* in 6S disaccharide (Δdi-6S), which was not previously observed in tissues from the germline *Bpnt2*-knockout mouse. Results from visual cortex are shown in **Figure 15C**, and results from hippocampus are shown in **Figure 15D**. Representative HPLC traices from visual cortex samples are shown in **Figures 15E, 15F**.

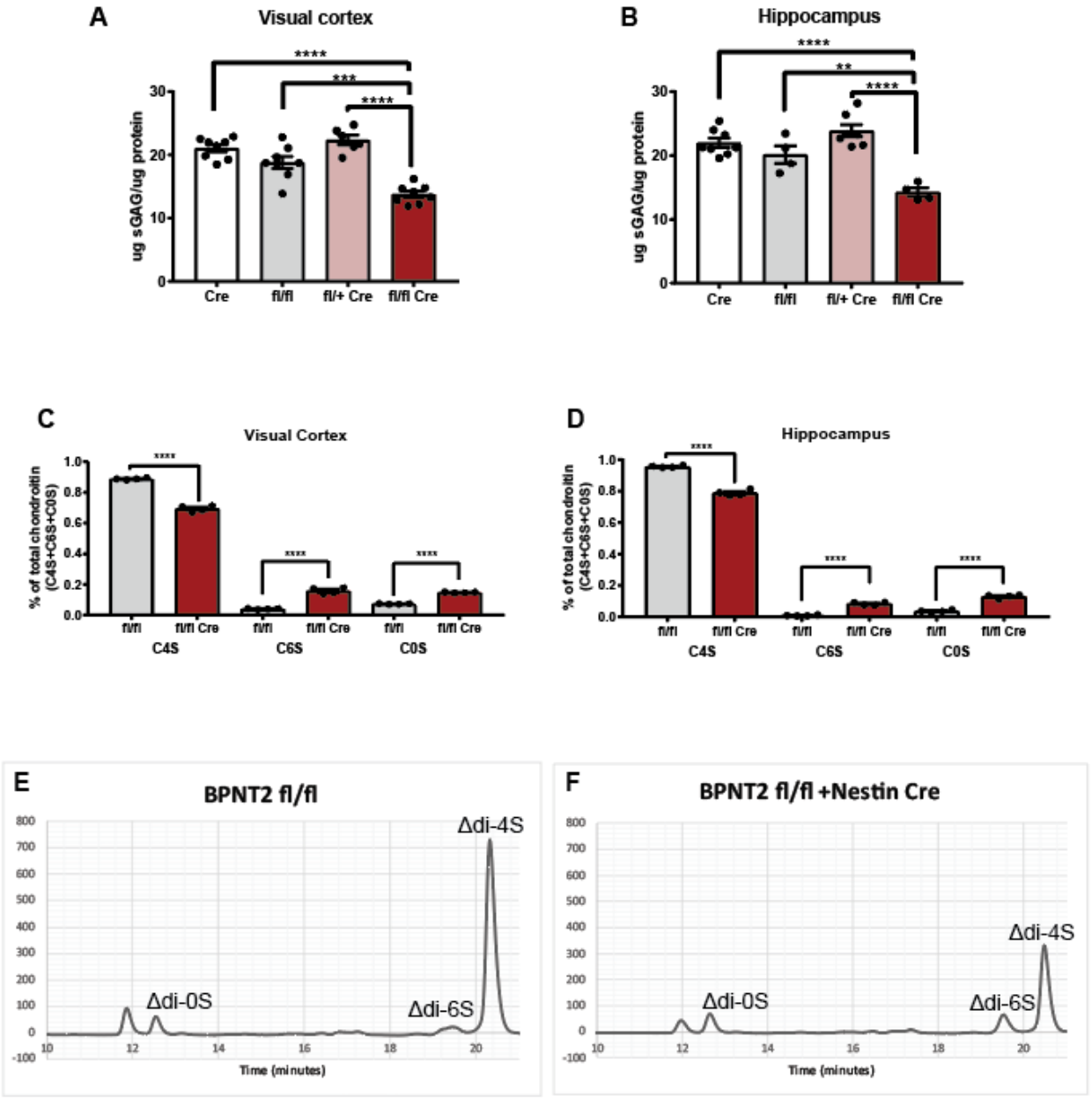

Figure 15. *Bpnt2*$^{fl/fl}$ Nestin-Cre mice exhibit altered glycosaminoglycan sulfation in brain tissues. Quantification of total GAG sulfation in A. visual cortex tissue and B. hippocampal tissue using DMMB assay. C. Quantification of chondroitin sulfate disaccharides in visual cortex tissue as measured by HPLC. D. Quantification of chondroitin sulfate disaccharides in hippocampal tissue as measured by HPLC. E. and F. Representative HPLC traces from chondroitin disaccharide HPLC performed on cortical tissue. Δdi-0S: unsulfated chondroitin disaccharide, Δdi-6S: chondroitin-6-sulfate disaccharide, Δdi-4S: chondroitin-4-sulfate disaccharide. P-values denote results of Tukey's post-hoc analyses following significant one-way ANOVA. **p<0.01, ***p<0.001, ****p<0.0001.

Perineuronal nets (as measured by WFA staining) are not grossly altered in *Bpnt2*$^{fl/fl}$ Nestin-Cre mice.

Other groups have examined genetic manipulations that affect the development of chondroitin sulfate proteoglycans in the brain and have identified alterations in perineuronal nets[96,97], as measured by conventional histological methods (namely, WFA staining). We therefore decided to evaluate perineuronal net staining in cortical and hippocampal regions of *Bpnt2*$^{fl/fl}$ Nestin-Cre mouse brain relative to *Bpnt2*$^{fl/fl}$ controls. Tissues sections were stained with WFA and then analyzed using commercially available PipsqueakAI software, which automatically detects perineuronal nets and reports fluorescence intensity relative to background staining[145]. We did not observe gross alterations in WFA fluorescence (**Figure 16A**), nor did we observe significant alterations in PNN staining measurements in cortical (**Figure 16B**) or hippocampal (**Figure 16C**) regions. As a secondary measure, we also analyzed the number of PNNs detected by PipsqueakAI per field of view in both cortical (**Figure 16D**) and hippocampal regions (**Figure 16E**), and we did not observe significant differences in number of PNNs.

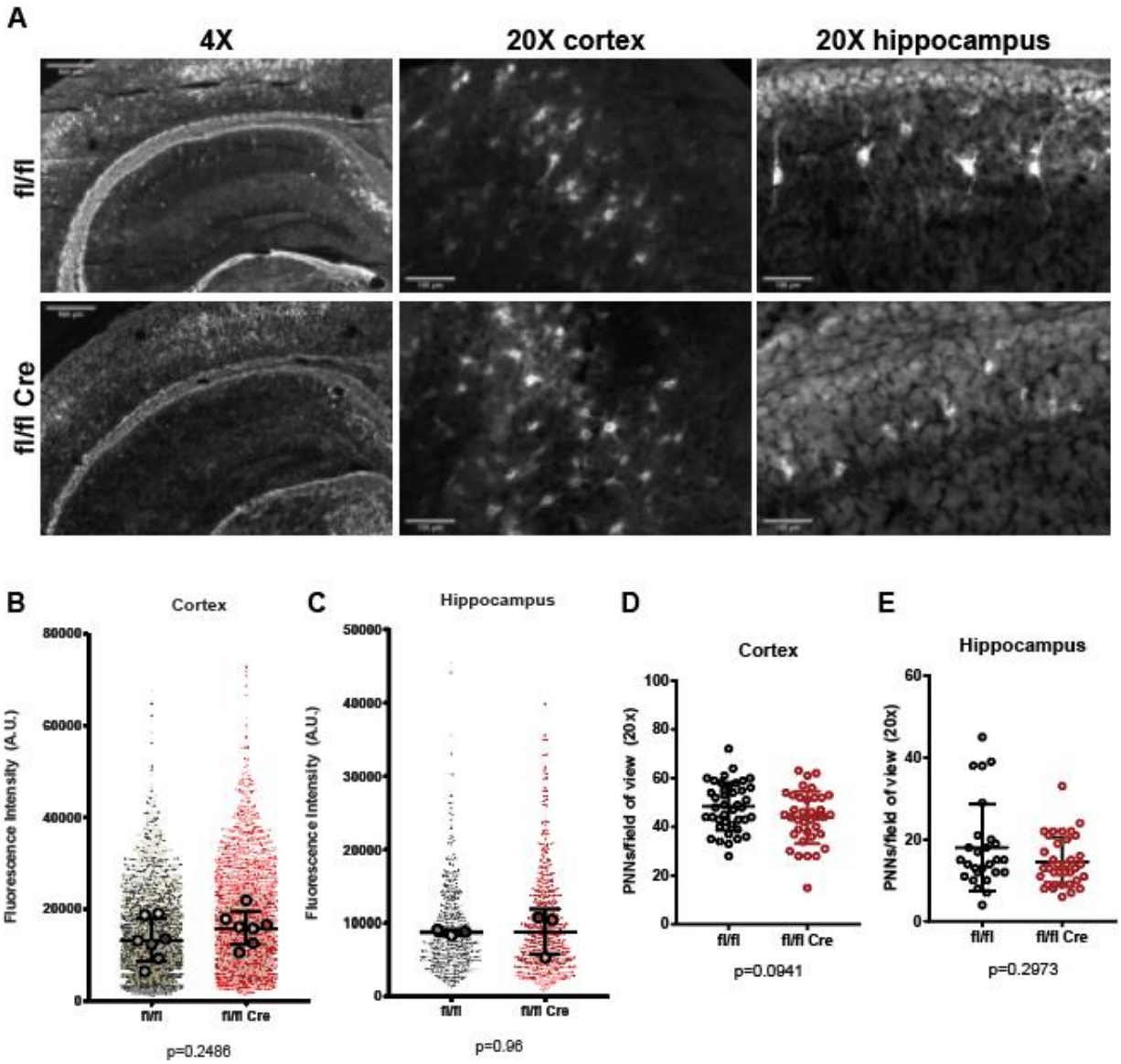

Figure 16. *Bpnt2*$^{fl/fl}$ Nestin-Cre mice do not exhibit gross alterations in perineuronal net staining. A. Representative PNN staining from *Bpnt2*$^{fl/fl}$ and *Bpnt2*$^{fl/fl}$ Nestin-Cre animals. Quantification of perineuronal net intensity from tissue sections from B. cortical and C. hippocampal brain regions using Pipsqueak AI. D. and E. Analysis of number of PNNs detected per tissue section using Pipsqueak AI software. For B/C, p-values indicate results of two-sided student's t-test. For D/E, p-values indicate results of Mann-Whitney U-test.

***Bpnt2*$^{fl/fl}$ Nestin-Cre mice do not exhibit alterations in behavior across a selection of behavioral tests.**

As a final analysis of the consequences of loss of BPNT2 in the nervous system, we subjected mice to a series of neurobehavioral experiments, which have been previously associated with alterations in PNNs, including open-field activity analysis[96], novel object recognition[97,142], accelerating rotarod[96], and acoustic startle response[96]. We also performed an elevated zero maze assessment of anxiety-like behaviors as a control experiment, and the tail-suspension test. (Altered performance on the tail suspension test is associated with lithium treatment[146], which we deemed relevant as BPNT2 is a direct inhibitory target of lithium.) However, we did not observe statistically significant alterations in behavioral performance between *Bpnt2*$^{fl/fl}$ and *Bpnt2*$^{fl/fl}$ Nestin-Cre mice on any of the assays performed (**Figures 17A-17G**).

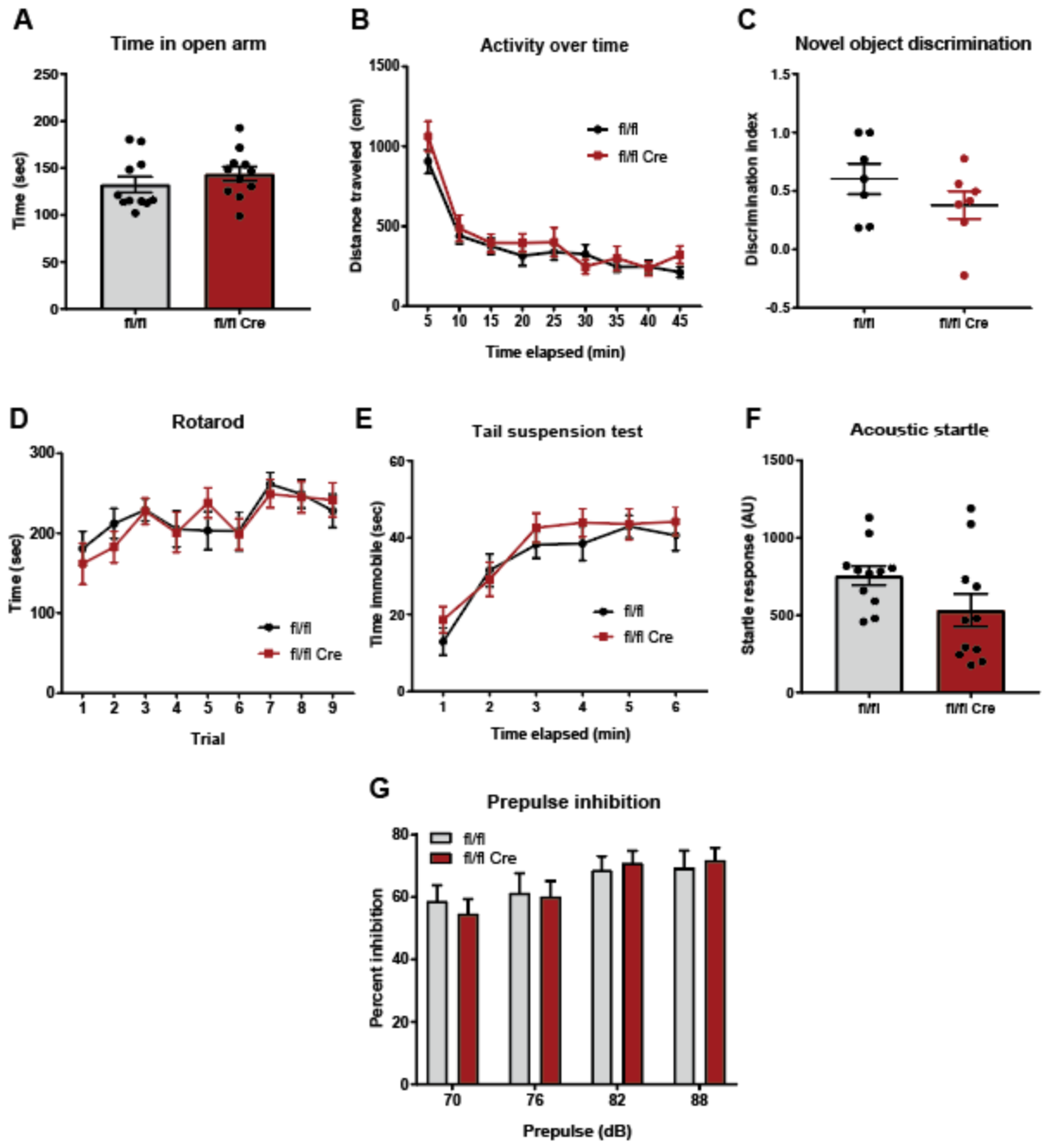

Figure 17. *Bpnt2*$^{fl/fl}$ Nestin-Cre mice do not exhibit gross abnormalities on key behavioral assays. A. Elevated zero maze. B. Open field activity assessment, performed over 45 minutes. C. Novel object recognition. D. Accelerating rotarod motor learning assay. E. Tail suspension test. F. Acoustic startle. G. Prepulse inhibition.

Discussion.

BPNT2 is an enzyme that breaks down the by-product of glycosaminoglycan sulfation reactions. Loss of BPNT2 impairs chondroitin-4-sulfation, which is an important component of the extracellular matrix across a variety of tissues. BPNT2 is also an inhibitory target of lithium, which is a widely prescribed mood stabilizer[2] used to treat bipolar disorder, which motivates us to investigate the function of BPNT2 specifically in the brain. In this work, we report the generation of a nervous system-specific *Bpnt2*-knockout mouse, which is viable and does not portray obvious phenotypic aberrations. This is in contrast to our previous reports of severe skeletal defects in the germline *Bpnt2*-knockout mouse, which lead to perinatal lethality[18], presumably due to pulmonary insufficiency. We now report that absence of functional BPNT2 in the nervous system does not result in lethality, and was not the cause of lethality in the germline knockout mouse.

Global knockout of BPNT2 impairs total-body chondroitin sulfation[18]. The effect of this impairment in cartilage is abnormal long bone development (chondrodysplasia)[18,46,47], which can be observed in the human disorder characterized by homozygous BPNT2 mutations. To our knowledge, in-depth studies of the neurocognitive profiles of human patients with homozygous *BPNT2* mutations have not been reported, but there is reason to suspect that brain function could be affected. Of the six published cases of homozygous *BPNT2* mutation in humans, one patient was noted to have intellectual disability[47].

Because chondroitin sulfate is an abundant glycosaminoglycan in the central nervous system, we sought to determine whether the loss of BPNT2 specifically in the nervous system would alter chondroitin sulfate biology in the brain. Analysis of brain tissue from *Bpnt2*$^{fl/fl}$ Nestin-Cre mice indeed demonstrated diminished chondroitin-4-sulfation, which corresponded to an increase in unsulfated chondroitin, as expected. However, we also identified a correspondent increase in chondroitin-6-sulfate. While such an increase was not identified in the cartilage of somatic *Bpnt2*-knockout mice, we did observe this increase in fibroblast cell lines taken from the *Bpnt2*-knockout mouse[147]. Chondroitin-6-sulfate is the next most abundant form of chondroitin sulfate after chondroitin-4-sulfate, and the two have been show to have opposing roles in regulating synaptic plasticity[78]. Chondroitin-6-sulfate promotes plasticity and is the

predominant species in the brain in early life, while chondroitin-4-sulfate inhibits plasticity and is more abundant in adult brain[78].

What is especially noteworthy about our observed increase in chondroitin-6-sulfate in the brains of our experimental animals is that changes in chondroitin-6-sulfate have been identified in the brains of human patients with bipolar disorder[74]. Specifically, decreases in chondroitin-6-sulfate were identified in patients with bipolar disorder relative to healthy controls, and exposure to lithium appeared to have a corrective effect; that is, lithium was associated with an increase in chondroitin-6-sulfate, as measured by immunohistochemistry[74]. We now report that the loss of a lithium-inhibited enzyme increases chondroitin-6-sulfation in the brain. Because we have previously shown that alterations in sulfation seen with *Bpnt2*-knockout stem from a loss of the enzyme's catalytic activity, we postulate that lithium-mediated inhibition of BPNT2 could underlie the effects on chondroitin-6-sulfate seen with lithium treatment of human patients.

Given the biochemical alteration of the chondroitin sulfation profile seen in brain tissue from *Bpnt2*$^{fl/fl}$ Nestin-Cre mice, it is interesting that we did not observe differences in PNN histology. Previous work has analyzed the consequences of nervous system-specific deletion of the proteoglycan core protein aggrecan, which plays a critical role in glycosaminoglycan biology[97]. Somatic homozygous mutations in aggrecan cause skeletal malformations as well as perinatal lethality[148], very similar to what is seen with homozygous *Bpnt2*-knockout. Nervous system-specific deletion of aggrecan (using the Nestin-Cre driver) completely abolishes WFA staining in the brain[97]. When undertaking the studies presented in this work, we considered it possible that we would observe a similarly dramatic effect in a nervous system-specific *Bpnt2* knockout. The somatic deletion of another gene relevant for chondroitin synthesis (CSGalNacT1, an enzyme critical for sugar chain synthesis), results in milder skeletal abnormalities, but still produces measurable disruption of WFA staining in brain tissue as well as behavioral anomalies[96]. The absence of such changes in a nervous system-specific *Bpnt2* knockout mouse is therefore an unexpected finding that could indicate a unique role of the BPNT2 enzyme. We can measure significant alterations in cerebral chondroitin sulfation that coincide with loss of BPNT2, but these are not so severe as to result in concomitant alterations in the PNN number or intensity. Nevertheless, chondroitin-sulfates (especially

chondroitin-4-sulfate) are one of the major components of adult PNNs[79]; where, then, is the loss of chondroitin-4-sulfate occurring?

Not all chondroitin-4-sulfate in the brain is localized to the WFA-reactive perineuronal nets themselves. Much of the chondroitin-4-sulfate in the brain is present in the loose extracellular matrix, which is not aggregated around specific cells. It could be that this loose matrix, which does not have as robust of a marker as condensed, pericellular PNNs do, is where the decrease in chondroitin-4-sulfate is physiologically relevant. To again contrast BPNT2 with other proteins that are important for chondroitin biology, the loss of aggrecan and CSGalNacT1 would be expected to affect the chondroitin species regardless of their locus of sulfation. However, this work and our prior work[147] suggest that of the three predominant species of chondroitin-sulfate, only chondroitin-4-sulfate is decreased with loss of BPNT2, while the ratios of chondroitin-6-sulfate and unsulfated chondroitin to total chondroitin are both elevated. While the increase in unsulfated chondroitin is to be expected, the increase in chondroitin-6-sulfate could be an attempt at a compensatory response. As WFA does not stain a specific sulfation moiety, this could explain why we did not observe alterations in WFA staining. There is also some work which suggests that the WFA-reactive, condensed PNNs are richer in chondroitin-6-sulfate and unsulfated chondroitin than the loose extracellular matrix is[149], despite the major component of condensed PNNs still being chondroitin-4-sulfate. It may be that the degree of decrease in chondroitin-4-sulfate, coupled with the correspondent increase in chondroitin-6-sulfate, is not sufficient to alter PNNs histologically.

The lack of apparent alteration in PNNs could, in part, explain why we did not observe behavioral alterations in *Bpnt2*$^{fl/fl}$ Nestin-Cre mice. If the PNNs are robust to the changes we observed in chondroitin-4-sulfate, then we would expect them to function normally, and behaviors associated with PNNs would be unchanged in the absence of BPNT2. However, the selection of behavioral assays used in this work is by no means exhaustive. One analytical metric that is strongly associated with PNNs is ocular dominance plasticity, which is the ability to shift which eye is dominant by occluding vision in the dominant eye. This propensity for plasticity is typically present in juvenile animals, but not adults. Disruption of PNNs is associated with renewed ocular dominance plasticity, even after the closure of the juvenile critical

period[97,144]. Future studies may investigate whether *Bpnt2*$^{fl/fl}$ Nestin-Cre animals display differences in assessments of ocular dominance plasticity, given their altered chondroitin sulfation profile.

Additional data relevant to this chapter can be found in the Appendix. **Appendix I** shows that depletion of BPNT2 in differentiated mouse neuroblastoma-2A cells (N2A) reduces the expression of WFA, as measured by immunostaining; this is a model of loss of BPNT2 in a cell line of neuronal lineage. **Appendix J** shows that AAV-Cre-mediated knockdown of BPNT2 in primary *Bpnt2*$^{fl/fl}$ neurons does not affect WFA staining; this is a secondary model of loss of BPNT2 in neurons. **Appendix K** shows that mice treated with dietary lithium carbonate do not display significant alterations in total GAG sulfation, nor in chondroitin sulfation specifically.

CHAPTER IV

CONCLUSIONS AND FUTURE DIRECTIONS

Motivation and principal findings.

This work has discussed the modulation of chondroitin sulfation by the catalytic activity of bisphosphate nucleotidase 2 (BPNT), a lithium-inhibited enzyme. It has also discussed the consequences of the deletion of BPNT2 in the brain, which has relevance for understanding potential effects of lithium treatment.

Despite widespread usage in psychiatric disease across many decades, the mechanism of action of lithium remains undefined. The discovery of a family of lithium-inhibited phosphatases[16] provided new opportunities to investigate lithium's effects. Studies of BPNT2, a member of this family, showed that BPNT2 is crucial for chondroitin-4-sulfation, which is a necessary step in the development of cartilage and long bones. While it was initially unclear how it contributed to the regulation of chondroitin sulfation patterns, it was soon discovered that BPNT2 acted immediately downstream of Golgi-localized sulfotransferase enzymes to convert the sulfation by-product phosphoadenosine phosphate (PAP) to adenosine monophosphate (AMP)[18].

Despite the discovery that BPNT2's catalytic activity is downstream of Golgi-localized sulfation reactions, it was still unknown (prior to this work) whether the catalytic function had direct impact on the sulfation reaction itself. It was known, however, that homozygous mutations in BPNT2 in humans resulted in dysplastic bone and joint development[46,47].

Because of BPNT2's inhibition by lithium, I was particularly interested in the function of BPNT2 in the brain. Human patients with BPNT2 mutations were not reported to have notable neurological or psychiatric symptoms, though several of the 6 patients identified were infants or toddlers at the time of publication. One patient was noted to have intellectual disability, suggesting a potential role for BPNT2 in the central nervous system. And if the catalytic activity of BPNT2 was indeed regulating chondroitin

sulfation, then it's inhibition by lithium could feasibly affect chondroitin sulfation in the brain. There is significant evidence that chondroitin sulfate is important in the nervous system, as it is a major component of a neuronal extracellular matrix structure called the perineuronal net (PNN)[79,141]. PNNs are known to be dysregulated in various neuropsychiatric diseases, including bipolar disorder[73–75] (which lithium treats). Additionally, there is evidence that lithium negatively regulates chondroitin sulfate in neuronal models[104], though the mechanistic basis for this is unknown.

The major hypothesis driving this research was that the catalytic function of BPNT2 was necessary for chondroitin-4-sulfation, and that the deletion of BPNT2 specifically in the nervous system would alter cerebral chondroitin sulfation patterns. From the work described herein, I found that the chondrodysplastic findings indeed stem from a loss of BPNT2 catalytic activity, and that BPNT2 does indeed regulate chondroitin sulfation patterns in the brain.

This chapter outlines some of what I view as the most important implications of this work, especially those which have clinical relevance. I discuss the implications of this work in regards to lithium's mechanism of action in treating bipolar disorder, as well as implications for patients with mutations in BPNT2 resulting in chondrodysplasia. I also revisit the discussion of chondroitin sulfation and perineuronal nets, which have relevance across a broad array of neuropsychiatric disease states. Along the way, I discuss limitations of this work, and I conclude by outlining the future directions of this research.

Implications for lithium's "mechanism of action".

To test the first part of this hypothesis, I generated catalytically inactive BPNT2, and observed that its expression did not restore levels of glycosaminoglycan sulfation in *Bpnt2*-knockout cells. I also noted that the location of point mutations in *BPNT2* associated with human chondrodysplasia occur in close proximity to the core catalytic motif. Furthermore, I found that lithium chloride impairs overall glycosaminoglycan sulfation, and specifically chondroitin-4-sulfation, in the same manner that *Bpnt2*-

knockout does, and that lithium does not exert this effect in *Bpnt2*-knockout cells, suggesting that lithium modulates glycosaminoglycan sulfation by inhibiting BPNT2.

This is a significant discovery, in part because lithium seems to have some role in modulating extracellular matrix in the nervous system. This role has been studied specifically in the context of spinal cord injury, in which lithium potentiates the axon-regenerating effects that are seen following digestion of chondroitin chains with chondroitinase enzyme[104]. Lithium, along with several other drugs used to treat bipolar disorder, also promotes the spread of axonal growth cones[112]. It is possible that lithium's inhibition of BPNT2 contributes to some of these effects.

This is not to say that inhibition of BPNT2 is the only way by which lithium could alter neuronal extracellular matrix and neuron outgrowth. Lithium has known effects on many more proteins than just BPNT2. Classically, lithium is seen as an inhibitor of GSK-3β, and this mechanism has been investigated as the means by which lithium could alter the extracellular matrix[150], chondroitin sulfates[135], and neuronal growth cones[135,151]. There is certainly evidence to suggest that GSK-3β inhibition alone is sufficient to produce these alterations, as specific GSK-3 inhibitors reproduce these effects in the absence of lithium[135,151].

But GSK-3β inhibition is just one popular hypothesis about how lithium exerts its effects. A secondary, but still popular, hypothesis is that of inositol-depletion[152]. Because several members of the lithium-inhibited phosphatase family are inositol phosphatases, lithium may be depleting levels of inositol sugar, in favor of maintaining pools of phosphorylated inositol species. Some research has shown that while several mood stabilizers (including lithium) modulate axonal growth cones, these effects can be reversed by the addition of inositol to neuron cultures[112].

Apart from the most popular hypotheses about how lithium works, we cannot ignore that an entire family of phosphatase enzymes was identified based on their inhibition by lithium, and while this family includes BPNT2 and inositol phosphatases, it also includes BPNT1. As discussed in the introduction,

BPNT1 performs the same reaction as BPNT2, but in the cytosol instead of the Golgi. The consequences of BPNT1-knockout are vastly different from BPNT2-knockout, and likely stem from a metabolically toxic accumulation of PAP. The consequences of BPNT1 inhibition by lithium remain an important area of study, and it would be interesting to generate a nervous-system specific BPNT1-knockout mouse, which would hopefully provide insights into the role of BPNT1 in the brain. While BPNT1 inhibition is far from a common hypothesis for how lithium elicits its effects, it has been shown that BPNT1 expression is downregulated in the brains of patients with bipolar disorder[153]. It has also been shown that deletion of BPNT1 in *C. elegans* produces selective neuronal dysfunction, which can be recapitulated by treating worms with lithium[154]. These findings imply an important function of BPNT1 either in psychiatric disease states or in the efficacy of lithium treatment.

The second part of my hypothesis was that selective deletion of BPNT2 in the nervous system would produce measurable alterations in chondroitin sulfation in the brain. The results of this work demonstrate that such selective deletion does indeed produce changes in chondroitin sulfation, including changes in chondroitin-6-sulfate that are consistent with chondroitin-6-sulfation patterns in bipolar patients who have been treated with lithium[74]. This is an exciting discovery, and BPNT2 inhibition could indeed be driving chondroitin-6-sulfate changes seen with chronic lithium treatment. However, as noted in Appendix K, my preliminary investigations into the effects of dietary lithium treatment on chondroitin sulfation patterns in mouse brain did not recapitulate either the findings seen in my *Bpnt2*$^{fl/fl}$ Nestin-Cre mice, or the findings from brain samples of bipolar patients treated with lithium[74]. There are many ways in which that experiment could be improved, and results may ultimately show that chronic treatment of mice with lithium actually produces measurable alteration in chondroitin sulfation (for example, longer exposure to lithium, more frequent monitoring of serum lithium levels to ensure adequate dosage, alternate methods of lithium administration, etc.).

This work is *not* an attempt to explain how BPNT2 inhibition is the means by which lithium elicits its mood stabilizing effects. Given lithium's exceptionally simple structure (a monoelemental cation), it

certainly has a wide range of effects. Some of these produce favorable symptom alleviation, and others produce undesirable toxic effects. There is sufficient evidence to cause me to suspect that the mechanisms underlying symptom alleviation are manifold. While it would be nice to pinpoint the precise mechanism of efficacy (and hopefully exclude the mechanisms of toxicity), the brain is an especially complicated network, and we are still far removed from understanding its scope.

What this work *does* is demonstrate that one such consequence of lithium treatment is almost certainly BPNT2 inhibition, and BPNT2 inhibition can alter chondroitin sulfation in the brain. Lithium treatment alone may or may not be sufficient to produce measurable changes in cerebral chondroitin sulfation patterns, and whether such an alteration would even prove to be clinically significant remains to be seen. However, BPNT2 deserves to be recognized as a target of lithium and its effects on chondroitin sulfation should be considered in future investigations of lithium's effects.

BPNT2-associated chondrodysplasia in humans.

Putting aside bipolar disorder and lithium, BPNT2 has a much more tangible clinical connection in that it defines an autosomal recessive disorder characterized by skeletal and joint defects (Chondrodysplasia-GPAPP type)[46–48]. While exceptionally rare (as all reported patients were born to parents of consanguineous lineage), this disorder is now included on genetic panels run on patients with chondrodysplasia of unknown cause.

The mouse equivalents of two of the mutations known to cause this disorder were studied in Chapter II. Both were missense mutations, T183P and D177N. As discussed in Chapter II, these mutations occur in close proximity to the core catalytic motif. The replacement of threonine with proline likely induces a severe structural alteration, which likely disturbs the protein folding, and prevent the three-dimensional structural motif from properly forming. The replacement of aspartic acid with asparagine initially seems less

detrimental, but this generated a novel N-glycosylation consensus sequence, which is indeed glycosylated when this variant is expressed in mammalian cells.

These missense mutations appear to be just as severe as the other identified mutations (a nonsense mutation resulting in an early stop codon after amino acid 187, which produces a truncated protein which will not have the full three-dimensional structural motif, and a frameshift mutation beginning at amino acid 108, which will prevent the formation of the metal binding locus entirely). However, the differences between the phenotypes of patients with different mutations is difficult to discern, as so few patients have been identified. Despite this, all mutations are predicted to disrupt the enzyme's catalytic activity.

As noted previously, the only reported neurological finding from any of these patients was that one patient (aged 11 at the time, T183P mutation) displayed signs of intellectual disability[47]. Intellectual disability is associated with a genetic cause or syndrome in up to 25% of cases[155], so it is possible that the intellectual disability stems from the BPNT2 mutation. As mentioned previously, all but one of the other patients with BPNT2 mutations were younger than 5 years, or deceased in early infancy[47], so it may have been difficult to assess their neurodevelopmental state.

While we did not observe behavioral alterations in mice lacking BPNT2 in the nervous system, we did observe biochemical differences. Chondroitin sulfate is especially abundant in bone, but it is also abundant and important in the brain[79]. Given the importance of the extracellular matrix in higher cortical development and organization[156], it is not surprising that several genes associated with intellectual disability also have known functions in regulating stature[157,158], skeletal development[159], and collagen/cartilage[160].

It is therefore possible that an altered chondroitin sulfation profile in the brain of patients with BPNT2 mutations could contribute to neurodevelopmental differences. Of course, it would be interesting to see whether these patients in fact exhibited decreased chondroitin-4-sulfate and elevated unsulfated chondroitin in their brains post-mortem, but given the very small sample size, such studies would be difficult. Additionally, mutations in BPNT2 are likely to be less severe than full genetic knockout. While

these mutations were severe enough to produce deficits in sulfation in cultured fibroblasts, it is unknown whether such deficits would be observed in their brain tissue.

If BPNT2 homozygous mutations were more common in the population, there would be many more questions to ask. Again, because BPNT2 is inhibited by a common psychotropic drug, I would be interested to know whether such patients displayed altered susceptibility to psychiatric disease. Would they be less prone to bipolar disorder? If they were diagnosed with bipolar disorder, would they respond to lithium? Does any region of their brain show alterations in perineuronal nets? These questions could provide more insight into the specific function of BPNT2 (and by extension, chondroitin sulfate) in normal cerebral function.

Disorders associated with cerebral chondroitin sulfate and perineuronal nets.

Much of the introduction of this work focused on perineuronal nets (PNNs). It appears that the most well-known role of chondroitin sulfate in the brain is its role in the composition of PNNs[79]. As such, it was only natural to hypothesize that any process that affected chondroitin sulfation in the brain may also be affecting PNN structure. Despite this well-established connection, this work identified decreases in overall GAG sulfation (and specifically decreases in chondroitin-4-sulfate) that did not correlate with decreases in perineuronal net staining in either of two brain regions.

In Chapter III, we postulated that PNNs may be more robust to changes in chondroitin sulfate level, and the sulfation changes may not have been severe enough to modify the intensity of PNNs. We also noted that much of the loose extracellular matrix in the brain is also composed on chondroitin-4-sulfate. Because the loose matrix is not easily visualized, this may be where the chondroitin sulfation changes are manifesting. It may also be that the most common marker of PNNs, WFA, is not specific to a locus of sulfation, and while the sulfation levels may be changing, the levels of chondroitin sugar chains themselves may not be changing, producing to visible change in WFA staining. The most objective, quantitative metric

of PNNs is to measure levels of chondroitin sulfate specifically, using a method such as HPLC. This work did use HPLC, and found sulfation changes. Therefore, there may still be significant alteration in PNN function that is not readily visualized.

However, one might expect that in the presence of such changes, there would be a change in a functional output. Thus, I decided to evaluate various neurobehavioral traits in mice lacking BPNT2 in the CNS. The behavioral tests selected were based on behaviors seen in other mice with disrupted chondroitin proteoglycan synthesis, all of which were correlated with changes in PNNs. But, no changes in behavior were identified. This could simply be because the absence of PNN changes meant there would not be changes in PNN-associated behaviors. However, I also evaluated a lithium-related behavior (immobility time on the tail suspension test[161]), and found no difference between mice lacking BPNT2 in the brain and controls.

The loss of BPNT2 function in the brain is one way to model the effects of lithium-mediated inhibition of BPNT2. If we had therefore hypothesized that deletion of BPNT2 from the nervous system mimicked treatment with lithium, we might have anticipated decreased immobility time on the tail suspension test in the experimental animals (a correlate for diminished depressive behavior), but the behavioral consequences of lithium treatment are far from robustly established[146]. It is difficult to study effects of lithium in mice in part because it is difficult to develop an animal model of bipolar disorder[162]. Some of lithium's most well-established effects in rodent models are attenuation of drug-induced symptoms (including attenuation of amphetamine-induced hyperlocomotion[163], exacerbation of pilocarpine-induced seizures[164], and attenuation of reserpine-induced hypoactivity[165]). Studies of these effects were beyond the scope of the research described in this dissertation, but it would be interesting to see whether deletion of BPNT2 modified the effects of these drugs in the same way that lithium does.

Future directions.

There are several important future directions for this research. Some experiments have already been mentioned in this chapter.

Building off of the work in Chapter II: While we know that the loss of the catalytic activity of BPNT2 is sufficient to impair glycosaminoglycan sulfation, we still do not know exactly how this occurs. As discussed in the conclusion of Chapter II, it is possible that the loss of BPNT2 activity causes PAP to accumulate locally in the Golgi lumen, and this feedback-inhibits the Golgi-localized glycosaminoglycan sulfotransferases. While we did not observe any PAP accumulation in BPNT2-knockout cells, luminal PAP can be difficult to measure, as subcellular fractionation studies can cause the PAP to leak out before the Golgi fraction can be analyzed. However, an alternative mechanism may be more likely anyways; there is some evidence that the PAPS transporter (PAPST), which is embedded in the Golgi membrane, may be an antiporter, and in order to shuttle PAPS into the Golgi, AMP must be shuttled out. In the absence of BPNT2 activity, AMP production within the Golgi would be limited, and PAPS would not make it into the Golgi, thereby preventing the sulfate donor molecule from being used for GAG sulfation reactions. Capasson and Hirschberg reported evidence for such an antiport mechanism[133], which could be seen specifically with guanosine nucleotide substrates in Golgi vesicles isolated from rat liver[166]. This guanosine antiport appeared to be equimolar[133], implying that a deficit in the analogous adenosine nucleotide AMP would certainly result in deficient PAPS import into the Golgi. Without PAPS, no sulfation can occur. Future experiments to confirm the PAPS transporter indeed functions as an AMP antiporter would likely involved the generation of liposomes engineered to express the PAPS transporter, which could be loaded with radiolabeled 5'-AMP, according to published methods[167]. Various concentrations of PAPS could then be added to the liposomal reaction mixture, and AMP export could be measured in the non-liposomal fraction.

Such an antiport mechanism would provide an explanation for impaired Golgi-localized sulfation generally, and as previously described, Golgi-localized sulfotransferases are carbohydrate sulfotransferases whose primary purpose is to sulfate glycosaminoglycans[31,39,168]. While the studies presented in this

dissertation all evaluated overall glycosaminoglycan sulfation, the only specific GAG that was analyzed was chondroitin. The original publication of the BPNT2-knockout mouse phenotype also evaluated heparan sulfation, and found significantly more modest deficits in sulfation relative to that of chondroitin[18]. Chondroitin-4-sulfate, in particular, was identified as a key GAG in part because BPNT2-knockout so closely mirrored C4ST1-knockout[45]. Notably, the phenotype of this mouse did not resemble the phenotype of heparan sulfotransferase-knockout mice[169,170]. Nevertheless, it is certainly possible that other species of GAG are under-sulfated in the absence of BPNT2. Future experiments should analyze the relative deficits of these molecules, including dermatan- and keratan-sulfates. Future work could also examine changes in these molecules in the brains of *Bpnt2*$^{fl/fl}$ Nestin-Cre mice. However, I would anticipate minor alterations in the levels of these sulfated GAGs, primarily because chondroitin-sulfate (chondroitin-4-sulfate, specifically) is so much more abundant in both the whole mammalian organism[171] and also in the central nervous system[172]. If we embrace the PAPS/AMP antiporter hypothesis, then the loss of BPNT2 will impair production of AMP, reduce PAPS import into the Golgi, and thereby impair GAG sulfation. However, when the GAG sulfation process is impaired indiscriminately (as would be in BPNT2-knockout, compared to say, a heparan sulfotransferase-knockout), I would hypothesize that the effects would be seen across sulfated GAG species in proportion to the amount of that GAG which needs to be synthesized. Because of how much more chondroitin gets sulfated relative to other GAG species, the effects stemming from impaired chondroitin sulfation are likely to be seen first. The original research described in this work supports this notion, as evidenced by how chondroitin-4-sulfate levels were significantly lower in both *Bpnt2*-knockout MEFs and *Bpnt2*$^{fl/fl}$ Nestin-Cre brain tissue, *but this decrease was countered by a relative increase in chondroitin-6-sulfate*, which is significantly less abundant. If the loss of BPNT2 made all sulfation impossible, then we would not expect this counterintuitive increase in another sulfation moiety. I suspect that the loss of BPNT2 does not halt all sulfation, but instead limits the pool of sulfate donor molecules (PAPS), causing cells to prioritize sulfation of less abundant GAGs, at the cost of chondroitin-4-sulfate, primarily. If this suspicion were true, I would anticipate low-to-no change in the less common sulfated GAGs, which would translate to minimal phenotypic manifestations.

Building off the work in Chapter III: While a broad panel of behavioral tests was selected for the *Bpnt2*$^{fl/fl}$ Nestin-Cre mice, these tests were not exhaustive. Additional tests could be performed to evaluate for other behavioral changes, including assay to measure fear memory, memory consolidation, and propensity to extinguish memories (behaviors which have also been associated with perineuronal nets[62,63,99,173]). Mice could also be subjected to some kind of stress prior to behavioral analysis, including stress paradigms (like isolation[174,175], social defeat stress[176], or unpredictable chronic mild shocks[177]) which are meant to mimic depressive symptoms. If BPNT2 inhibition mimics lithium treatment, then inducing mood symptoms in a mouse model may cause behavioral effects to become more pronounced. And because lithium is meant to treat both the depressive and manic symptoms of bipolar disorder, then a manic-like state could be induced pharmacologically, for example, using amphetamines[163]; perhaps then, we may observe a behavioral difference in mice lacking BPNT2 in the nervous system.

An additional experiment which could be useful would be to treat experimental mice with lithium, and compare them behavioral to wild-type mice on lithium, to see if lithium has any effects in mice that do not have BPNT2 in their brains. Future experiments that make use of lithium should monitor serum lithium levels regularly, and perhaps confirm that lithium dosage is adequate to achieve canonical effects, such as inhibitory phosphorylation of GSK-3β[178,179]. Brains of mice in these studies should also be subjected to histological PNN analysis and biochemical sulfation analyses.

As discussed at the end of Chapter III, experimental mice could be subjected to analyses of phenomena associated explicitly with PNNs, such as the duration of the critical period associated with establishment of ocular dominance at mouse adolescence.

Given my experience in performing this research and my familiarity with this field of work, I would be particularly excited about the propensity of BPNT2 inhibition to facilitate healing from spinal cord injury. As described several times throughout the course of this work, lithium treatment has been associated with augmentation of chondroitinase's ability to promote axon regeneration in cellular models of spinal cord injury[104]. *In vivo* trials of lithium have (as yet) been less successful[108]. Chondroitinase ABC (the

enzyme used in these studies) digests chondroitin chains down to their disaccharide components, but does not affect their sulfation (as we used it prior to our disaccharide HPLC analyses in both Chapters II and II—see corresponding "Methods" sections). I am curious as to whether axon regeneration would be improved following injury to spinal ganglial neurons taken from *Bpnt2*$^{fl/fl}$ Nestin-Cre mice, or whether the absence of BPNT2 could augment their regenerative potential in conjunction with chondroitinase treatment. It may be that both digestion of the disaccharide chain as well as inhibition of disaccharide sulfation could result in fewer extracellular obstacles to axon regrowth.

The proposed future studies for these experimental mice thus far have all been focused on BPNT2's regulation of GAG sulfation. While GAGs are abundant and are the major substrate for Golgi sulfotransferases, other large endogenous molecules need to be sulfated as well. For example, sulfatides are a major class of sulfated lipids[180] found at the membranes of eukaryotic cells. Like sulfated GAGs, they serve structural purposes, as well as facilitate protein trafficking and cell adhesion. The sulfotransferase responsible for sulfatide synthesis, cerebroside sulfotransferase (CST), is distinct from most members of the Golgi sulfotransferase family[181], but it has been shown to localize to Golgi membranes[182]. Sulfatides have a particularly important role in the central nervous system, where they are a crucial component of the myelin sheath encasing axons[183]. Like chondroitin-4-sulfate, sulfatide is known to inhibit axonal outgrowth and prevent axonal regeneration following nerve injury[184]. Knockout of the CST enzyme in mice leads to hindlimb weakness (beginning around 6 weeks of age), tremors, and progressive ataxia[185]. These symptoms are quite similar to symptoms of severe lithium toxicity, including the syndrome of irreversible lithium-effectuated neurotoxicity (SILENT)[6], which is thought to be s result of demyelinating processes in the brain[6]. While we did not observe ataxic symptoms in *Bpnt2*$^{fl/fl}$ Nestin-Cre mice, future work could look at these mice when they are aged, and see whether they begin to display such symptoms in later life. Future studies should also evaluate levels of sulfatide in the brains of these mice biochemically (using HPLC or mass spectrometry), to see whether any significant alterations are present. Such alterations, if they exist,

could also be present (to a degree) in patients with BPNT2 mutations, and this may inform any observed neurological phenotypes.

Final thoughts.

The catalytic function of bisphosphate nucleotidase 2 (BPNT2) is important for glycosaminoglycan sulfation generally, but especially for chondroitin sulfation. Chondroitin sulfate is abundant and especially important in the extracellular matrix of bone, cartilage, and nervous tissue. Loss of BPNT2 in these tissues results in measurable changes to the chondroitin sulfate profile, which could have clinically meaningful effects.

BPNT2 is also an established inhibitory target of the mood stabilizer lithium. While lithium is unlikely to have a single mechanism of action, elucidating the specific consequences of lithium treatment is an important step forward in the field. It may one day be discovered that BPNT2 has important therapeutic relevance as a regulator of the chondroitin sulfation profile.

As an important step forward, this work establishes that the inhibition of the enzymatic activity of BPNT2 drives the changes in sulfation profile, and that BPNT2 regulates chondroitin sulfation not only in the bone and cartilage, but also in the central nervous system.

APPENDIX A

Primer	Sequence
HPRT.Fwd	5'- GCAGTACAGCCCCAAAATGG-3'
HPRT.Rev	5'- ATCCAACAAAGTCTGGCCTGT-3'
BPNT2.Fwd	5'-CGCCGATGATAAGATGACCAG-3'
BPNT2.Rev	5'-GCATCCACATGTTCCTCAGTA-3'
Chst11.Fwd	5'-AAGTATGTTGCACCCAGTCAT-3'
Chst11.Rev	5'-ATGGCAGTGTTGGATAGCTC-3'
Chst3.Fwd	5'-TTCCTGGCATTTGTGGTCA-3'
Chst3.Rev	5'-AGATGCATTCTCCGATAAGAGC-3'
Slc35b2.Fwd	5'-AGGTCCTGAAGCTGGTCTT-3'
Slc35b2.Rev	5'-AATGCTCTCCTGGTGATGTG-3'
Slc35b3.Fwd	5'-CCTTCCTGTTTTCCCTCACTG-3'
Slc35b3.Rev	5'-CATTGCTTTCCTTCCTGTTGTC-3'

Appendix A. Table of primer sequences used for quantitative PCR analyses described in Chapter II.

APPENDIX B

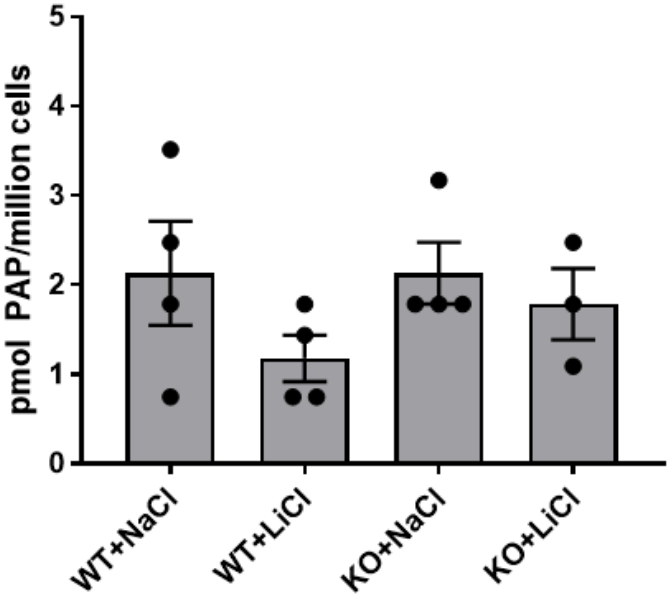

Appendix B. Lithium treatment does not alter PAP level in WT or *Bpnt2*-KO MEFs. Cells were treated with 10mM LiCl or 10mM NaCl and cultured as 3-dimensional cell pellets for 7 days prior to analysis. Error bars show mean +/- SEM. Findings were not significant across groups, as measured by one-way ANOVA.

APPENDIX C

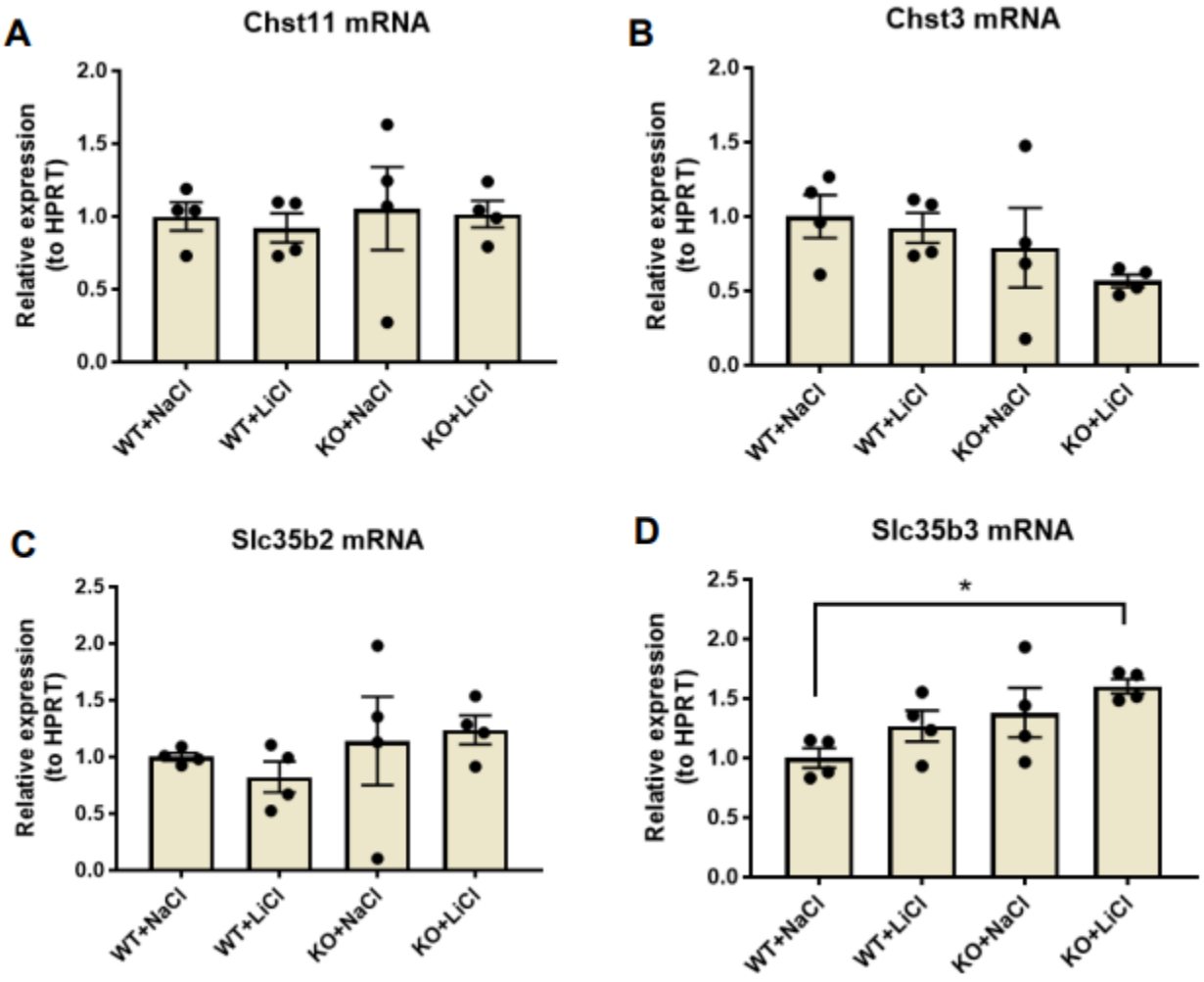

Appendix C. Gene expression analysis of members of the Golgi-localized sulfation pathway in WT and *Bpnt2*-KO MEFs, with and without lithium treatment. mRNA expression analysis as measured by quantitative PCR. *Chst11* (A) encodes chondroitin-4-sulfotransferase, *Chst3* (B) encodes chondroitin-6-sulfotransferase, *Slc35b2* (C) encodes PAPST1, *Slc35b3* (D) encodes PAPST2. Expression levels are relative to HPRT expression. Error bars show mean +/- SEM. Findings were not significant across groups, as measured by one-way ANOVA, with the exception of the increase in *Slc35b3* expression in KO+LiCl cells relative to WT+NaCl cells (*p=0.0325).

APPENDIX D

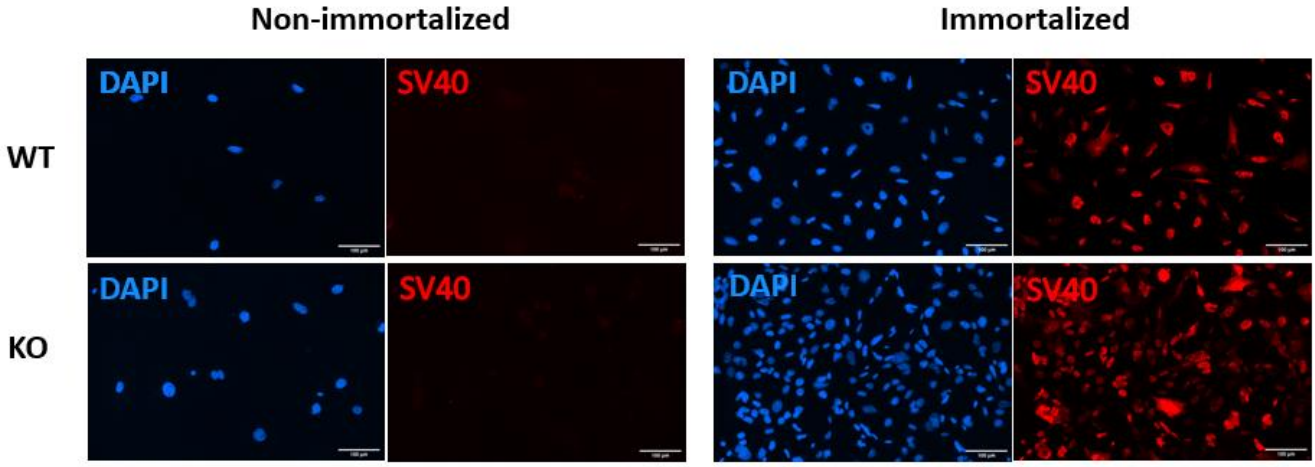

Appendix D. Validation of immortalization of primary MEF cultures. SV40 staining of MEFs at passage 10 (P10). Non-immortalized WT and *Bpnt2*-KO MEFs were thawed at P4. At P7, a subset of cells were immortalized using SV40 large and small T antigens packaged in lentivirus (using Addgene #22298). As non-immortalized cells underwent senescence, SV40-transduced cells continued to grow rapidly. At P10, both set of cells were plated onto coverslips and stained for SV40 T antigen (Abcam 16879, 1:500) to secondarily confirm immortalization. Both cell proliferation and presence of SV40 are easily detectable in immortalized cells. DAPI stains cell nuclei. Scale bars: 100 um.

APPENDIX E

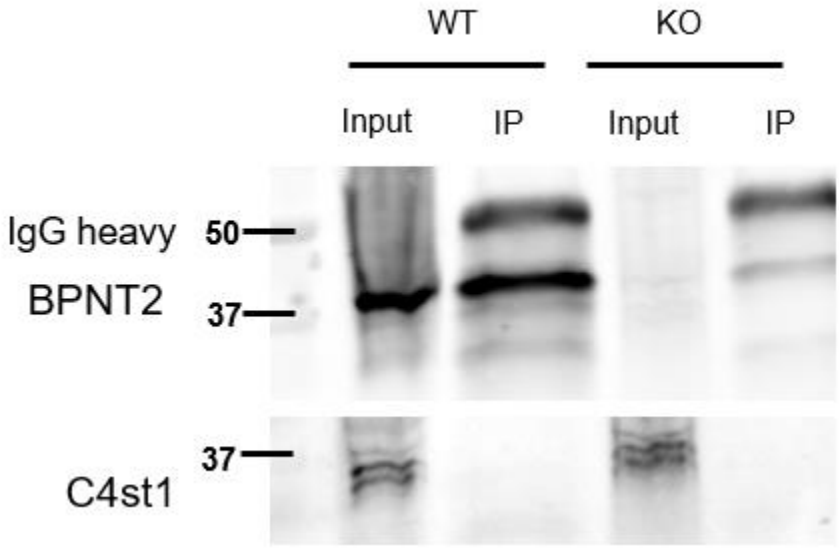

Appendix E. Co-immunoprecipitation studies of BPNT2 and C4st1. Immunoprecipitation of BPNT2 from WT and *Bpnt2*-KO MEF lysates (prepared in Triton-X100 buffer). BPNT2-immunoprecipitation is successful, as can be seen in WT IP lane, but C4st1 does not appear to be present in the IP lane, suggesting no pull-down of C4st1.

APPENDIX F

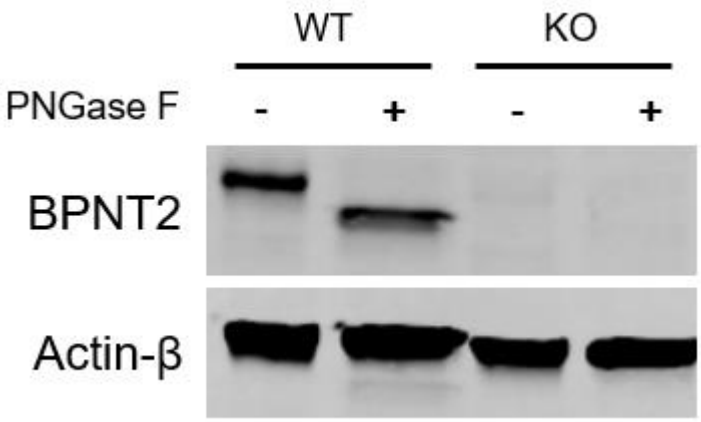

Appendix F. **Immunoblotting of BPNT2 following PNGase F digestion**. 10ug of protein from cell lysates was either left untreated or treated with PNGase F, according to manufacturer instructions, and lysates were loaded into a 12% SDS-PAGE gel. A decrease in size of BPNT2 protein is observable due to the cleavage of an N-glycosyl group present at N257. No band is present in *Bpnt2*-KO lanes.

APPENDIX G

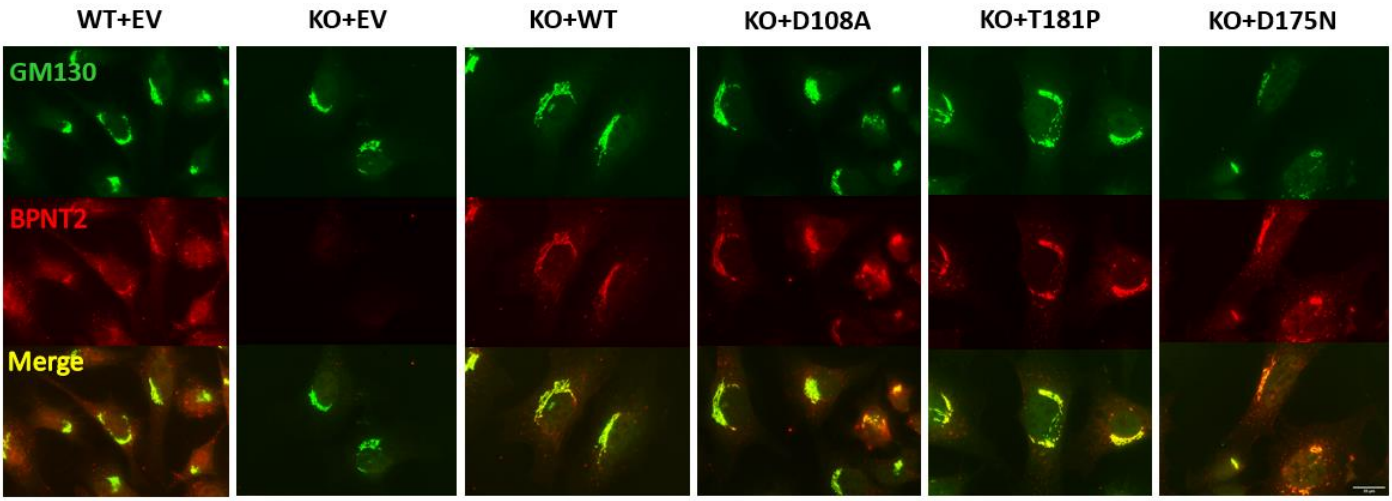

Appendix G. Immunofluorescent staining of BPNT2 and GM130 (Golgi marker) in mutant *Bpnt2* MEFs. WT BPNT2 is localted in the Golgi. Mutations in *Bpnt2* do not alter the protein's localization. Scale bar is 20 um.

APPENDIX H

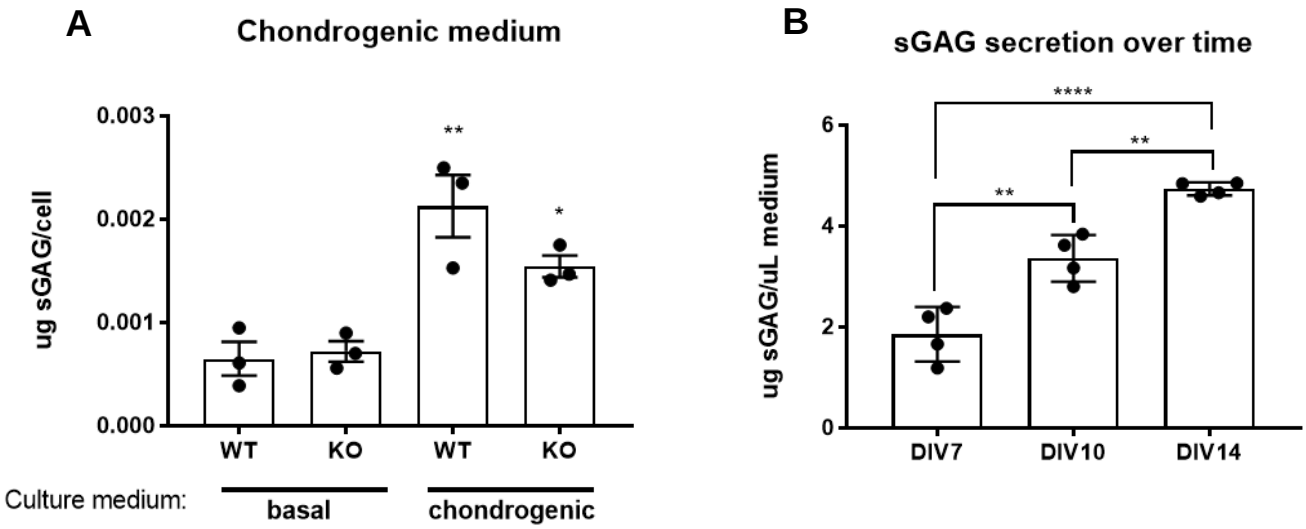

Appendix H. **Induction of chondrogenesis in MEF cultures.** A. Culturing MEFs in chondrogenic medium enhances chondrogenesis, magnifying differences in sulfation between WT and *Bpnt2*-KO MEFs. B. Culturing MEFs as pellets over 7-14 days enhances secretion of sulfated GAG into medium. Significance denotes results of one-way ANOVA. *p<0.05, **p<0.01, ****p<0.0001.

APPENDIX I

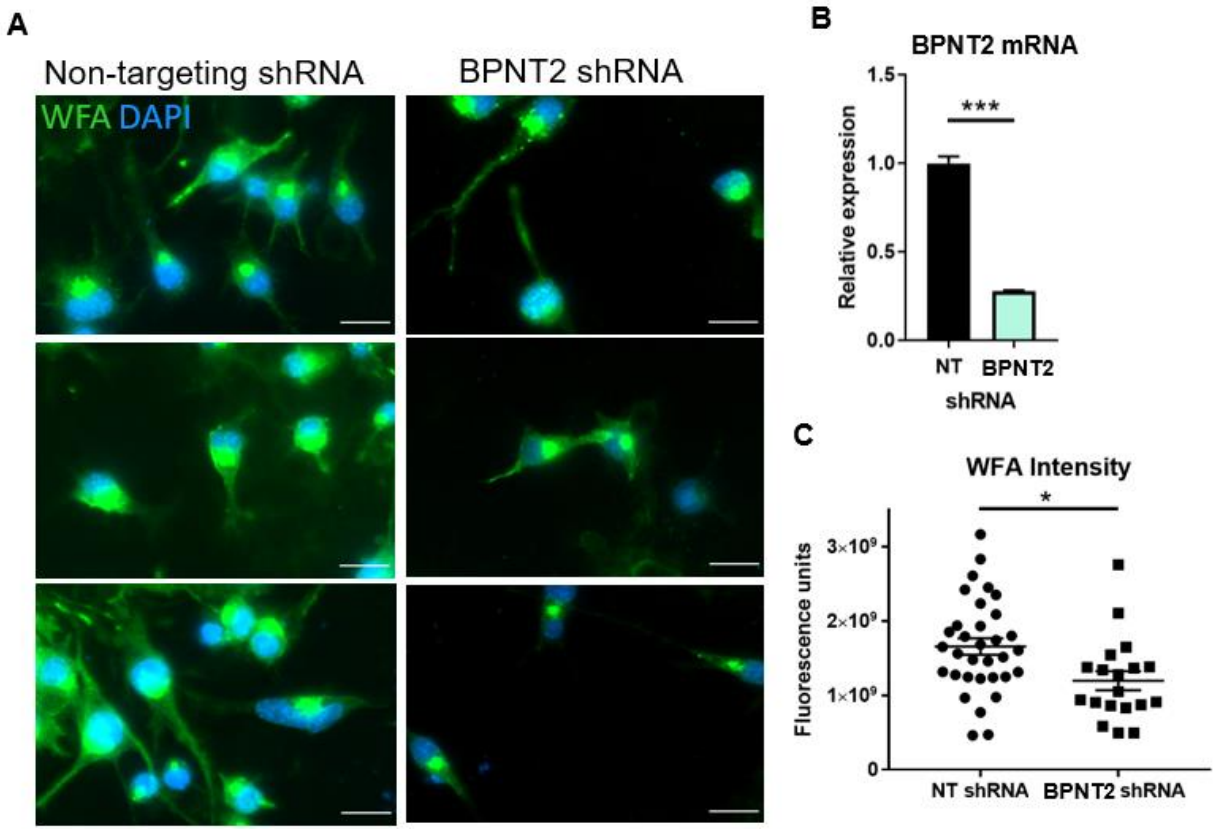

Appendix I. **Knockdown of BPNT2 in N2A cells decreases WFA fluorescence.** N2A cells were transiently transfected with either scrambled shRNA (non-targeting) or BPNT2 shRNA, then cultured in low-glucose medium for 5 days to promote neuronal differentiation. Approximately 75% knockdown of BPNT2 mRN was achieved. Following differentiation, cells were fixed and stained with WFA. WFA fluorescence was quantified by hand in ImageJ. Significance denotes result of two-sided student's t-test. *p<0.05. Scale bar is 20um.

APPENDIX J

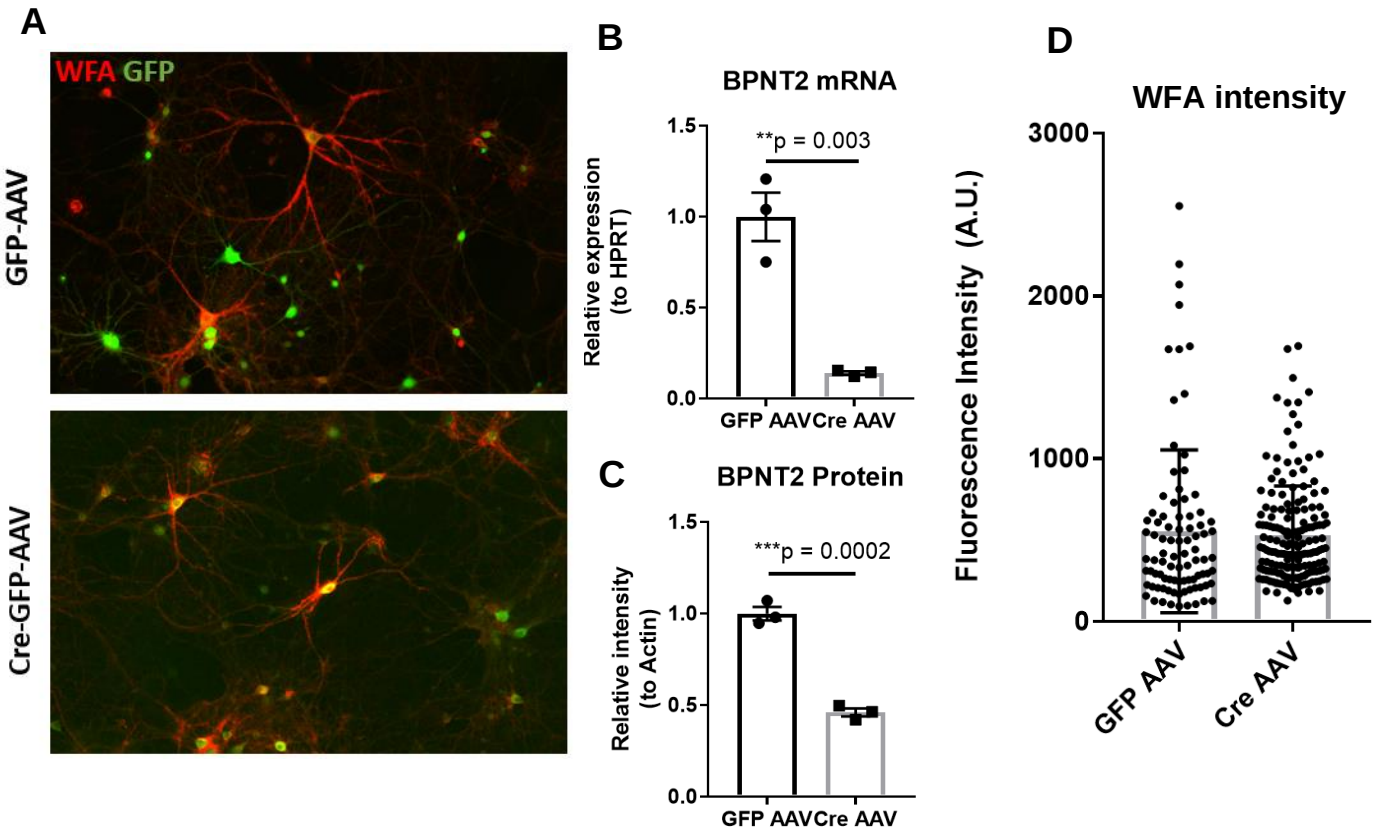

Appendix J. WFA staining of *Bpnt2*-KO primary neurons. Primary neurons were cultured from *Bpnt2*$^{fl/fl}$ mouse pups (P0). Cultures were treated with pre-designed AAV (adeno-associated virus) containing either GFP alone or GFP and Cre recombinase. Efficacy of viral transduction was confirmed with staining for GFP (A). Recombination of loxp sites was confirmed by measuring degree of knockout of *Bpnt2* mRNA and protein. Approximately an 80% reduction in mRNA (B) and a 50% reduction in BPNT2 protein (C) was observed. Neurons were fixed and stained with WFA, and fluorescence intensity was evaluated using Pipsqueak AI software. No significant change in WFA intensity was seen between GFP-AAV and Cre-GFP-AAV cells (D).

APPENDIX K

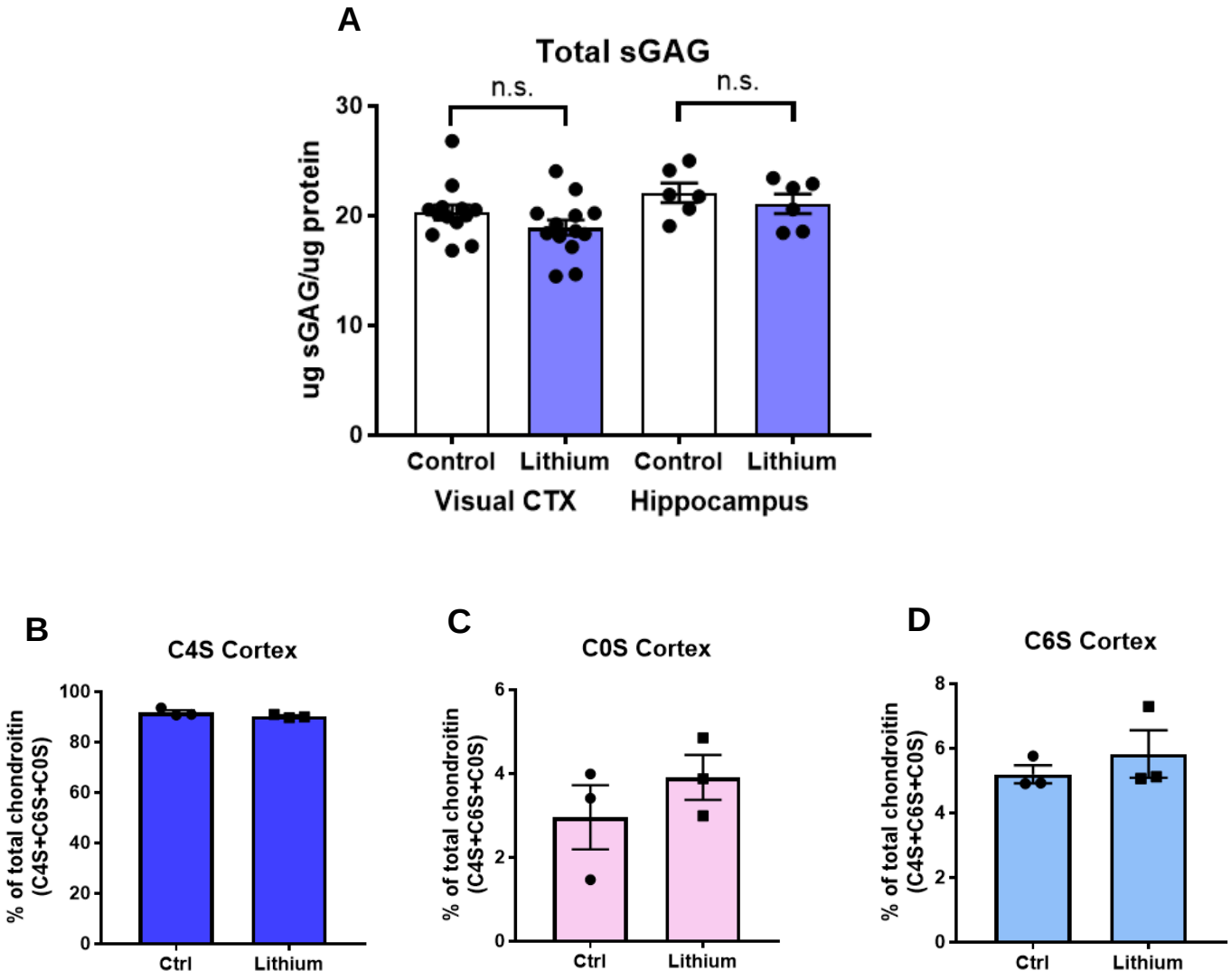

Appendix K. Sulfated GAG analysis on brain tissues from mice subjected to dietary lithium carbonate for 6-8 weeks. Mice were placed on lithium diet, and serum lithium concentration was measured from trunk blood collected at time of sacrifice. Serum lithium concentrations ranged from 0.5 mM to 0.9 mM. DMMB analysis was performed on both visual cortex and hippocampal samples. No change in overal GAG sulfation was observed (A). Chondroitin disaccharide HPLC was performed on a subset of visual cortex samples, and no significant changes were seen in C4S (B), C0S (C), or C6S (D).

REFERENCES

1. Schou, M., Juel-Nielsen, N., Stromgren, E. & Voldby, H. The treatment of manic psychoses by the administration of lithium salts. *J. Neurol. Neurosurg. Psychiatry* **17**, 250–260 (1954).
2. Cade, J. F. J. Lithium salts in the treatment of psychotic excitement. *Med. J. Aust.* **2**, 349–352 (1949).
3. Phillips, M. L. & Kupfer, D. J. Bipolar disorder diagnosis: challenges and future directions. *Lancet Lond. Engl.* **381**, 1663–1671 (2013).
4. Association, A. P. *Diagnostic and Statistical Manual of Mental Disorders (DSM-5®)*. (American Psychiatric Pub, 2013).
5. Miller, J. N. & Black, D. W. Bipolar Disorder and Suicide: a Review. *Curr. Psychiatry Rep.* **22**, 6 (2020).
6. Adityanjee, null, Munshi, K. R. & Thampy, A. The syndrome of irreversible lithium-effectuated neurotoxicity. *Clin. Neuropharmacol.* **28**, 38–49 (2005).
7. Aiff, H. *et al.* Effects of 10 to 30 years of lithium treatment on kidney function. *J. Psychopharmacol. Oxf. Engl.* **29**, 608–614 (2015).
8. Gitlin, M. Lithium side effects and toxicity: prevalence and management strategies. *Int. J. Bipolar Disord.* **4**, (2016).
9. Connolly, K. R. & Thase, M. E. The Clinical Management of Bipolar Disorder: A Review of Evidence-Based Guidelines. *Prim. Care Companion CNS Disord.* **13**, (2011).
10. McKnight, R. F. *et al.* Lithium for acute mania. *Cochrane Database Syst. Rev.* **6**, CD004048 (2019).
11. Plans, L. *et al.* Association between completed suicide and bipolar disorder: A systematic review of the literature. *J. Affect. Disord.* **242**, 111–122 (2019).
12. Malhi, G. S., Tanious, M., Das, P., Coulston, C. M. & Berk, M. Potential mechanisms of action of lithium in bipolar disorder. Current understanding. *CNS Drugs* **27**, 135–153 (2013).

13. Naccarato, W. F., Ray, R. E. & Wells, W. W. Biosynthesis of myo-inositol in rat mammary gland. Isolation and properties of the enzymes. *Arch. Biochem. Biophys.* **164**, 194–201 (1974).
14. Hallcher, L. M. & Sherman, W. R. The effects of lithium ion and other agents on the activity of myo-inositol-1-phosphatase from bovine brain. *J. Biol. Chem.* **255**, 10896–10901 (1980).
15. Inhorn, R. C. & Majerus, P. W. Inositol polyphosphate 1-phosphatase from calf brain. Purification and inhibition by Li+, Ca2+, and Mn2+. *J. Biol. Chem.* **262**, 15946–15952 (1987).
16. York, J. D., Ponder, J. W. & Majerus, P. W. Definition of a metal-dependent/Li(+)-inhibited phosphomonoesterase protein family based upon a conserved three-dimensional core structure. *Proc. Natl. Acad. Sci.* **92**, 5149–5153 (1995).
17. Dollins, D. E. *et al.* A Structural Basis for Lithium and Substrate Binding of an Inositide Phosphatase. *J. Biol. Chem.* jbc.RA120.014057 (2020) doi:10.1074/jbc.RA120.014057.
18. Frederick, J. P. *et al.* A role for a lithium-inhibited Golgi nucleotidase in skeletal development and sulfation. *Proc. Natl. Acad. Sci. U. S. A.* **105**, 11605–11612 (2008).
19. Spiegelberg, B. D., Xiong, J. P., Smith, J. J., Gu, R. F. & York, J. D. Cloning and characterization of a mammalian lithium-sensitive bisphosphate 3'-nucleotidase inhibited by inositol 1,4-bisphosphate. *J. Biol. Chem.* **274**, 13619–13628 (1999).
20. Spiegelberg, B. D., Cruz, J. dela, Law, T.-H. & York, J. D. Alteration of Lithium Pharmacology through Manipulation of Phosphoadenosine Phosphate Metabolism. *J. Biol. Chem.* **280**, 5400–5405 (2005).
21. Ramaswamy, S. G. & Jakoby, W. B. (2')3',5'-Bisphosphate nucleotidase. *J. Biol. Chem.* **262**, 10044–10047 (1987).
22. López-Coronado, J. M., Bellés, J. M., Lesage, F., Serrano, R. & Rodríguez, P. L. A novel mammalian lithium-sensitive enzyme with a dual enzymatic activity, 3'-phosphoadenosine 5'-phosphate phosphatase and inositol-polyphosphate 1-phosphatase. *J. Biol. Chem.* **274**, 16034–16039 (1999).

23. Murguía, J. R., Bellés, J. M. & Serrano, R. A salt-sensitive 3'(2'),5'-bisphosphate nucleotidase involved in sulfate activation. *Science* **267**, 232–234 (1995).
24. Mechold, U., Ogryzko, V., Ngo, S. & Danchin, A. Oligoribonuclease is a common downstream target of lithium-induced pAp accumulation in Escherichia coli and human cells. *Nucleic Acids Res.* **34**, 2364–2373 (2006).
25. Harrison, R. L. & Jarvis, D. L. Protein N-Glycosylation in the Baculovirus–Insect Cell Expression System and Engineering of Insect Cells to Produce "Mammalianized" Recombinant Glycoproteins. in *Advances in Virus Research* vol. 68 159–191 (Academic Press, 2006).
26. Stipanuk, M. H. & Ueki, I. Dealing with methionine/homocysteine sulfur: cysteine metabolism to taurine and inorganic sulfur. *J. Inherit. Metab. Dis.* **34**, 17–32 (2011).
27. Hästbacka, J. *et al.* The diastrophic dysplasia gene encodes a novel sulfate transporter: positional cloning by fine-structure linkage disequilibrium mapping. *Cell* **78**, 1073–1087 (1994).
28. Venkatachalam, K. V. Human 3'-phosphoadenosine 5'-phosphosulfate (PAPS) Synthase: Biochemistry, Molecular Biology and Genetic Deficiency. *IUBMB Life* **55**, 1–11 (2003).
29. Sasaki, N. *et al.* The 3'-phosphoadenosine 5'-phosphosulfate transporters, PAPST1 and 2, contribute to the maintenance and differentiation of mouse embryonic stem cells. *PloS One* **4**, e8262 (2009).
30. Allali-Hassani, A. *et al.* Structural and Chemical Profiling of the Human Cytosolic Sulfotransferases. *PLOS Biol.* **5**, e97 (2007).
31. Gamage, N. *et al.* Human Sulfotransferases and Their Role in Chemical Metabolism. *Toxicol. Sci.* **90**, 5–22 (2006).
32. Lee, S.-J. *et al.* Single Nucleotide Polymorphisms in SULT1A1 and SULT1A2 in a Korean Population. *Drug Metab. Pharmacokinet.* **28**, 372–377 (2013).

33. Li, Y., Lindsay, J. & Zhou, L.-L. W. and S.-F. Structure, Function and Polymorphism of Human Cytosolic Sulfotransferases. *Current Drug Metabolism* vol. 9 99–105 http://www.eurekaselect.com/66419/article (2008).

34. Schmidt, H. H. *et al.* Deregulation of the carbohydrate (chondroitin 4) sulfotransferase 11 (CHST11) gene in a B-cell chronic lymphocytic leukemia with a t(12;14)(q23;q32). *Oncogene* **23**, 6991–6996 (2004).

35. Chopra, S. S. *et al.* Inherited CHST11/MIR3922 deletion is associated with a novel recessive syndrome presenting with skeletal malformation and malignant lymphoproliferative disease. *Mol. Genet. Genomic Med.* **3**, 413–423 (2015).

36. Shabbir, R. M. K., Nalbant, G., Ahmad, N., Malik, S. & Tolun, A. Homozygous CHST11 mutation in chondrodysplasia, brachydactyly, overriding digits, clino-symphalangism and synpolydactyly. *J. Med. Genet.* **55**, 489–496 (2018).

37. Kosho, T. CHST14/D4ST1 deficiency: New form of Ehlers–Danlos syndrome. *Pediatr. Int.* **58**, 88–99 (2016).

38. Reuter, M. S. *et al.* NDST1 missense mutations in autosomal recessive intellectual disability. *Am. J. Med. Genet. A.* **164**, 2753–2763 (2014).

39. Fukuda, M., Hiraoka, N., Akama, T. O. & Fukuda, M. N. Carbohydrate-modifying Sulfotransferases: Structure, Function, and Pathophysiology. *Journal of Biological Chemistry* http://www.jbc.org doi:10.1074/jbc.R100049200.

40. Pomin, V. H. & Mulloy, B. Glycosaminoglycans and Proteoglycans. *Pharmaceuticals* **11**, (2018).

41. Silbert, J. E. & Sugumaran, G. Biosynthesis of chondroitin/dermatan sulfate. *IUBMB Life* **54**, 177–186 (2002).

42. Mikami, T. & Kitagawa, H. Biosynthesis and function of chondroitin sulfate. *Biochim. Biophys. Acta BBA - Gen. Subj.* **1830**, 4719–4733 (2013).

43. Mitchell, K. J. *et al.* Functional analysis of secreted and transmembrane proteins critical to mouse development. *Nat. Genet.* **28**, 241–249 (2001).

44. Sohaskey, M. L., Yu, J., Diaz, M. A., Plaas, A. H. & Harland, R. M. JAWS coordinates chondrogenesis and synovial joint positioning. *Dev. Camb. Engl.* **135**, 2215–2220 (2008).

45. Klüppel, M., Wight, T. N., Chan, C., Hinek, A. & Wrana, J. L. Maintenance of chondroitin sulfation balance by chondroitin-4-sulfotransferase 1 is required for chondrocyte development and growth factor signaling during cartilage morphogenesis. *Development* **132**, 3989–4003 (2005).

46. Vissers, L. E. L. M. *et al.* Chondrodysplasia and abnormal joint development associated with mutations in IMPAD1, encoding the Golgi-resident nucleotide phosphatase, gPAPP. *Am. J. Hum. Genet.* **88**, 608–615 (2011).

47. Nizon, M. *et al.* IMPAD1 mutations in two Catel-Manzke like patients. *Am. J. Med. Genet. A.* **158A**, 2183–2187 (2012).

48. Kiper, P. Ö. Ş., Utine, G. E., Boduroğlu, K. & Alanay, Y. Catel-Manzke syndrome: a clinical report suggesting autosomal recessive inheritance. *Am. J. Med. Genet. A.* **155A**, 2288–2292 (2011).

49. Bajaj, K. *et al.* Stereochemical Criteria for Prediction of the Effects of Proline Mutations on Protein Stability. *PLOS Comput. Biol.* **3**, e241 (2007).

50. Li, S. C., Goto, N. K., Williams, K. A. & Deber, C. M. Alpha-helical, but not beta-sheet, propensity of proline is determined by peptide environment. *Proc. Natl. Acad. Sci. U. S. A.* **93**, 6676–6681 (1996).

51. Cowan, J. A. Structural and catalytic chemistry of magnesium-dependent enzymes. *Biometals* **15**, 225–235 (2002).

52. Severus, W. E. *et al.* What is the optimal serum lithium level in the long-term treatment of bipolar disorder--a review? *Bipolar Disord.* **10**, 231–237 (2008).

53. Hudson, B. H. *et al.* Role for cytoplasmic nucleotide hydrolysis in hepatic function and protein synthesis. *Proc. Natl. Acad. Sci. U. S. A.* **110**, 5040–5045 (2013).

54. Lasek, A. W., Chen, H. & Chen, W.-Y. Releasing Addiction Memories Trapped in Perineuronal Nets. *Trends Genet.* (2017) doi:10.1016/j.tig.2017.12.004.

55. Berretta, S., Pantazopoulos, H., Markota, M., Brown, C. & Batzianouli, E. T. Losing the sugar coating: potential impact of perineuronal net abnormalities on interneurons in schizophrenia. *Schizophr. Res.* **167**, 18–27 (2015).

56. Dzyubenko, E., Gottschling, C. & Faissner, A. Neuron-Glia Interactions in Neural Plasticity: Contributions of Neural Extracellular Matrix and Perineuronal Nets. *Neural Plast.* **2016**, (2016).

57. van 't Spijker, H. M. & Kwok, J. C. F. A Sweet Talk: The Molecular Systems of Perineuronal Nets in Controlling Neuronal Communication. *Front. Integr. Neurosci.* **11**, (2017).

58. Donegan, J. J. & Lodge, D. J. Hippocampal Perineuronal Nets Are Required for the Sustained Antidepressant Effect of Ketamine. *Int. J. Neuropsychopharmacol.* **20**, 354–358 (2016).

59. Tsien, R. Y. Very long-term memories may be stored in the pattern of holes in the perineuronal net. *Proc. Natl. Acad. Sci.* **110**, 12456–12461 (2013).

60. Miyata, S. & Kitagawa, H. Chondroitin 6-Sulfation Regulates Perineuronal Net Formation by Controlling the Stability of Aggrecan. *Neural Plast.* **2016**, 1305801 (2016).

61. Pantazopoulos, H. & Berretta, S. In Sickness and in Health: Perineuronal Nets and Synaptic Plasticity in Psychiatric Disorders. *Neural Plasticity* https://www.hindawi.com/journals/np/2016/9847696/ (2016) doi:10.1155/2016/9847696.

62. Thompson, E. H. *et al.* Removal of perineuronal nets disrupts recall of a remote fear memory. *Proc. Natl. Acad. Sci. U. S. A.* **115**, 607–612 (2018).

63. Gogolla, N., Caroni, P., Lüthi, A. & Herry, C. Perineuronal Nets Protect Fear Memories from Erasure. *Science* **325**, 1258–1261 (2009).

64. Ueno, H. *et al.* Age-dependent and region-specific alteration of parvalbumin neurons and perineuronal nets in the mouse cerebral cortex. *Neurochem. Int.* **112**, 59–70 (2018).

65. Brückner, G. & Grosche, J. Perineuronal nets show intrinsic patterns of extracellular matrix differentiation in organotypic slice cultures. *Exp. Brain Res.* **137**, 83–93 (2001).

66. Mauney, S. A. *et al.* Developmental pattern of perineuronal nets in the human prefrontal cortex and their deficit in schizophrenia. *Biol. Psychiatry* **74**, 427–435 (2013).

67. Morikawa, S., Ikegaya, Y., Narita, M. & Tamura, H. Activation of perineuronal net-expressing excitatory neurons during associative memory encoding and retrieval. *Sci. Rep.* **7**, (2017).

68. Baker, K. D., Gray, A. R. & Richardson, R. The development of perineuronal nets around parvalbumin gabaergic neurons in the medial prefrontal cortex and basolateral amygdala of rats. *Behav. Neurosci.* **131**, 289–303 (2017).

69. Benes, F. M. & Berretta, S. GABAergic Interneurons: Implications for Understanding Schizophrenia and Bipolar Disorder. *Neuropsychopharmacology* **25**, 1–27 (2001).

70. Brambilla, P., Perez, J., Barale, F., Schettini, G. & Soares, J. C. GABAergic dysfunction in mood disorders. *Mol. Psychiatry* **8**, 721–737, 715 (2003).

71. Kato, T. Molecular neurobiology of bipolar disorder: a disease of 'mood-stabilizing neurons'? *Trends Neurosci.* **31**, 495–503 (2008).

72. Khayachi, A. *et al.* Chronic lithium treatment alters the excitatory/ inhibitory balance of synaptic networks and reduces mGluR5-PKC signalling in mouse cortical neurons. *J. Psychiatry Neurosci. JPN* **46**, E402–E414 (2021).

73. Pantazopoulos, H., Woo, T.-U. W., Lim, M. P., Lange, N. & Berretta, S. Extracellular matrix-glial abnormalities in the amygdala and entorhinal cortex of subjects diagnosed with schizophrenia. *Arch. Gen. Psychiatry* **67**, 155–166 (2010).

74. Pantazopoulos, H. *et al.* Aggrecan and chondroitin-6-sulfate abnormalities in schizophrenia and bipolar disorder: a postmortem study on the amygdala. *Transl. Psychiatry* **5**, e496 (2015).

75. Steullet, P. *et al.* The thalamic reticular nucleus in schizophrenia and bipolar disorder: role of parvalbumin-expressing neuron networks and oxidative stress. *Mol. Psychiatry* **23**, 2057–2065 (2018).

76. Alcaide, J. *et al.* Alterations of perineuronal nets in the dorsolateral prefrontal cortex of neuropsychiatric patients. *Int. J. Bipolar Disord.* **7**, 24 (2019).

77. Lin, R., Rosahl, T. W., Whiting, P. J., Fawcett, J. W. & Kwok, J. C. F. 6-Sulphated Chondroitins Have a Positive Influence on Axonal Regeneration. *PLoS ONE* **6**, (2011).

78. Miyata, S., Komatsu, Y., Yoshimura, Y., Taya, C. & Kitagawa, H. Persistent cortical plasticity by upregulation of chondroitin 6-sulfation. *Nat. Neurosci.* **15**, 414–422, S1-2 (2012).

79. Miyata, S. & Kitagawa, H. Chondroitin sulfate and neuronal disorders. *Front. Biosci. Landmark Ed.* **21**, 1330–1340 (2016).

80. Wlodarczyk, J., Mukhina, I., Kaczmarek, L. & Dityatev, A. Extracellular matrix molecules, their receptors, and secreted proteases in synaptic plasticity. *Dev. Neurobiol.* **71**, 1040–1053 (2011).

81. Yamaguchi, Y. Lecticans: organizers of the brain extracellular matrix: *Cell. Mol. Life Sci.* **57**, 276–289 (2000).

82. Cichon, S. *et al.* Genome-wide association study identifies genetic variation in neurocan as a susceptibility factor for bipolar disorder. *Am. J. Hum. Genet.* **88**, 372–381 (2011).

83. Yu, Z. *et al.* Decreased Density of Perineuronal Net in Prelimbic Cortex Is Linked to Depressive-Like Behavior in Young-Aged Rats. *Front. Mol. Neurosci.* **13**, 4 (2020).

84. Li, Z., Gao, C., Peng, J., Liu, M. & Cong, B. Multi-omics analysis of pathological changes in the amygdala of rats subjected to chronic restraint stress. *Behav. Brain Res.* **392**, 112735 (2020).

85. Pesarico, A. P. *et al.* Chronic Stress Modulates Interneuronal Plasticity: Effects on PSA-NCAM and Perineuronal Nets in Cortical and Extracortical Regions. *Front. Cell. Neurosci.* **13**, 197 (2019).

86. Ohira, K., Takeuchi, R., Iwanaga, T. & Miyakawa, T. Chronic fluoxetine treatment reduces parvalbumin expression and perineuronal nets in gamma-aminobutyric acidergic interneurons of the frontal cortex in adult mice. *Mol. Brain* **6**, 43 (2013).

87. Alaiyed, S., Bozzelli, P. L., Caccavano, A., Wu, J. Y. & Conant, K. Venlafaxine stimulates PNN proteolysis and MMP-9-dependent enhancement of gamma power; relevance to antidepressant efficacy. *J. Neurochem.* **148**, 810–821 (2019).

88. Umemori, J., Winkel, F., Castrén, E. & Karpova, N. N. Distinct effects of perinatal exposure to fluoxetine or methylmercury on parvalbumin and perineuronal nets, the markers of critical periods in brain development. *Int. J. Dev. Neurosci.* **44**, 55–64 (2015).

89. Belichenko, P. V., Hagberg, B. & Dahlström, A. Morphological study of neocortical areas in Rett syndrome. *Acta Neuropathol. (Berl.)* **93**, 50–61 (1997).

90. Gu, B. *et al.* Ube3a reinstatement mitigates epileptogenesis in Angelman syndrome model mice. *J. Clin. Invest.* **129**, 163–168 (2019).

91. Wen, T. H. *et al.* Genetic Reduction of Matrix Metalloproteinase-9 Promotes Formation of Perineuronal Nets Around Parvalbumin-Expressing Interneurons and Normalizes Auditory Cortex Responses in Developing Fmr1 Knock-Out Mice. *Cereb. Cortex N. Y. N 1991* **28**, 3951–3964 (2018).

92. Baig, S., Wilcock, G. K. & Love, S. Loss of perineuronal net N-acetylgalactosamine in Alzheimer's disease. *Acta Neuropathol. (Berl.)* **110**, 393–401 (2005).

93. Rankin-Gee, E. K. *et al.* Perineuronal net degradation in epilepsy. *Epilepsia* **56**, 1124–1133 (2015).

94. Kobayashi, K., Emson, P. C. & Mountjoy, C. Q. Vicia villosa lectin-positive neurones in human cerebral cortex. Loss in Alzheimer-type dementia. *Brain Res.* **498**, 170–174 (1989).

95. Vazquez-Sanroman, D. B., Monje, R. D. & Bardo, M. T. Nicotine self-administration remodels perineuronal nets in ventral tegmental area and orbitofrontal cortex in adult male rats. *Addict. Biol.* **22**, 1743–1755 (2017).

96. Yoshioka, N. *et al.* Abnormalities in perineuronal nets and behavior in mice lacking CSGalNAcT1, a key enzyme in chondroitin sulfate synthesis. *Mol. Brain* **10**, (2017).

97. Rowlands, D. *et al.* Aggrecan Directs Extracellular Matrix-Mediated Neuronal Plasticity. *J. Neurosci.* **38**, 10102–10113 (2018).

98. Brakebusch, C. *et al.* Brevican-deficient mice display impaired hippocampal CA1 long-term potentiation but show no obvious deficits in learning and memory. *Mol. Cell. Biol.* **22**, 7417–7427 (2002).

99. Hylin, M. J., Orsi, S. A., Moore, A. N. & Dash, P. K. Disruption of the perineuronal net in the hippocampus or medial prefrontal cortex impairs fear conditioning. *Learn. Mem.* **20**, 267–273 (2013).

100. Zhou, X.-H. *et al.* Neurocan Is Dispensable for Brain Development. *Mol. Cell. Biol.* **21**, 5970–5978 (2001).

101. Yang, S. *et al.* Perineuronal net digestion with chondroitinase restores memory in mice with tau pathology. *Exp. Neurol.* **265**, 48–58 (2015).

102. Carulli, D. *et al.* Cerebellar plasticity and associative memories are controlled by perineuronal nets. *Proc. Natl. Acad. Sci. U. S. A.* **117**, 6855–6865 (2020).

103. Duncan, J. A., Foster, R. & Kwok, J. C. F. The Potential of Memory Enhancement through Perineuronal Net Modulation. *Br. J. Pharmacol.* (2019) doi:10.1111/bph.14672.

104. Yick, L.-W., So, K.-F., Cheung, P.-T. & Wu, W.-T. Lithium chloride reinforces the regeneration-promoting effect of chondroitinase ABC on rubrospinal neurons after spinal cord injury. *J. Neurotrauma* **21**, 932–943 (2004).

105. Kadomatsu, K. & Sakamoto, K. Mechanisms of axon regeneration and its inhibition: Roles of sulfated glycans. *Arch. Biochem. Biophys.* **558**, 36–41 (2014).

106. Snow, D. M., Mullins, N. & Hynds, D. L. Nervous system-derived chondroitin sulfate proteoglycans regulate growth cone morphology and inhibit neurite outgrowth: a light, epifluorescence, and electron microscopy study. *Microsc. Res. Tech.* **54**, 273–286 (2001).

107. Tong, M. *et al.* Lithium chloride contributes to blood-spinal cord barrier integrity and functional recovery from spinal cord injury by stimulating autophagic flux. *Biochem. Biophys. Res. Commun.* **495**, 2525–2531 (2018).

108. Yang, M. L. *et al.* Efficacy and safety of lithium carbonate treatment of chronic spinal cord injuries: a double-blind, randomized, placebo-controlled clinical trial. *Spinal Cord* **50**, 141–146 (2012).

109. Corvetti, L. & Rossi, F. Degradation of chondroitin sulfate proteoglycans induces sprouting of intact purkinje axons in the cerebellum of the adult rat. *J. Neurosci. Off. J. Soc. Neurosci.* **25**, 7150–7158 (2005).

110. Barritt, A. W. *et al.* Chondroitinase ABC promotes sprouting of intact and injured spinal systems after spinal cord injury. *J. Neurosci. Off. J. Soc. Neurosci.* **26**, 10856–10867 (2006).

111. Williams, R. S. B., Cheng, L., Mudge, A. W. & Harwood, A. J. A common mechanism of action for three mood-stabilizing drugs. *Nature* **417**, 292–295 (2002).

112. Shaltiel, G., Dalton, E. C., Belmaker, R. H., Harwood, A. J. & Agam, G. Specificity of mood stabilizer action on neuronal growth cones. *Bipolar Disord.* **9**, 281–289 (2007).

113. Berry-Kravis, E. *et al.* Open-label treatment trial of lithium to target the underlying defect in fragile X syndrome. *J. Dev. Behav. Pediatr. JDBP* **29**, 293–302 (2008).

114. Liu, Z. & Smith, C. B. Lithium: A Promising Treatment for Fragile X Syndrome. *ACS Chem. Neurosci.* **5**, 477–483 (2014).

115. Siegel, M. *et al.* Preliminary Investigation of Lithium for Mood Disorder Symptoms in Children and Adolescents with Autism Spectrum Disorder. *J. Child Adolesc. Psychopharmacol.* **24**, 399–402 (2014).

116. Eisele, B. S. *et al.* Sulfation of glycosaminoglycans depends on catalytic activity of lithium-inhibited phosphatase BPNT2 in vitro. *J. Biol. Chem.* **0**, (2021).

117. Hudson, B. H. & York, J. D. Roles for nucleotide phosphatases in sulfate assimilation and skeletal disease. *Adv. Biol. Regul.* **52**, (2012).

118. Hudson, B. H., Hale, A. T., Irving, R. P., Li, S. & York, J. D. Modulation of intestinal sulfur assimilation metabolism regulates iron homeostasis. *Proc. Natl. Acad. Sci. U. S. A.* **115**, 3000–3005 (2018).

119. Soares da Costa, D., Reis, R. L. & Pashkuleva, I. Sulfation of Glycosaminoglycans and Its Implications in Human Health and Disorders. *Annu. Rev. Biomed. Eng.* **19**, 1–26 (2017).

120. Langford, R., Hurrion, E. & Dawson, P. A. Genetics and pathophysiology of mammalian sulfate biology. *J. Genet. Genomics Yi Chuan Xue Bao* **44**, 7–20 (2017).

121. Huang, X., Holden, H. M. & Raushel, F. M. Channeling of Substrates and Intermediates in Enzyme-Catalyzed Reactions. *Annu. Rev. Biochem.* **70**, 149–180 (2001).

122. Kehl, T. *et al.* About miRNAs, miRNA seeds, target genes and target pathways. *Oncotarget* **8**, 107167–107175 (2017).

123. Lin, E.-S. & Yang, Y.-S. Colorimetric Determination of the Purity of 3′-Phospho Adenosine 5′-Phosphosulfate and Natural Abundance of 3′-Phospho Adenosine 5′-Phosphate at Picomole Quantities. *Anal. Biochem.* **264**, 111–117 (1998).

124. Zheng, C. & Levenston, M. E. Fact versus artifact: Avoiding erroneous estimates of sulfated glycosaminoglycan content using the dimethylmethylene blue colorimetric assay for tissue-engineered constructs. *Eur. Cell. Mater.* **29**, 224–236 (2015).

125. Bigge, J. C. *et al.* Nonselective and efficient fluorescent labeling of glycans using 2-amino benzamide and anthranilic acid. *Anal. Biochem.* **230**, 229–238 (1995).

126. Yoshida, K., Miyauchi, S., Kikuchi, H., Tawada, A. & Tokuyasu, K. Analysis of unsaturated disaccharides from glycosaminoglycuronan by high-performance liquid chromatography. *Anal. Biochem.* **177**, 327–332 (1989).

127. Estes, B. T. & Guilak, F. Three-dimensional Culture Systems to Induce Chondrogenesis of Adipose-Derived Stem Cells. *Methods Mol. Biol. Clifton NJ* **702**, 201–217 (2011).

128. Hale, A. T. *et al.* Modulation of sulfur assimilation metabolic toxicity overcomes anemia and hemochromatosis in mice. *Adv. Biol. Regul.* **76**, 100694 (2020).

129. Lee, H. S., Qi, Y. & Im, W. Effects of N -glycosylation on protein conformation and dynamics: Protein Data Bank analysis and molecular dynamics simulation study. *Sci. Rep.* **5**, 1–7 (2015).

130. Petrescu, A.-J., Milac, A.-L., Petrescu, S. M., Dwek, R. A. & Wormald, M. R. Statistical analysis of the protein environment of N-glycosylation sites: implications for occupancy, structure, and folding. *Glycobiology* **14**, 103–114 (2004).

131. Mourão, P. A. Distribution of chondroitin 4-sulfate and chondroitin 6-sulfate in human articular and growth cartilage. *Arthritis Rheum.* **31**, 1028–1033 (1988).

132. James, M. O. Enzyme Kinetics of Conjugating Enzymes: PAPS Sulfotransferase. in *Enzyme Kinetics in Drug Metabolism: Fundamentals and Applications* (eds. Nagar, S., Argikar, U. A. & Tweedie, D. J.) 187–201 (Humana Press, 2014). doi:10.1007/978-1-62703-758-7_10.

133. Capasso, J. M. & Hirschberg, C. B. Mechanisms of glycosylation and sulfation in the Golgi apparatus: evidence for nucleotide sugar/nucleoside monophosphate and nucleotide sulfate/nucleoside monophosphate antiports in the Golgi apparatus membrane. *Proc. Natl. Acad. Sci. U. S. A.* **81**, 7051–7055 (1984).

134. Ozeran, J. D., Westley, J. & Schwartz, N. B. Kinetics of PAPS translocase: evidence for an antiport mechanism. *Biochemistry* **35**, 3685–3694 (1996).

135. Dill, J., Wang, H., Zhou, F. & Li, S. Inactivation of glycogen synthase kinase 3 promotes axonal growth and recovery in the CNS. *J. Neurosci. Off. J. Soc. Neurosci.* **28**, 8914–8928 (2008).

136. Benard, V., Vaiva, G., Masson, M. & Geoffroy, P. A. Lithium and suicide prevention in bipolar disorder. *L'Encephale* **42**, 234–241 (2016).

137. Saccà, F. *et al.* A randomized controlled pilot trial of lithium in spinocerebellar ataxia type 2. *J. Neurol.* **262**, 149–153 (2015).

138. Karimi, A. *et al.* Evaluation of lithium serum level in multiple sclerosis patients: A neuroprotective element. *Mult. Scler. Relat. Disord.* **17**, 244–248 (2017).

139. Forlenza, O. V., De-Paula, V. J. R. & Diniz, B. S. O. Neuroprotective Effects of Lithium: Implications for the Treatment of Alzheimer's Disease and Related Neurodegenerative Disorders. *ACS Chem. Neurosci.* **5**, 443–450 (2014).

140. Neuroprotective Effects of Lithium in Patients with Bipolar. http://www.currentpsychopharmacology.com/articles/137888/neuroprotective-effects-of-lithium-in-patients-with-bipolar-disorder.

141. Sorg, B. A. *et al.* Casting a Wide Net: Role of Perineuronal Nets in Neural Plasticity. *J. Neurosci.* **36**, 11459–11468 (2016).

142. Romberg, C. *et al.* Depletion of Perineuronal Nets Enhances Recognition Memory and Long-Term Depression in the Perirhinal Cortex. *J. Neurosci.* **33**, 7057–7065 (2013).

143. Lord, S. J., Velle, K. B., Mullins, R. D. & Fritz-Laylin, L. K. SuperPlots: Communicating reproducibility and variability in cell biology. *J. Cell Biol.* **219**, (2020).

144. Pizzorusso, T. *et al.* Reactivation of Ocular Dominance Plasticity in the Adult Visual Cortex. *Science* **298**, 1248–1251 (2002).

145. Slaker, M. L., Harkness, J. H. & Sorg, B. A. A standardized and automated method of perineuronal net analysis using Wisteria floribunda agglutinin staining intensity. *IBRO Rep.* **1**, 54–60 (2016).

146. O'Donnell, K. C. & Gould, T. D. The Behavioral Actions of Lithium in Rodent Models. *Neurosci. Biobehav. Rev.* **31**, 932–962 (2007).

147. Eisele, B. S. *et al.* Sulfation of glycosaminoglycans depends on catalytic activity of a lithium-inhibited phosphatase. *bioRxiv* 2021.06.24.449779 (2021) doi:10.1101/2021.06.24.449779.

148. Watanabe, H. *et al.* Mouse cartilage matrix deficiency (cmd) caused by a 7 bp deletion in the aggrecan gene. *Nat. Genet.* **7**, 154–157 (1994).

149. Deepa, S. S. *et al.* Composition of perineuronal net extracellular matrix in rat brain: a different disaccharide composition for the net-associated proteoglycans. *J. Biol. Chem.* **281**, 17789–17800 (2006).

150. Tsai, L.-K., Leng, Y., Wang, Z., Leeds, P. & Chuang, D.-M. The mood stabilizers valproic acid and lithium enhance mesenchymal stem cell migration via distinct mechanisms. *Neuropsychopharmacol. Off. Publ. Am. Coll. Neuropsychopharmacol.* **35**, 2225–2237 (2010).

151. Guidotti, S. *et al.* Lithium Chloride Dependent Glycogen Synthase Kinase 3 Inactivation Links Oxidative DNA Damage, Hypertrophy and Senescence in Human Articular Chondrocytes and Reproduces Chondrocyte Phenotype of Obese Osteoarthritis Patients. *PLOS ONE* **10**, e0143865 (2015).

152. Yu, W. & Greenberg, M. L. Inositol depletion, GSK3 inhibition and bipolar disorder. *Future Neurol.* **11**, 135–148 (2016).

153. Shaltiel, G., Kozlovsky, N., Belmaker, R. H. & Agam, G. 3'(2')-Phosphoadenosine 5'-phosphate phosphatase is reduced in postmortem frontal cortex of bipolar patients. *Bipolar Disord.* **4**, 302–306 (2002).

154. Meisel, J. D. & Kim, D. H. Inhibition of Lithium-Sensitive Phosphatase BPNT-1 Causes Selective Neuronal Dysfunction in C. elegans. *Curr. Biol. CB* **26**, 1922–1928 (2016).

155. Schaefer, G. B. & Bodensteiner, J. B. Evaluation of the child with idiopathic mental retardation. *Pediatr. Clin. North Am.* **39**, 929–943 (1992).

156. Amin, S. & Borrell, V. The Extracellular Matrix in the Evolution of Cortical Development and Folding. *Front. Cell Dev. Biol.* **8**, 1486 (2020).

157. Şıklar, Z. & Berberoğlu, M. Syndromic Disorders with Short Stature. *J. Clin. Res. Pediatr. Endocrinol.* **6**, 1–8 (2014).

158. Bober, M. B., Bellus, G. A., Nikkel, S. M. & Tiller, G. E. Hypochondroplasia. in *GeneReviews®* (eds. Adam, M. P. et al.) (University of Washington, Seattle, 1993).

159. Ilyas, M., Mir, A., Efthymiou, S. & Houlden, H. The genetics of intellectual disability: advancing technology and gene editing. *F1000Research* **9**, F1000 Faculty Rev-22 (2020).

160. Ghibellini, G., Brancati, F. & Castori, M. Neurodevelopmental attributes of joint hypermobility syndrome/Ehlers-Danlos syndrome, hypermobility type: Update and perspectives. *Am. J. Med. Genet. C Semin. Med. Genet.* **169C**, 107–116 (2015).

161. Redrobe, J. P. & Bourin, M. Effects of pretreatment with clonidine, lithium and quinine on the activities of antidepressant drugs in the mouse tail suspension test. *Fundam. Clin. Pharmacol.* **11**, 381–386 (1997).

162. Beyer, D. K. E. & Freund, N. Animal models for bipolar disorder: from bedside to the cage. *Int. J. Bipolar Disord.* **5**, 35 (2017).

163. Phan, D.-H. *et al.* Lithium attenuates d-amphetamine-induced hyperlocomotor activity in mice via inhibition of interaction between cyclooxygenase-2 and indoleamine-2,3-dioxygenase. *Clin. Exp. Pharmacol. Physiol.* **47**, 790–797 (2020).

164. Müller, C. J., Bankstahl, M., Gröticke, I. & Löscher, W. Pilocarpine vs. lithium-pilocarpine for induction of status epilepticus in mice: development of spontaneous seizures, behavioral alterations and neuronal damage. *Eur. J. Pharmacol.* **619**, 15–24 (2009).

165. Lerer, B., Ebstein, R. P., Felix, A. & Beimaker, R. H. Lithium Amelioration of Reserpine-Induced Hypoactivity in Rats. *Int. Pharmacopsychiatry* **15**, 338–343 (1980).

166. Leelavathi, D. E., Estes, L. W., Feingold, D. S. & Lombardi, B. Isolation of a Golgi-rich fraction from rat liver. *Biochim. Biophys. Acta BBA - Biomembr.* **211**, 124–138 (1970).

167. Ashykhmina, N. *et al.* PAPST2 Plays Critical Roles in Removing the Stress Signaling Molecule 3'-Phosphoadenosine 5'-Phosphate from the Cytosol and Its Subsequent Degradation in Plastids and Mitochondria. *Plant Cell* **31**, 231–249 (2019).

168. Negishi, M. *et al.* Structure and Function of Sulfotransferases. *Arch. Biochem. Biophys.* **390**, 149–157 (2001).

169. Bullock, S. L., Fletcher, J. M., Beddington, R. S. P. & Wilson, V. A. Renal agenesis in mice homozygous for a gene trap mutation in the gene encoding heparan sulfate 2-sulfotransferase. *Genes Dev.* **12**, 1894–1906 (1998).

170. Ringvall, M. & Kjellén, L. Mice deficient in heparan sulfate N-deacetylase/N-sulfotransferase 1. *Prog. Mol. Biol. Transl. Sci.* **93**, 35–58 (2010).

171. Hascall, V. C. & Sajdera, S. W. Physical properties and polydispersity of proteoglycan from bovine nasal cartilage. *J. Biol. Chem.* **245**, 4920–4930 (1970).

172. Djerbal, L., Lortat-Jacob, H. & Kwok, J. Chondroitin sulfates and their binding molecules in the central nervous system. *Glycoconj. J.* **34**, 363–376 (2017).

173. Banerjee, S. B. *et al.* Perineuronal Nets in the Adult Sensory Cortex Are Necessary for Fear Learning. *Neuron* **95**, 169-179.e3 (2017).

174. Arakawa, H. Ethological approach to social isolation effects in behavioral studies of laboratory rodents. *Behav. Brain Res.* **341**, 98–108 (2018).

175. Mumtaz, F., Khan, M. I., Zubair, M. & Dehpour, A. R. Neurobiology and consequences of social isolation stress in animal model-A comprehensive review. *Biomed. Pharmacother. Biomedecine Pharmacother.* **105**, 1205–1222 (2018).

176. Golden, S. A., Covington, H. E., Berton, O. & Russo, S. J. A standardized protocol for repeated social defeat stress in mice. *Nat. Protoc.* **6**, 1183–1191 (2011).

177. Willner, P. Animal models as simulations of depression. *Trends Pharmacol. Sci.* **12**, 131–136 (1991).

178. Chalecka-Franaszek, E. & Chuang, D. M. Lithium activates the serine/threonine kinase Akt-1 and suppresses glutamate-induced inhibition of Akt-1 activity in neurons. *Proc. Natl. Acad. Sci. U. S. A.* **96**, 8745–8750 (1999).

179. Zhang, F., Phiel, C. J., Spece, L., Gurvich, N. & Klein, P. S. Inhibitory Phosphorylation of Glycogen Synthase Kinase-3 (GSK-3) in Response to Lithium: EVIDENCE FOR AUTOREGULATION OF GSK-3 *. *J. Biol. Chem.* **278**, 33067–33077 (2003).

180. Xiao, S., Finkielstein, C. V. & Capelluto, D. G. S. The enigmatic role of sulfatides: new insights into cellular functions and mechanisms of protein recognition. *Adv. Exp. Med. Biol.* **991**, 27–40 (2013).

181. Honke, K. *et al.* Molecular Cloning and Expression of cDNA Encoding Human 3'-Phosphoadenylylsulfate:galactosylceramide 3'-Sulfotransferase *. *J. Biol. Chem.* **272**, 4864–4868 (1997).

182. Yaghootfam, A. *et al.* Cerebroside sulfotransferase forms homodimers in living cells. *Biochemistry* **46**, 9260–9269 (2007).

183. Norton, W. T. & Poduslo, S. E. Myelination in rat brain: method of myelin isolation. *J. Neurochem.* **21**, 749–757 (1973).

184. Winzeler, A. M. *et al.* The lipid sulfatide is a novel myelin-associated inhibitor of CNS axon outgrowth. *J. Neurosci. Off. J. Soc. Neurosci.* **31**, 6481–6492 (2011).

185. Honke, K. *et al.* Paranodal junction formation and spermatogenesis require sulfoglycolipids. *Proc. Natl. Acad. Sci. U. S. A.* **99**, 4227–4232 (2002).